BROCKMAN SYNCLINE REGIONAL GROUNDWATER MODEL

Cumulative Impact Assessment

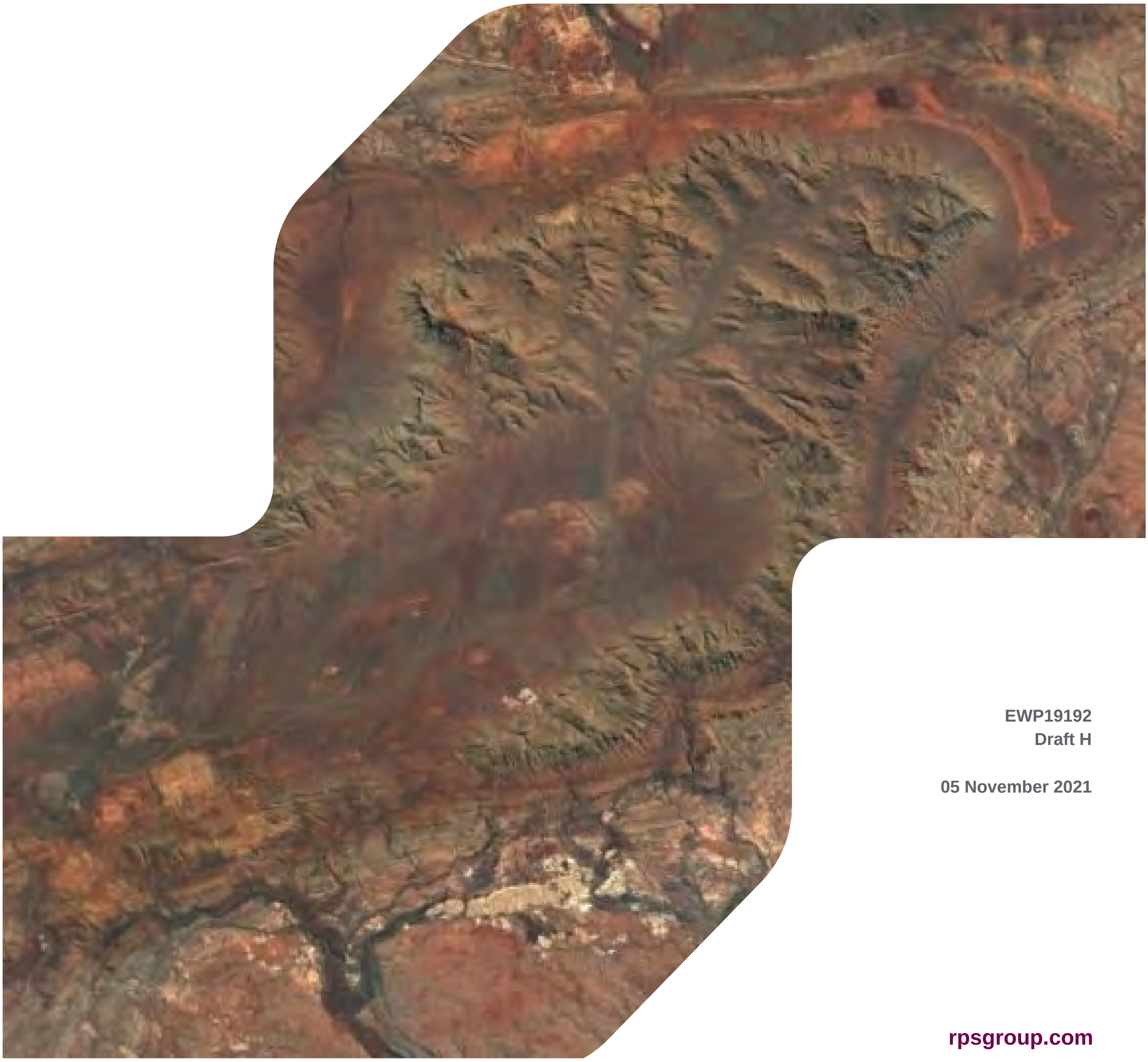

EWP19192
Draft H

05 November 2021

rpsgroup.com

Document status

Version	Purpose of document	Authored by	Reviewed by	Approved by	Review date
Draft A	Draft for client review	CasTur	RonCol	RonCol	18/01/2020
Draft B	Update to include comments	CasTur	RonCol	RonCol	19/02/2020
Draft C	Correction to timing	CasTur			29/04/2020
Draft D	Change figure layout	CasTur			06/05/2020
Draft E	Update to new mine plan	CasTur	RonCol	RonCol	12/02/2021
Draft F	Update to include comments	CasTur	RonCol	RonCol	24/02/2021
Draft G	Update to include new closure	CasTur	RonCol	RonCol	28/06/2021
Draft H	Update to closure plan	CasTur			04/11/2021

Approval for issue

Prepared by:

RPS

Cassie Turvey
Senior Groundwater Modeller

Level 2, 27-31 Troode Street
West Perth WA 6005

T +61 8 9211 1111
E cassie.turvey@rpsgroup.com.au

Prepared for:

Rio Tinto

Paul Hedley
Superintendent Hydrogeology

Level 10, 152-158 St Georges Tce
Perth WA 6000

Contents

Tables

Figures

Graphs

Appendices

1 INTRODUCTION

Hamersley Iron Pty Ltd (the Proponent) is currently preparing a broad ranging Part IV submission for additional mining in several separate deposits that are contained within the Brockman Syncline area. The submission is to be referred to the EPA. RPS has been engaged by Rio Tinto Group (Rio Tinto) on behalf of the Proponent to undertake numerical groundwater modelling for the cumulative impact assessment for the Brockman Syncline proposal (the Proposal). This report presents the results of the modelling to be incorporated into the broader Part IV submission.

The Proposal area, located approximately 45km north west of Tom Price, includes a Development Envelope and a conceptual footprint as well as existing approved operations at Nammuldi-Silvergrass, Brockman Syncline 2 and Brockman Syncline 4.

1.1 Scope of work

The scope of work includes:

- Construction and calibration of a numerical groundwater flow model suitable for assessment of potential impacts of the Proposal.
- Modelling of the proposed mine during operations and post closure.
- Modelling and quantification of cumulative impacts of mining within the Brockman Syncline, including Rio Tinto approved and proposed pits as well as nearby projects, such as the Fortescue Metals Group (FMG) Eliwana mine.
- Preparation of this groundwater model Cumulative Impact Assessment report.

Outputs from this work are proposed to feed into various components of the Part IV submission as well as provide preliminary estimates of dewatering infrastructure requirements, mine water balance assessments and input to optimisation of long-term mine planning.

This report represents a revision to earlier reporting (RPS, 2021) to incorporate updates to the mine closure plan.

2 MINE PLAN

2.1 Existing Mine Plan

Existing and proposed mine locations within the Brockman Syncline are shown in Figure 1. Current mining has progressed below watertable within the Nammuldi Hub (Lens AB, Lens CD, Lens EF), Brockman Syncline 2 Hub (BS2ED), and the Brockman Syncline 4 Hub at BS4. The progressive historic schedule for mine development is not readily available to be included here; in lieu of the mine schedule, mine floor levels were taken from monthly end of mine LiDAR surfaces to derive the past progression of the mine floor over time for modelling purposes.

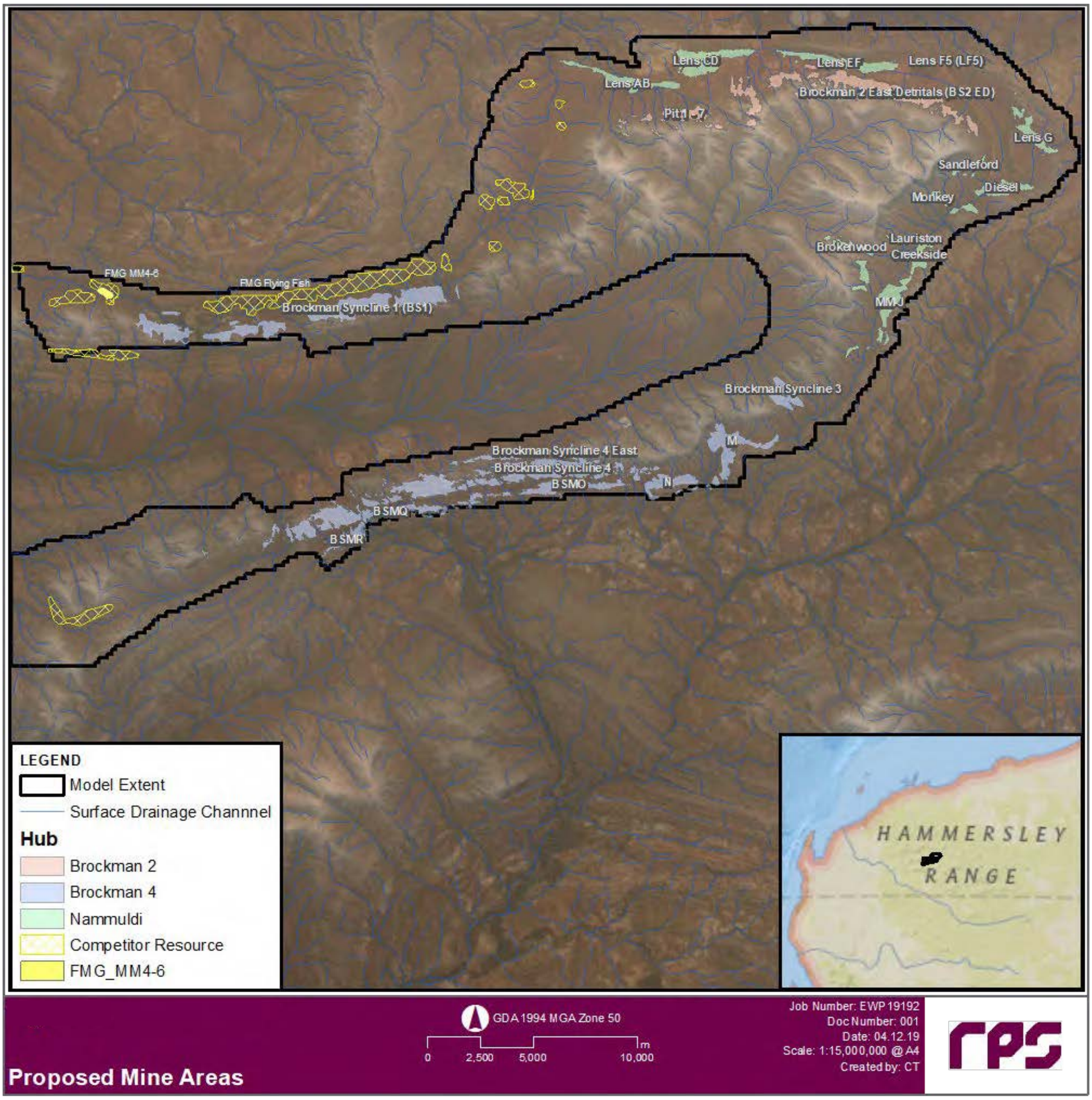

Figure 1 Existing and proposed mining areas

2.2 Future Mine Plan

Current mine plans forecast mining to year 2047 within the Nammuldi hub and 2045 at BS4. Several versions of the mine plan were provided by Rio Tinto as mine planning optimisation is still being undertaken. Ultimately, 2020 Life of Mine (LoM) planning was used, with the final version of the mine schedule and associated pit shells used in predictive modelling presented in Appendix A. Only pits that are currently proposed to go below water table were included in the model.

2.3 Nearby Mines

FMG's Eliwana mine is located directly north of BS1. With reference to Golder 2019, the majority of pits that occur in the vicinity of BS1 are not currently proposed to go below water table, with the exception of pit MM4-6, located at the most north-westerly point in the groundwater model (Figure 1). Available information suggests excavation of this pit goes below water table from December 2031 to Dec 2034, with a final pit floor of 450mAHD (approximately 50m below natural groundwater levels). A groundwater abstraction borefield is proposed to be established at the Flying Fish deposit if the final mine plan results in a water deficit for part or all of the mine life.

3 CONCEPTUAL MODEL OVERVIEW

The groundwater system is highly compartmentalised due to the presence of low permeability sub-vertical dykes and fault features, as well as very low permeability units within the steeply dipping geology forming barriers to horizontal flow. Within the Brockman Syncline, in areas of proposed mining, the main regional aquifers include the mineralised BIF of the Marra Mamba Iron Formation (particularly the Mount Newman Member) and Brockman Iron Formations (Dales Gorge and Joffre members), as well as the Wittenoom Dolomite (Paraburdoo Member).

Localised shallow aquifers may also exist in the alluvial/detrital sediments, although these are likely to be mainly perched/disconnected aquifers formed during periods of significant rainfall (i.e. after cyclonic rainfall). Recharge to the groundwater system is minimal and occurs only via recharge from alluvial systems during extended wet periods. The conceptualisation of groundwater flow in the system is shown in plan view in Figure 2 and section view in Figure 3.

Groundwater discharge occurs at localised areas where deeper alluvial sediments occur in combination with a sharply incised topography (i.e. gorge). One such location, known locally as Plunge Pool, is considered to form an aquatic groundwater dependant ecosystem (GDE) and occurs between the BS3 and M deposits. The BoM GDE Atlas (BoM, 2019) identifies another un-named GDE mapped by the then Department of Water (now DWER) south of the Maybelline deposit and east of BS2. It is understood that this location has not been ground-truthed by Rio Tinto. However, aerial imagery does not indicate any obvious presence of potential groundwater dependent vegetation. Studies being undertaken by Rio Tinto indicate several other potential GDEs occur across the syncline, however the likelihood of groundwater dependence is not yet fully understood. Mapped potential GDEs are shown in Figure 4.

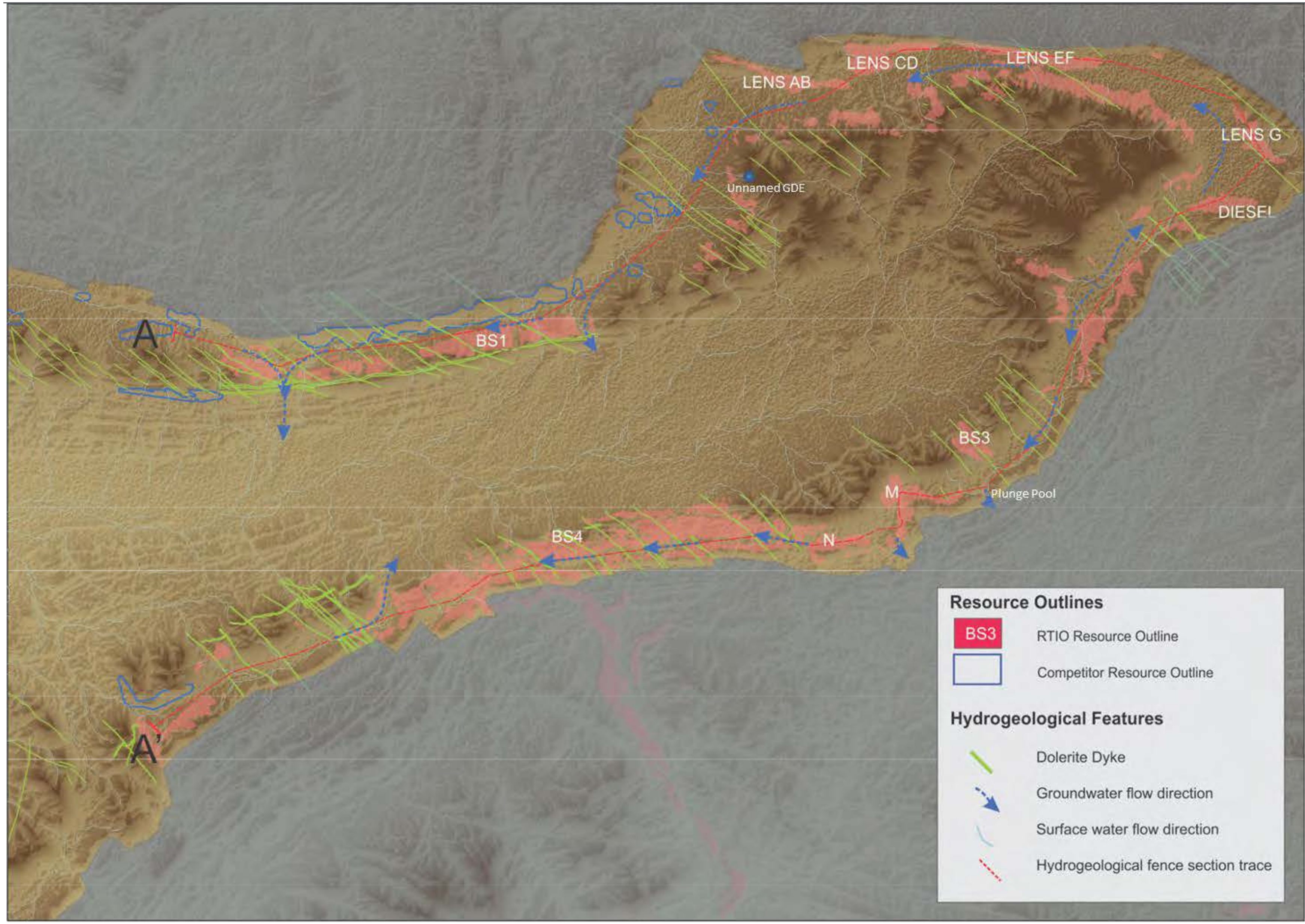

Figure 2 Plan view groundwater conceptual model

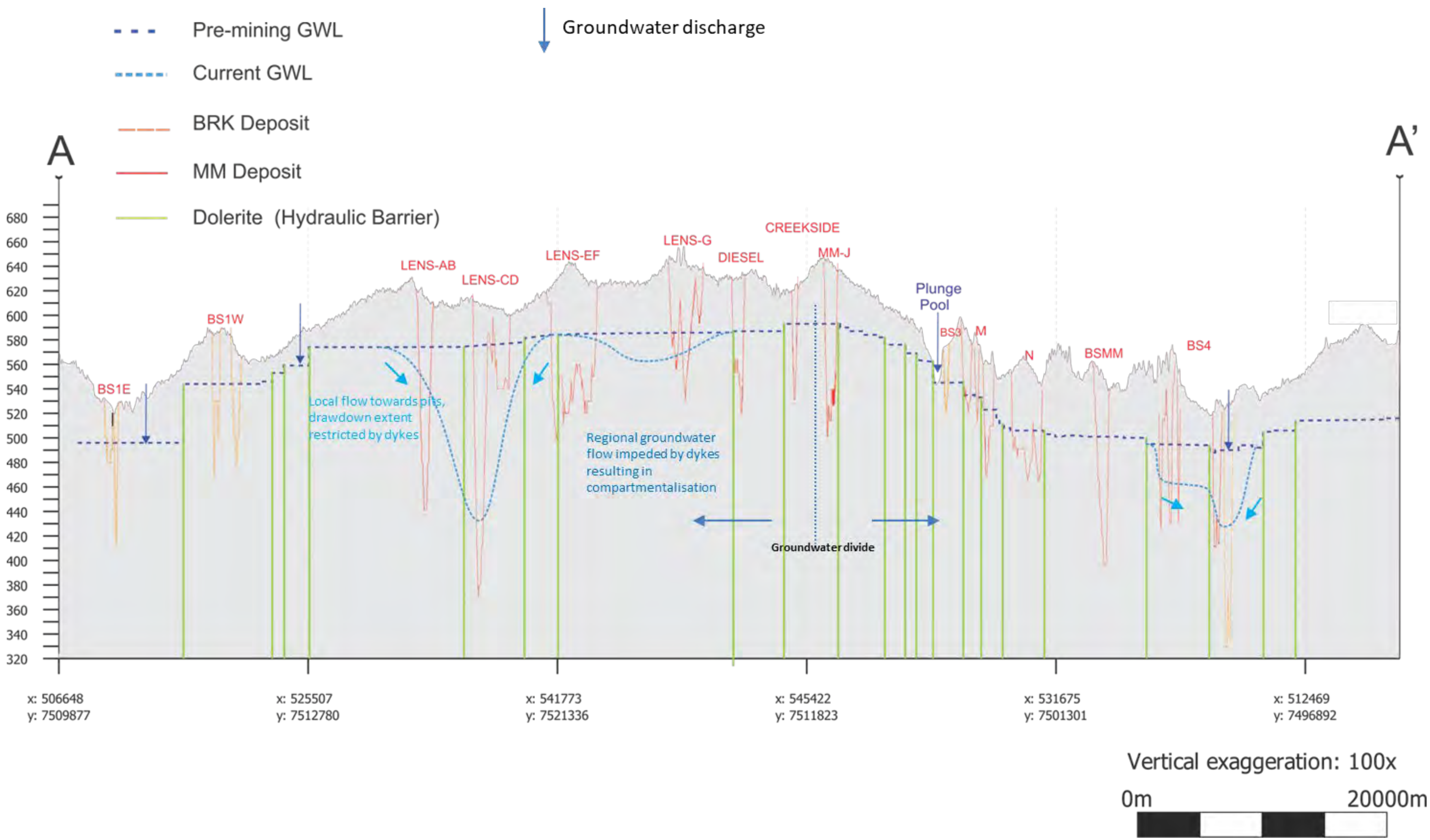

Figure 3 **Conceptual section view for groundwater model**

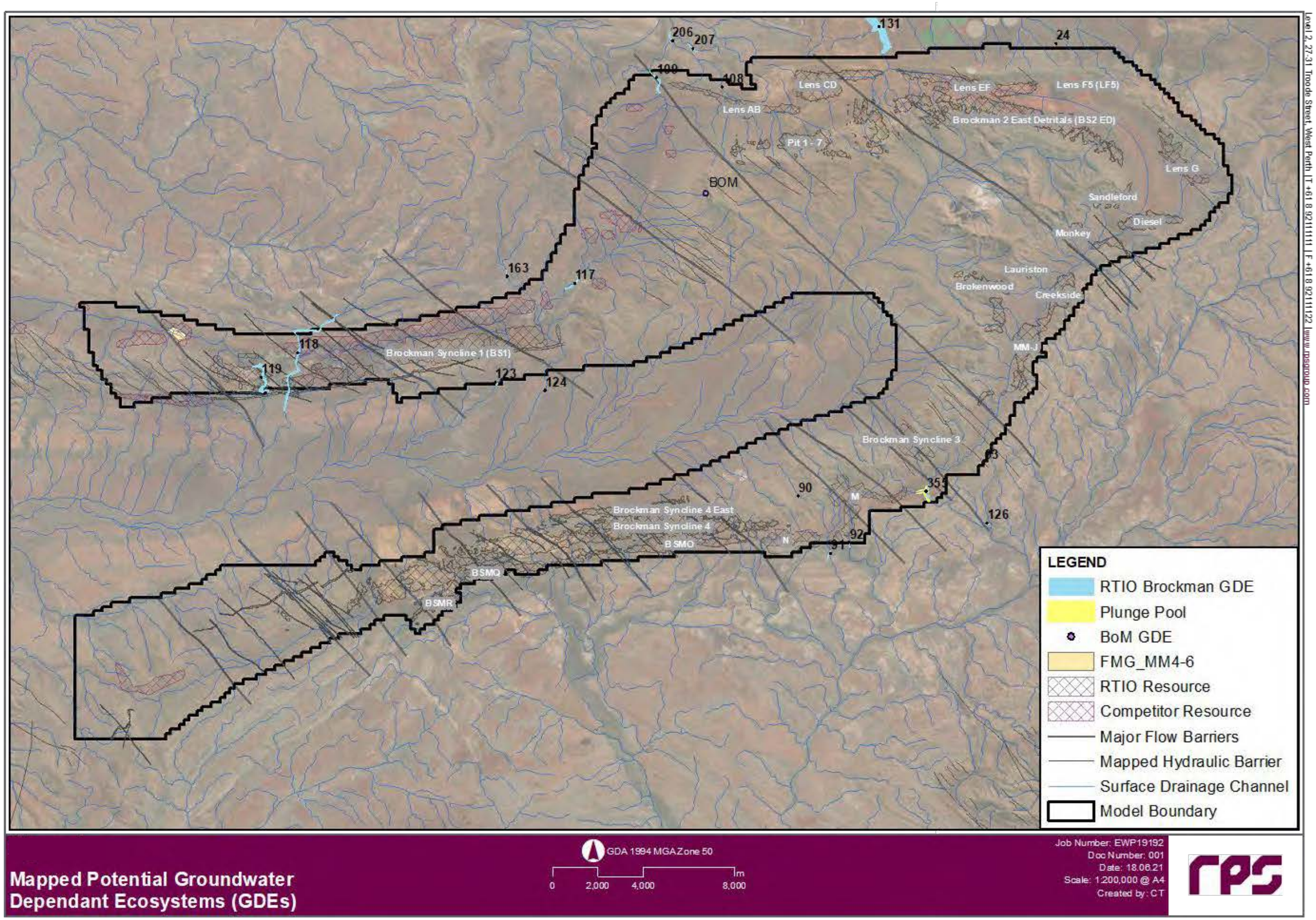

Figure 4 Mapped GDEs

3.1 Model Implementation

3.1.1 Mine Progression

The MODFLOW drain package was used to simulate pit floor progression over time, with the drain stage set at 10m below the scheduled floor level to capture the planned dewatering target. Additionally, existing dewatering wells remained in the model to the end of mining, with dewatering bores switched off at the end of life of the proposed pit, and supply bores pumping until 2050. The rate of flow in the bores is automatically decreased using the Auto Flow Reduction option available in MODFLOW-USG, such that the flow rate declines with declining head. Existing dewatering bores that are "mined through" are superseded by the MODFLOW drain package. The FMG water supply borefield at Flying Fish was simulated using the MODFLOW drain package such that drawdown matched that predicted by Golder (2018).

3.1.2 Closure

The closure plan for mining within the Brockman Syncline is to backfill the majority of the below water table pits to above pre-mining groundwater level with the aim of minimising exposure of potential acid forming (PAF) material and reducing long-term drawdown impacts in areas of known GDEs (Table 1). The remaining pits are currently proposed to stay as open voids.

Table 1 Proposed closure outcome for below water table pits

Backfill		Open Void
BS4 Pit2	Creekside	BS4MM O1,2,3
BS4 Pit3	Diesel	BS4MM Q
BS4 Pit4	END 1	BS4MN N1,2
BS4 Pit5	MMJ	BS4MN M2
BS4 Pit6	BS1_E1	Lens B
BS4 Pit7	BS1_W1	Lens CD
BS4 Pit10	BS1_E2	Lens EF
BS4 Pit11	BS1_W2	Lens G
BS4 Pit12	BSMR	
BS4 Pit15	B2ED Pit 8	
BS4 Pit16	B2ED Pit 10	
BS4 Pit17	B2ED Pit 11	
BS4 Pit18	B2ED Pit 12	
Lens A	B2ED Pit 13	

The MODFLOW-USG Time-Variant Materials (TVM) package was used to change the hydraulic properties to represent either spoil fill or an open void pit (with new hydraulic properties activated following the end of mining for each pit) as shown in Table 2.

Table 2 Hydraulic properties applied at end of mining in the groundwater model

Closure Option	kh [m/d]	kv [m/d]	Sy	Ss [m^{-1}]	Net Recharge
Backfill	5	5	0.2	1.0e-6	1.5% rainfall
Pit Void	100	100	1	1.0e-6	0% rainfall

The likely higher infiltration characteristics of the spoil were accommodated by allocating enhanced rainfall recharge (1.5% of rainfall) using the MODFLOW recharge package. Topography was not altered in response to the proposed final rehabilitated landform.

The representation of the pit voids using the high hydraulic conductivity and storage method is relatively simplistic but is common modelling practice and is deemed appropriate for the purpose of estimating water level recovery and lake filling. In the case of pit lake formation, the model only represents the groundwater contribution to pit lake development, and further assessment to include surface water runoff, direct rainfall and evaporation at the lake surface should be undertaken. Given the low level of lake recovery and excess evaporation (i.e. evaporation >> rainfall) it is likely that the pits will remain a groundwater sink, assuming that the pits have sufficient post-closure bunding to prevent significant ingress of surface water.

4 MODEL CONSTRUCTION

4.1 Model Code

The model was run using the MODFLOW-USG code (Panday et al., 2013) through the Groundwater Vistas V7 Pro graphical user interface (Rumbaugh, 2017). The MODFLOW-USG code was chosen primarily due to the ability to refine the model mesh at mine locations as well as for its stability in handling dry cells when run using the Newton solver (Niswonger et al., 2011), which is important in models simulating significant drawdown.

4.2 Model Grid and Extent

Quadtree mesh refinement was used over an area of 564km^2 to create a model mesh with 200m x 200m regional grid cells, and refinement to 50m x 50m cells along mapped structures and pit areas (Figure 5), resulting in 78,135 cells per model layer, with 6 model layers giving a total of 468,810 model cells. The option to pinch out layers of less than a certain thickness (a feature of MODFLOW-USG) was not employed in order to facilitate the speed of building model input files using GIS software.

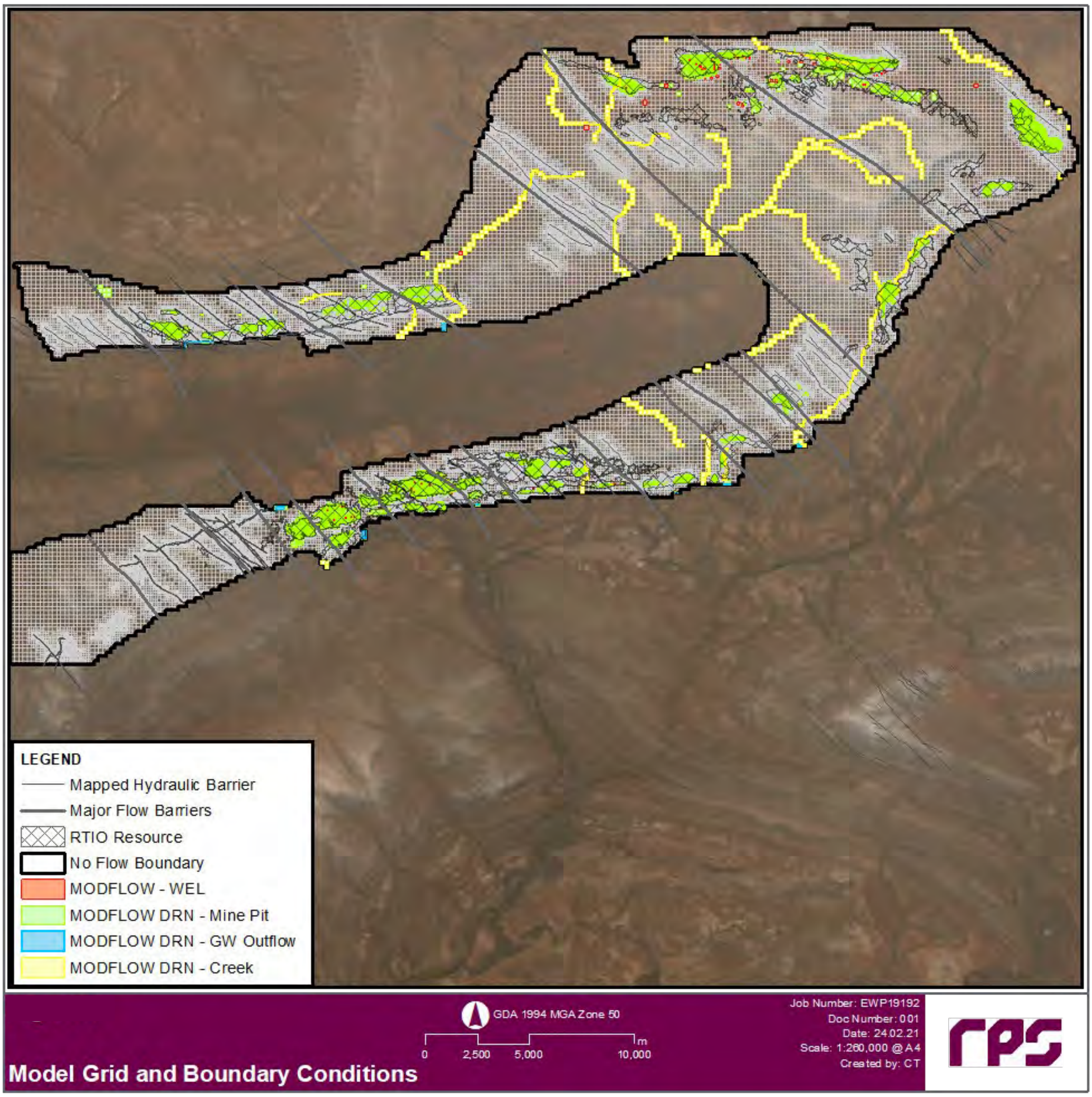

Figure 5 Model grid and boundary conditions

4.3 Layers

The top of model Layer 1 was set using the available digital elevation model DEM derived from LiDAR. The base of Layer 1 was set 2m below the pre-mining water level based on the conceptual understanding that water levels are controlled by dykes that are not present in the regolith/alluvium horizon. The base of Layer 1 extended below the pre-mining water level to match observations in the drillhole data base (with some interpretation of alluvial depth along channels based on nearby data). The thickness of Layer 1 ranges from 2m to approximately 550m (thickest in areas of high elevation due to the significant depth to water). The thickness of Layer 1 (tertiary sediment) that is saturated below pre-mining groundwater level is shown in Figure 6. For simplicity all of model layer one was set as one hydraulic zone in the model, although localised areas of high hydraulic conductivity are known to occur in areas of calcrete and channel iron deposits.

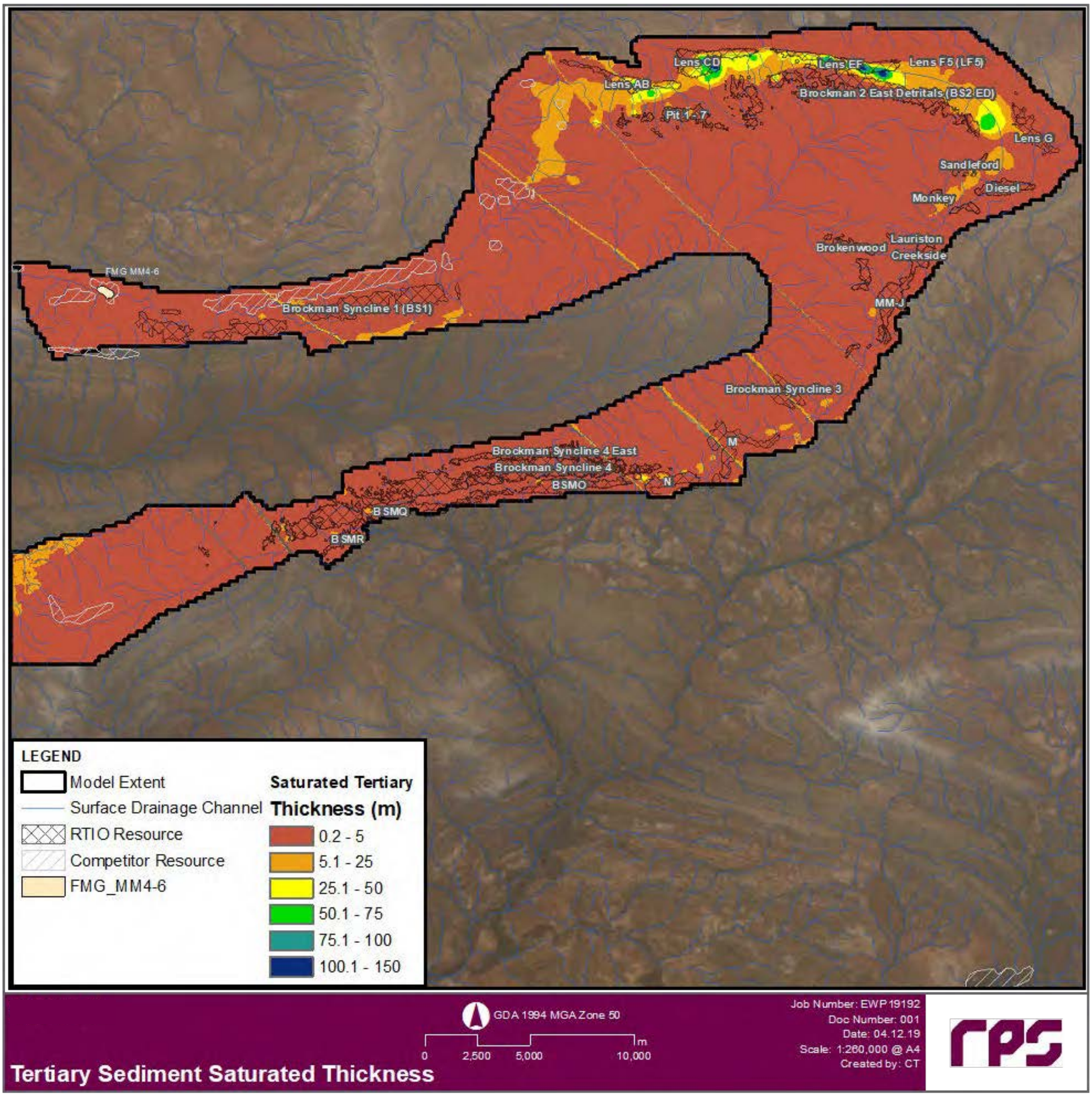

Figure 6 Saturated thickness of model Layer 1

Layers 2 to 6 include BIF, shale and dolerite dykes based on a simplification of mapped geology and structure in Rio Tinto's Leapfrog geological model. Simplified model zonation is shown in Figure 6. Layers 2 to 6 each have a thickness of 40m as shown in Figure 8.

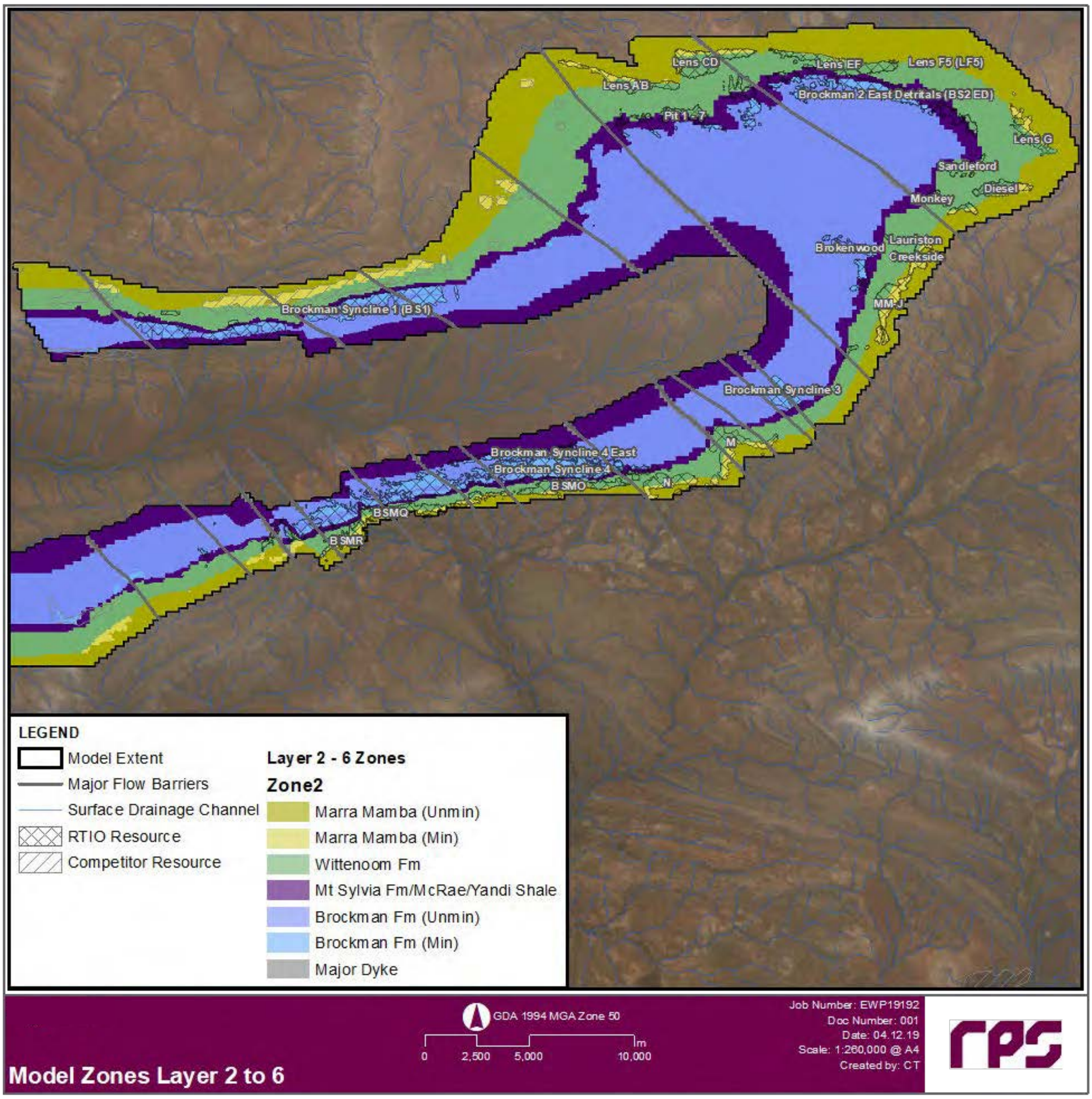

Figure 7 Model parameter zones Layer 2 to 6

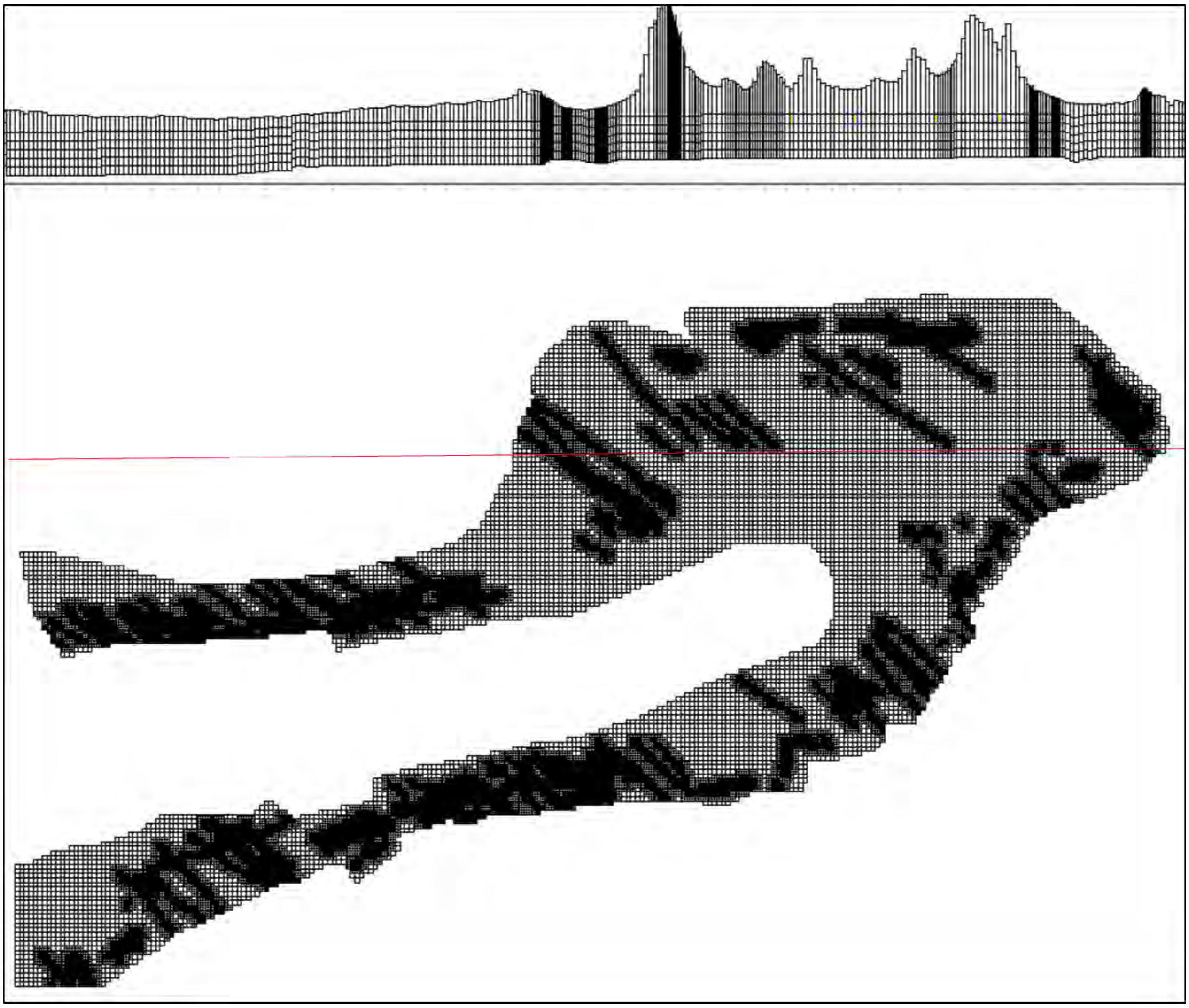

Figure 8 **Example model section showing layer distribution**

4.4 Boundary Conditions

4.4.1 No Flow

A no-flow boundary formed the edge of the model extent and represents the mapped extent of the Jeerinah Formation (outer boundary and stratigraphically below the Marra Mamba Formation) and the Weeli Wolli Formation (inner boundary and stratigraphically above the Brockman Formation), both of which are considered significant regional aquitards.

4.4.2 Drains

The MODFLOW Drain package was used to represent outflow locations at selected alluvial channels (with the drain stage set at the level of the closest pre-mining water level records). The conductance was calculated based on cell dimensions and the hydraulic conductivity of the cell in which the drain was mapped.

Drains were also used to represent surface water creeks (drain stage equal to topography), allowing groundwater discharge only in the event of elevated groundwater levels. However, these drains were largely inactive in the model due to the disconnected nature of surface drainage in the region, except in the locations where specific outflow features where mapped.

The drain package was also used to represent mine pit development over time. The conductance was set to 100,000 m^2/day, which is sufficiently high that there is no restriction to outflow. The drain stage was set to 10m below the proposed pit floor to simulate advanced dewatering to approximately one bench below mining (i.e. normal operational dewatering situation).

4.4.3 Wells

The MODFLOW well package was used to represent advanced dewatering and drawdown from water supply using metered abstraction volumes obtained from Rio Tinto's EnviroSys database.

4.4.4 Recharge and Evapotranspiration

Recharge was set at 1% rainfall only in locations where alluvial material is mapped. Evapotranspiration (ET) was not included in the model due to issues with model stability when included. As ET is expected to occur only in areas of shallow groundwater table (alluvial areas), the applied recharge is considered net of ET. It is likely that recharge only occurs after large or sustained periods of rainfall with subsequent creek flow. Therefore a linear application of 1% rain is considered an oversimplification but being such a minor component of the water balance, detailed analysis of the rainfall duration resulting in recharge is not warranted for this study.

4.5 Model Variants and Timing

Both steady-state and transient model phases have been developed, as summarised in **Table 3**.

Table 3 Model stress period set-up

Model Period	Time
Steady-state model of pre-mining conditions.	Period to January 2008. Model stress period 1
Transient model of the transition from pre-mining to the current state of the BS mines.	January 2008 to end 2019. Model stress periods 2-49.
Transient predictive model extending to and beyond the proposed end of mining, simulating both the proposed mining period and the recovery period.	Early 2020 to 2350. Model stress periods 50-97.

A quarterly (3 month) stress period length was applied in the calibration phase (2008 to 2019). Predictive modelling to the end of mining (2020 - 2050) was simulated with an annual stress period length. Stress periods in the recovery phase were designated annual durations and then increasingly longer into the post-mining recovery phase. This serves to capture finer detail during the early post-mining recovery phase, when groundwater levels recover most rapidly, the rate of recovery slowing with time thereafter. Three time steps per stress period were applied with a time step multiplier of 1.414, providing a mildly increasing time step duration. The MODFLOW-USG option for adaptive time stepping was applied to aid convergence, and hence the number of steps was variable in practice, increasing as required if numerical difficulties were encountered.

Due to the relative speed and functionality of the MODFLOW-USG model, all stress periods are included within a single model run, i.e. steady state in stress period 1, followed by historical transient simulation leading into the transient predictive and recovery phase. Complete model run time ranges from approximately 10 minutes to 45 minutes depending on the hydraulic parameterisation and transient stresses applied.

5 MODEL CALIBRATION

5.1 Steady State Calibration

Limited calibration was undertaken manually in the steady state model with the aim to quickly derive suitable initial heads and support the conceptual model prior to undertaking transient calibration. Due to the lack of seasonal response in observed water levels the degree of calibration was minimal, rather it consisted of iterations of initial head levels and location of outflow areas. Resulting initial head contours are shown in Figure 9 relative to representative pre-mining water levels showing the compartmentalisation between dykes.

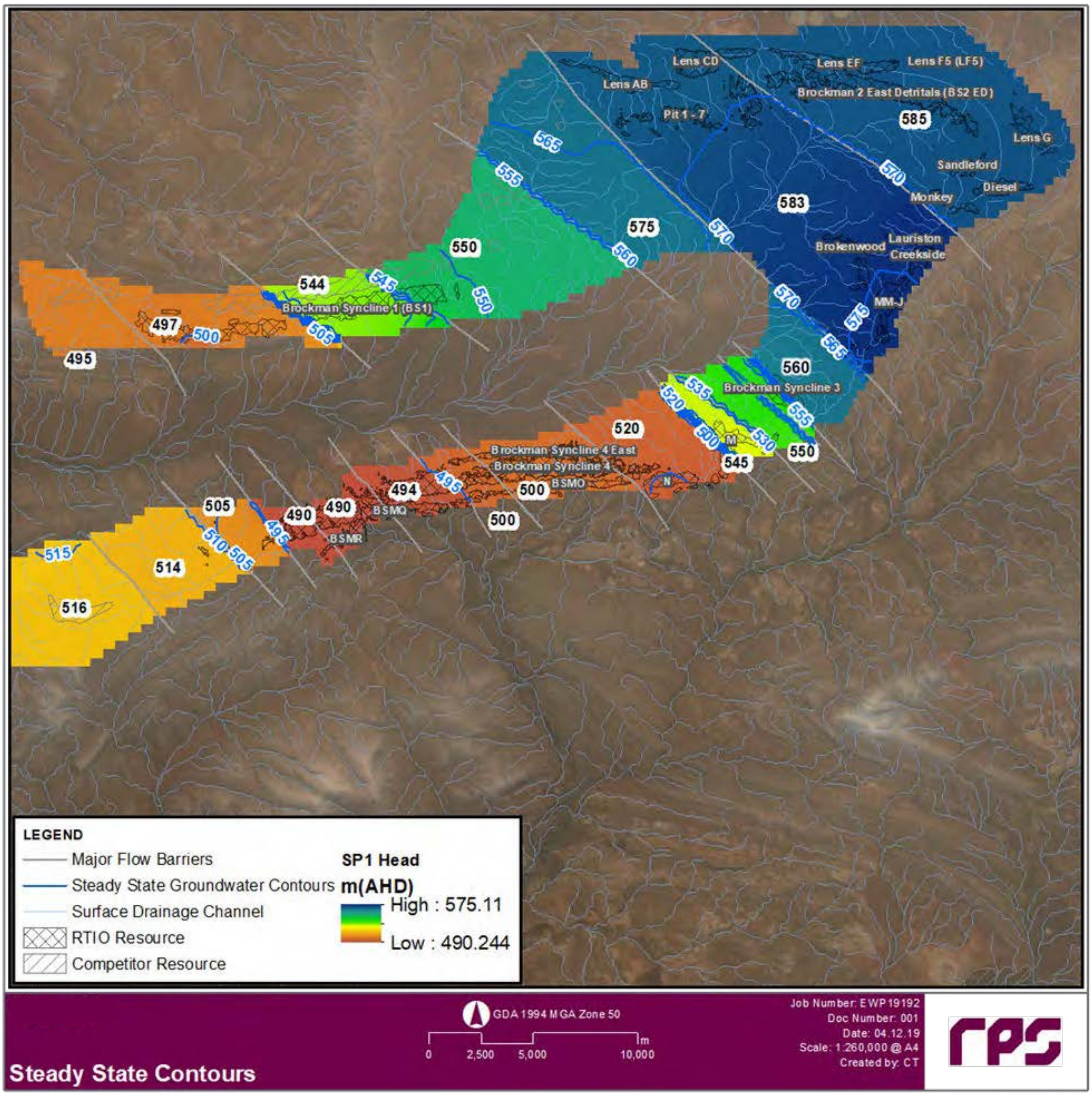

Figure 9 Steady state contours (initial heads)

The SRMS for the steady-state run was 4.9%, which is less than the 5% recommended by Barnet et al., (2012). Graph 1 shows the scatter plot of modelled vs observed groundwater levels.

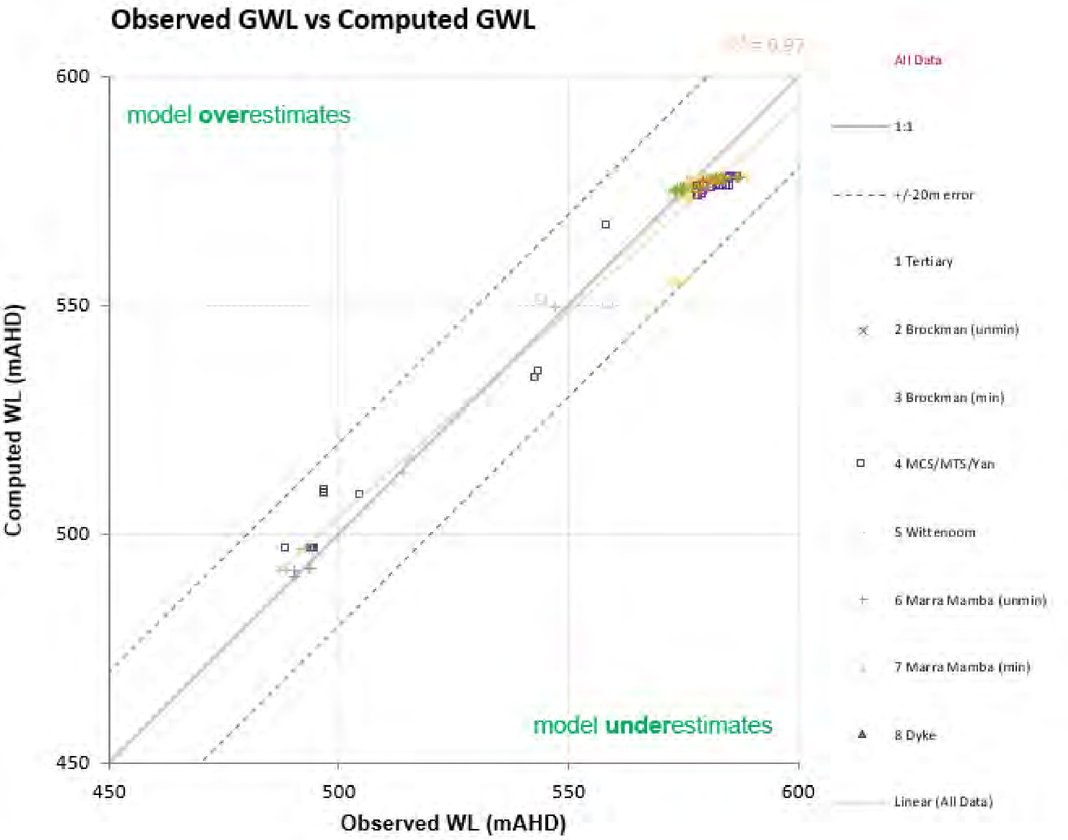

Graph 1 Steady state calibration scatter plot

5.1.1 Steady-State Water Balance

The water balance for the steady-state (pre–mining) model is given in Table 4. Simply put, recharge to the model is in equilibrium with water exiting the model via outflow from connection with alluvium at the specified outflow locations shown in Figure 5. A small balance error of 0.06% exists and is not surprising given the high degree of compartmentalisation in the model. This is well below the 1% error suggested as allowable by Barnett et al,. 2012.

Table 4 Steady state water balance

	Inflow (m^3/day)	Outflow (m^3/day)
Recharge	484.55	-
Drains	-	484.25
Total	484.55	484.25
Error (%)	0.06	

5.2 Transient Calibration

Transient calibration was undertaken both manually and using the automated calibration utility PEST (Doherty, 2010) against measured water levels (taken from Rio Tinto's HydroChart database). The transient model was run with the first period set to steady-state so that the pre-mining water levels were recalculated during each parameter iteration. Final parameters were modified slightly from calibrated values in consultation with Rio Tinto staff and are summarised in Table 5 below. Results presented herein are based on this parameter set.

Table 5 Modelled hydraulic parameters

Model Layer	Geology	Hydraulic Conductivity (m/day)	Specific Storage (m-1)	Specific Yield
1	Regolith	4.4	1x10-6	0.02
2 - 6	Dykes	1x10-7	1x10-6	0.005
2 - 6	Brockman (Unmineralised)	0.1	1x10-6	0.05
2 - 6	Brockman (Mineralised)	1.5	1x10-6	0.05
2 - 6	Yandicoogina Shale / Mt McRae Shale / Mt Sylvia Formation	0.01	1x10-6	0.01
2 - 6	Wittenoom Formation	1	1x10-6	0.05
2 - 6	Marra Mamba (Unmineralised)	0.1	1x10-6	0.05
2 - 6	Marra Mamba (Mineralised)	2.8	1x10-6	0.08

A mean residual of 3.0m and SRMS value of 5.8% suggests transient calibration overall is good. However, the minimum and maximum residual were -54.2 and 55.20m respectively, indicating that significant over and under prediction of water levels occur in some locations. A scatter plot of transient modelled vs observed results is given in Graph 2, and error distribution histogram (Graph 3) in transient calibration hydrographs provided in Appendix B, which suggest that on the whole drawdown trends from dewatering are represented in the model but several locations where not able to be well matched using the current model set-up. This is likely to be a combination of the coarse scale grid and simplification of applied geology (which is not able to account for localised heterogeneities), plus uncertainty in applied abstraction rates where data records were erroneous (as discussed in Section 4.4.3). Spatial representation of the average residual at each target location shows that generally areas where the model levels are too high (negative residuals) are close to areas where levels are too low (positive residuals). Modelled heads in most areas to be mined below water table are considered to be well represented overall (Figure 10).

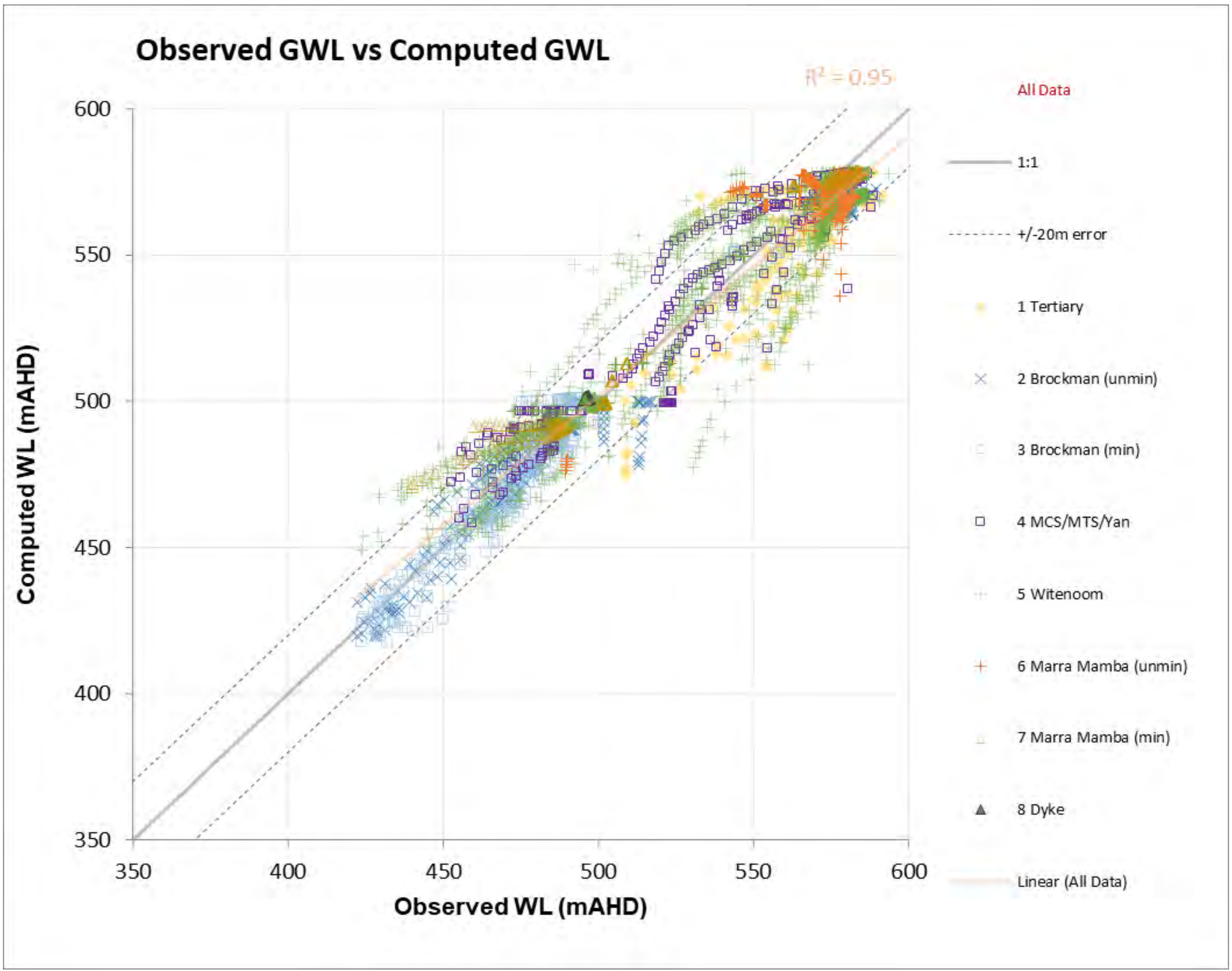

Graph 2 Transient calibration scatter plot

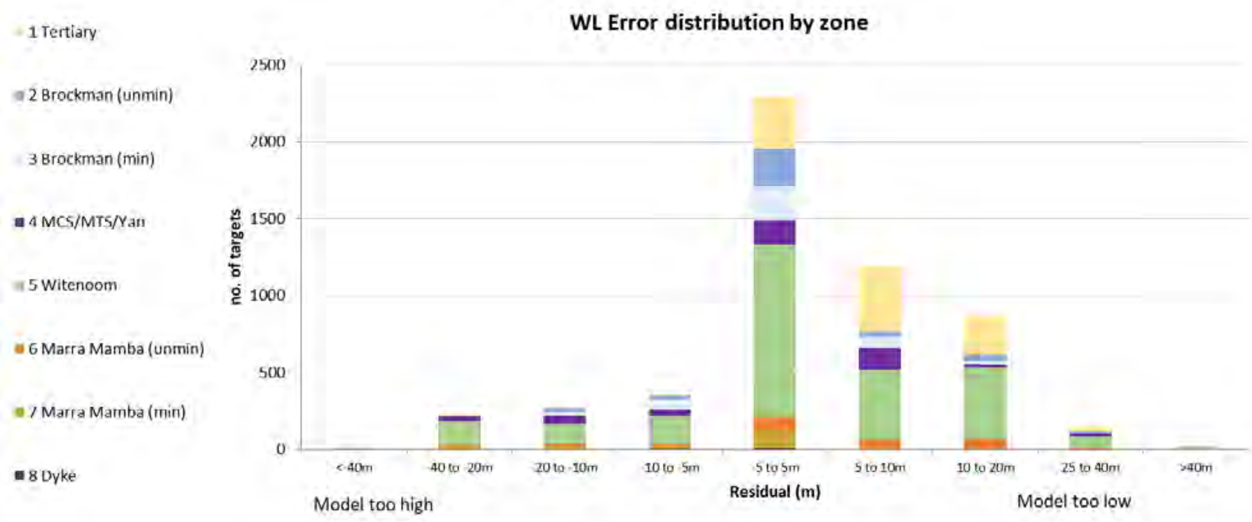

Graph 3 Transient calibration error distribution

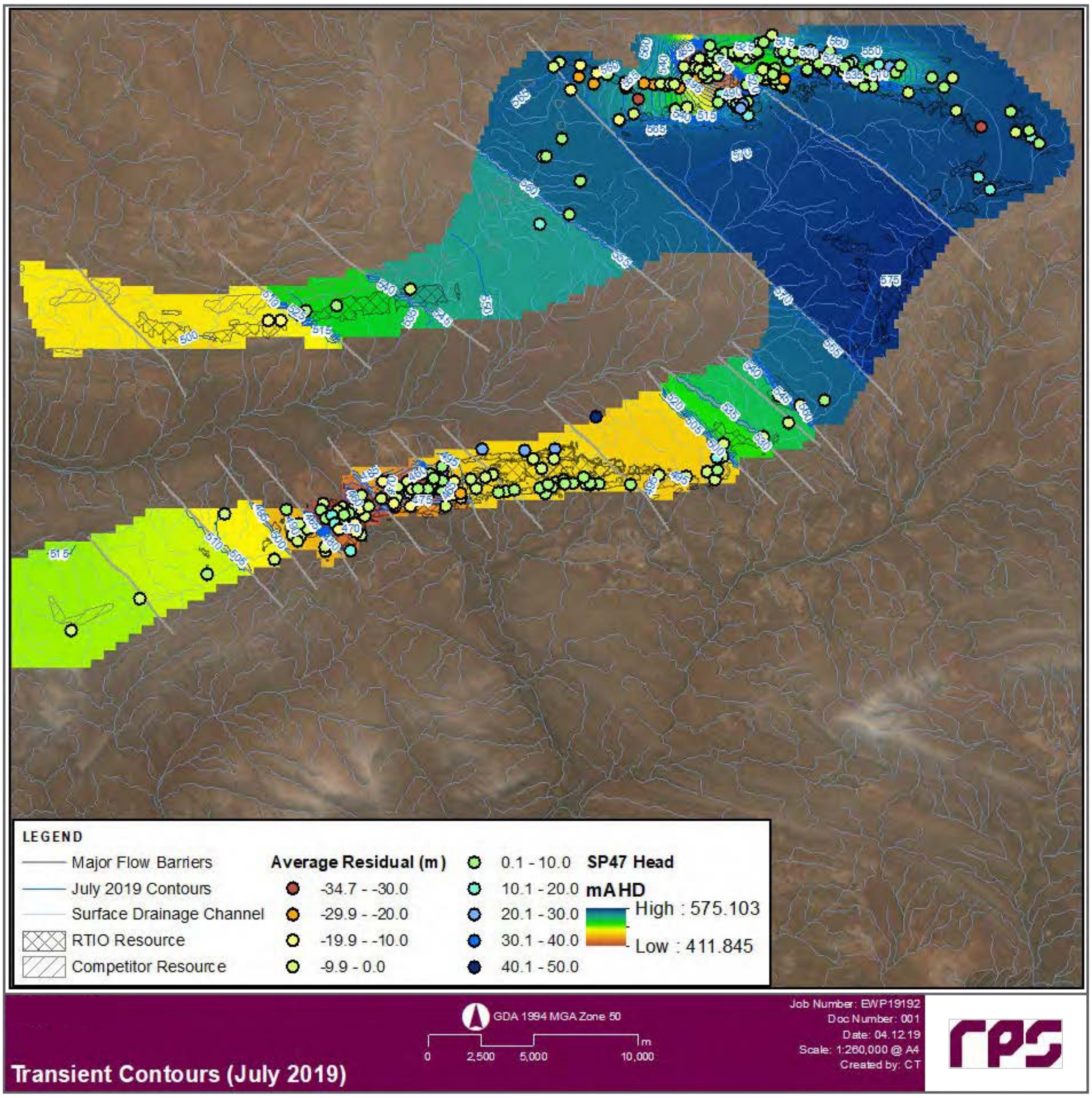

Figure 10 Transient contours (at July 2019)

5.2.1 Water Balance

The water balance to the transient calibration period (July 2019) is presented in Table 6 below. The water balance shows that dewatering due to mining activities (wells and drains) dominates the water balance, with dewatering draining the aquifer storage (>99% of the water balance) with comparatively very little volume of recharge occurring to the system.

Table 6 Transient water balance

	Inflow (m^3/day)	Outflow (m^3/day)
Recharge	456	
Drains	0	2,173
Wells	0	24,450
Storage	26,873	706
Total	27,329	27,329
Error %	0.00	
Change in Storage	261,670	

Groundwater abstraction simulated by the groundwater model for the period between 2016 to 2018 was compared to reported values in the 2018 Triennial Aquifer Reviews (Rio Tinto, 2019a,b). On average the model is simulating between 80-90% of the reported dewatering volumes at the Nammuldi Lens CD and Lens EF deposits, and the combined volumes from multiple pits and dewatering borefields at Brockman Syncline 4. Graph 4 shows the actual vs simulated dewatering at each site. This slight underestimation in inflows is likely to be due to the model having a bias towards simulating modelled water levels that are too low. Therefore, predicted future volumes should be viewed with a minimum 20% increase when planning for water management.

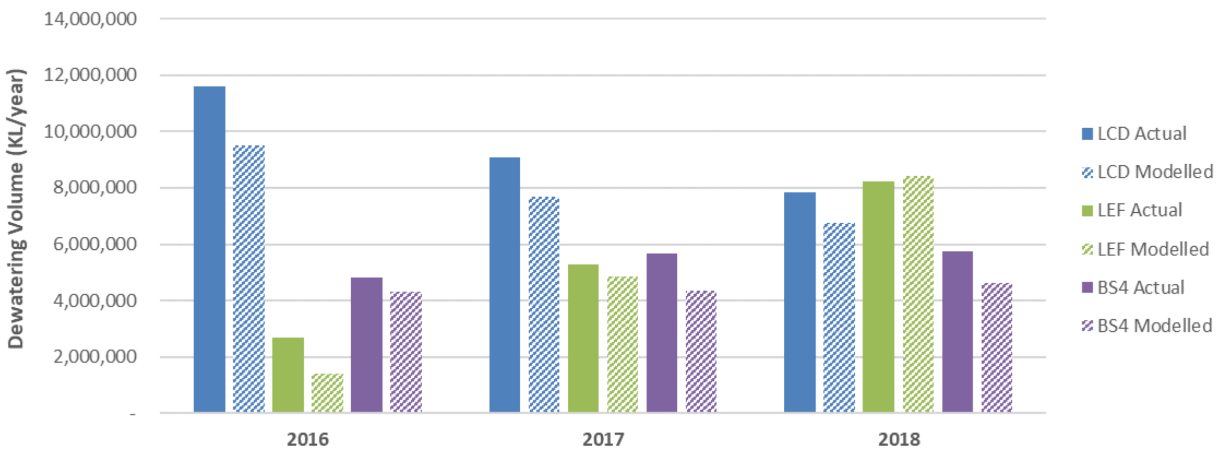

Graph 4 Actual vs modelled dewatering

6 ASSESSMENT OF MODEL PERFORMANCE AND LIMITATIONS

6.1 Model Confidence Level

Under the MDBC (2001) modelling guideline, the model is best categorised as an Impact Assessment Model of medium complexity. That guide (MDBC, 2001) describes this model type as follows:

> *"Impact Assessment model - a moderate complexity model, requiring more data and a better understanding of the groundwater system dynamics, and suitable for predicting the impacts of proposed developments or management policies."*

The most recent modelling guideline (Barnett *et al.*, 2012), developed a system to further classify the confidence level for groundwater models. Models are classified as Class 1, Class 2 or Class 3 in order of increasing confidence based on key indicators such as available data, calibration procedures, consistency between calibration and predictive analysis, and level of stresses. Under these guidelines, this model would be classified as a Confidence Level 2 (Class 2) groundwater model, with the following key indicators (based on Table 2-1 of Barnett *et al.*, 2012):

- Daily rainfall and evaporation data are available (Level 3 – higher than Level 2).
- Groundwater head observations and metered abstraction volumes are available with reasonable coverage around ore deposit locations, but without spatial coverage throughout the full model domain (Level 2).
- Scaled RMS error and other calibration measures are acceptable (Level 2).
- Suggested use is for prediction of impacts of proposed developments in medium value aquifers (Level 2).

6.2 Limitations

While MODFLOW-USG has allowed the use of quite fine model resolution in many areas of interest, the scale of model cells (50 m laterally around the pits) limits the ability to accurately simulate some behaviours and features, particularly where hydraulic gradients are steep, such as near to open cut pits and wells.

Simplified geology has been applied in the model, with known members of high/lower conductivity, generalised into a single zone for each. This is likely to have the most significant impact on model results in the Wittenoom Formation where the Paraburdoo Member often has a substantially higher hydraulic conductivity than its neighbours, and in locations where proposed pits come into contact with saturated shallow sediments (e.g. channel iron deposits and calcrete) that may result in localised areas of substantially increased inflow. Parameter sensitivity results for early model runs indicated that the permeability of CID and calcrete were important in matching modelled and observed heads. Future models with the purpose of dewatering design optimisation should consider these zones as they have the potential to have a significant impact on the timing and volume of dewatering at nearby pits.

Not all mapped structures (dykes and faults) are included, only those that appear to induce a significant change in water level across strike. Minor features may also have a controlling influence of groundwater flow within the syncline.

There is poor understanding of the depth of Tertiary material away from near pit exploration areas that may influence groundwater connectivity across the syncline (particularly as the base of the Tertiary represents to top of the dykes on the model).

Bore abstraction data was applied in each model stress period at the rate indicated by available flowmeter records in EnviroSys. However, there are several instances when this data appeared erroneous (potentially due to flowmeter malfunction/replacement etc). Where the flow rate was clearly incorrect this was manually adjusted by inferring a flow rate. However, occasional short-term irregularities in calibration hydrographs suggest there may be instances where these errors went undetected for an extended period and/or the inferred rates are not representative of actual historical abstraction. Parameter calibration was largely based on the water level response to dewatering abstraction so any erroneous abstraction volumes will have negatively affected calibration. It is considered the overall trends are adequate given the limitations resulting from a coarse regional grid and other simplification as discussed above, and broad uncertainty in predictions related to parameterisation are covered in uncertainty analysis.

The pit design, timings and closure landforms are likely to vary from what has been modelled for future scenarios as the short-term planning is expected to be optimised on an on-going basis commensurate with current mining conditions. Depending on the magnitude of changes this is likely to not only affect the timing of predicted dewatering volumes but may also affect the overall amount, as the timing of the interaction of drawdown resulting from dewatering of adjacent pits has the ability to significantly affect the volume of dewatering required at each location, particularly for shallower pits.

No inclusion of any surplus water management options were included in the modelling upon agreement with Rio Tinto staff. Other locations in the Pilbara where surplus water management includes discharge to surface drainage, infiltration or injection have resulted in some recirculation of dewatering that has the potential to result in increased pit inflows. This has the potential to occur here if surplus water is disposed of within the Brockman Syncline.

7 PREDICTIVE MODELLING

The following section outlines the predictive scenarios run to inform the assessment of cumulative impacts and effects on the groundwater system from the various mines within the Brockman Syncline, including the nearby FMG Eliwana MM4-6 below water table mine pit and potential water supply borefield at Flying Fish.

7.1 Modelling Approach

Three main predictive model scenarios were run:

1. A 'No-mining' or 'Null' run (as per Barnett et al, 2012), without any past or future mining. Hereafter referred to as the 'Null' run or condition.

2. The 'RTIO only' run, i.e. a run with the proposed mine schedule and closure plan, for RTIO pits only. Throughout the report discussion this is simplified to "without FMG".

3. The 'Cumulative run', i.e. a run with RTIO mining as per scenario 2 and inclusive of proposed below water table mining and water supply abstraction at FMG's Eliwana mine. Throughout the report discussion this is simplified to "with FMG".

Comparison of these three runs then allows a cumulative impact assessment to be carried out. Due to the significant number of pits to be mined, individual model runs for each pit/mine area were not undertaken to assess the individual impact relating to each pit.

All models used the calibrated historic period, as described in Section 5, as a run-in precursor to the predictive simulation period. The 'Null' run that did not include any historical or future mining in the area.

7.2 Predicted Pit Inflows

Predicted daily inflow rates for individual Nammuldi/BS2 hub pits are shown in Graph 5, and cumulative inflows in Graph 6. Maximum predicted daily inflow is approximately 30ML/day at Lens EF in 2020. Life of mining dewatering across the Nammuldi hub is predicted to be in the order of 425 GL. Lens CD and Lens EF are expected to be the dominant contributors to total dewatering volume (totalling around 70% of cumulative inflow volumes) until the end of mining in 2050.

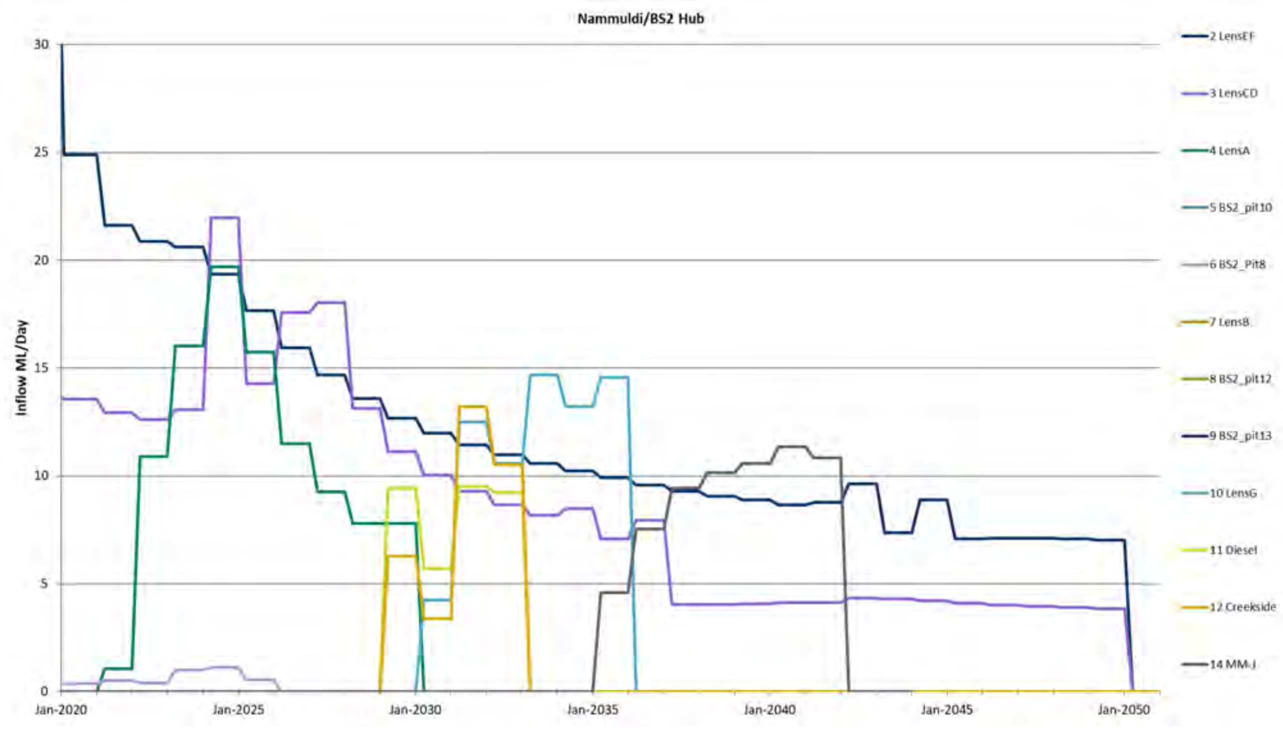

Graph 5 Predicted inflow rate – Nammuldi/BS2 hubs

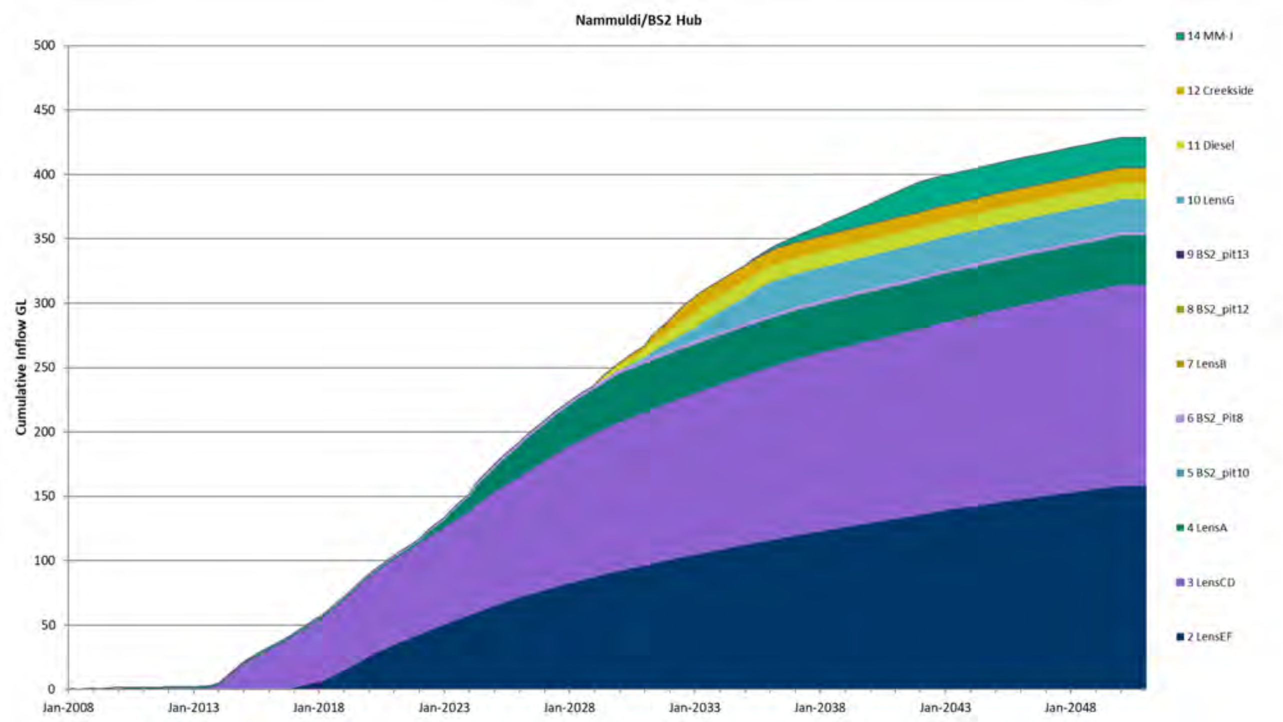

Graph 6 Predicted cumulative inflow – Nammuldi/BS2 hubs

Predicted BS4 hub daily inflow rates for individual pits are shown in Graph 7, and cumulative inflows in Graph 8. Under the current mine plan, the highest short-term inflows are expected from Pit 18 (approximately 11ML/day). Cumulative inflows over the life of mining total approximately 145 GL. Approximately 60% of the overall dewatering volumes are predicted from BS4 main area (Pits 2 and 5 combined, Pits 3 and 4 combined, Pit 11and Pit 18), 20% from the BS1 area and the remainder from the BSMM and BSMN areas.

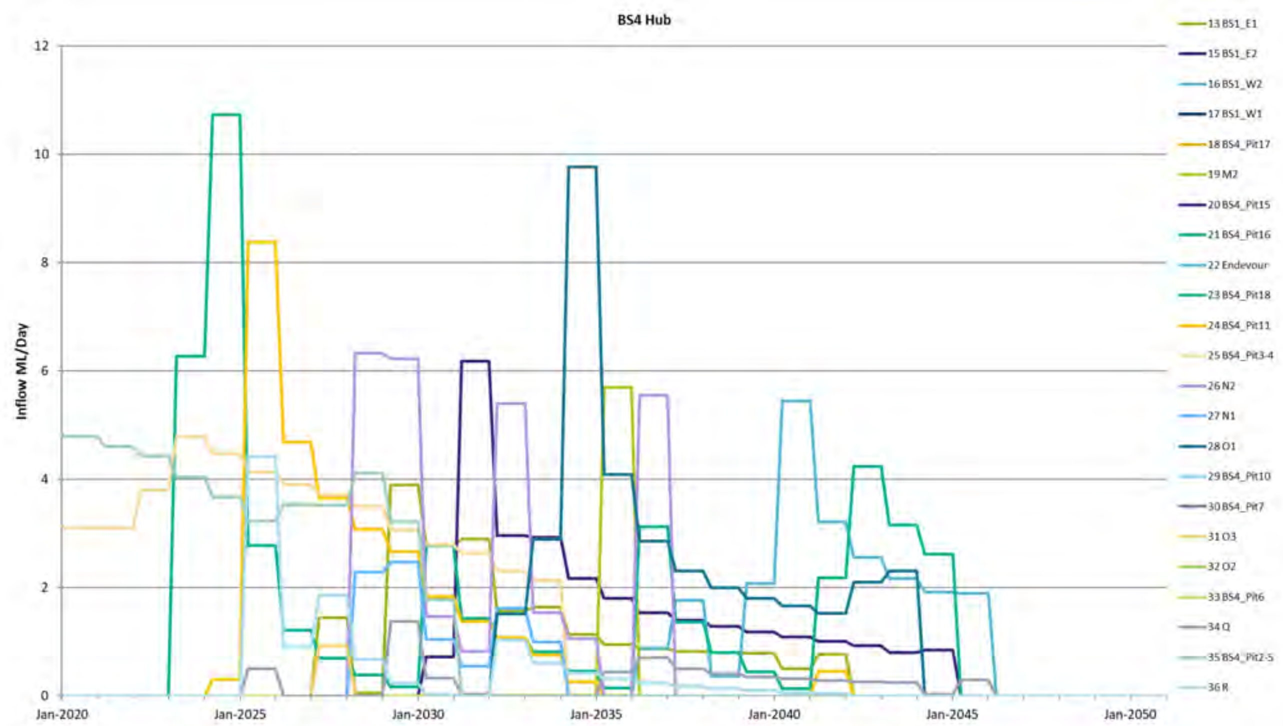

Graph 7 Predicted inflow rate – BS4 hub

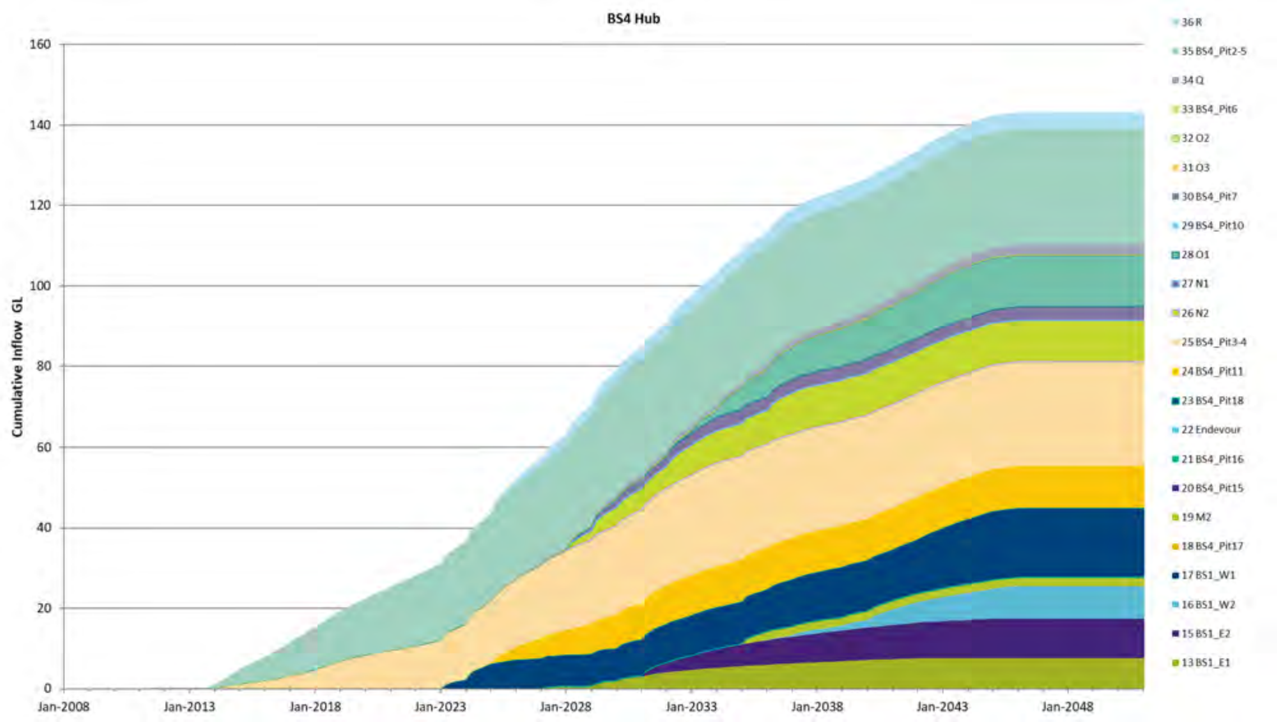

Graph 8 Predicted cumulative inflow – BS4 hub

Table 7 provides the total predicted dewatering volume by hub (GL/year) from 2020 onwards. Predicted annual dewatering volumes within the Nammuldi hubs are predicted to ramp-up to approximately 23 GL/year over the coming five to ten years, decreasing to around 4 GL/year towards the end of mine life. Within the Brockman 4 hub peak dewatering volumes of up to 9 GL/year are predicted, with the greatest dewatering volume currently forecast for the period 2024 to 2029.

Table 7 Predicted annual dewatering by hub

Year	NAM/BS2 (GL/yr)	BS4 (GL/yr)
2020	14.2	2.9
2021	13.2	2.8
2022	16.3	3.0
2023	18.5	5.5
2024	22.7	7.0
2025	17.6	8.6
2026	16.4	5.2
2027	15.3	5.8
2028	12.6	7.5
2029	17.3	8.5
2030	12.9	5.7
2031	20.4	5.8
2032	18.2	6.8
2033	12.2	5.2
2034	11.6	5.6

Year	NAM/BS2 (GL/yr)	BS4 (GL/yr)
2035	13.2	4.9
2036	9.1	5.8
2037	8.3	3.1
2038	8.5	2.1
2039	8.6	2.5
2040	8.8	3.4
2041	8.7	3.5
2042	5.1	3.7
2043	4.3	3.2
2044	4.8	2.0
2045	4.1	0.8
2046	4.1	0.0
2047	4.0	0.0
2048	4.0	0.0
2049	4.0	0.0
2050	0.0	0.0

7.3 Predicted Water Levels

Due to the different timing of completion of mining within the various pits across the Brockman Syncline, the timing of the minimum water level at each location is variable. The overall predicted minimum water level over the complete duration of mining (with FMG) is presented in Figure 11 and minimum water levels without FMG in Figure 12. Transient hydrographs of the water level at each pit location are presented in Appendix C. The lowest water levels occur at BS4 Pit 2 (around 320mAHD) and Nammuldi Lens CD (350mAHD). The hydrographs in several of the shallower pit locations show that the drawdown in the vicinity of these pits continues to develop below the pit floor over time as the cone of depression induced from the adjacent larger, deeper pits continues to propagate regionally.

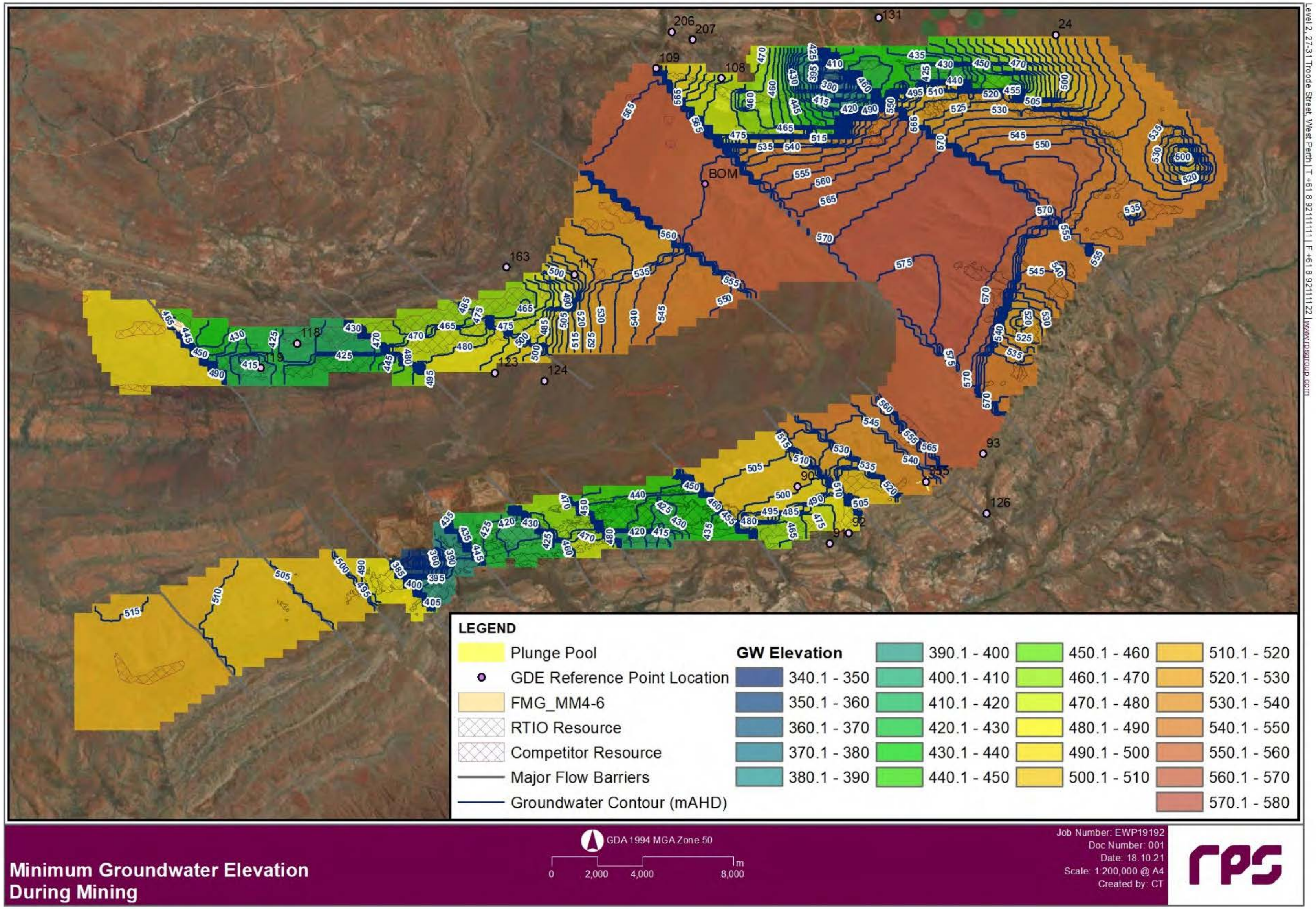

Figure 11 Minimum predicted groundwater level during mining with FMG (to 2050)

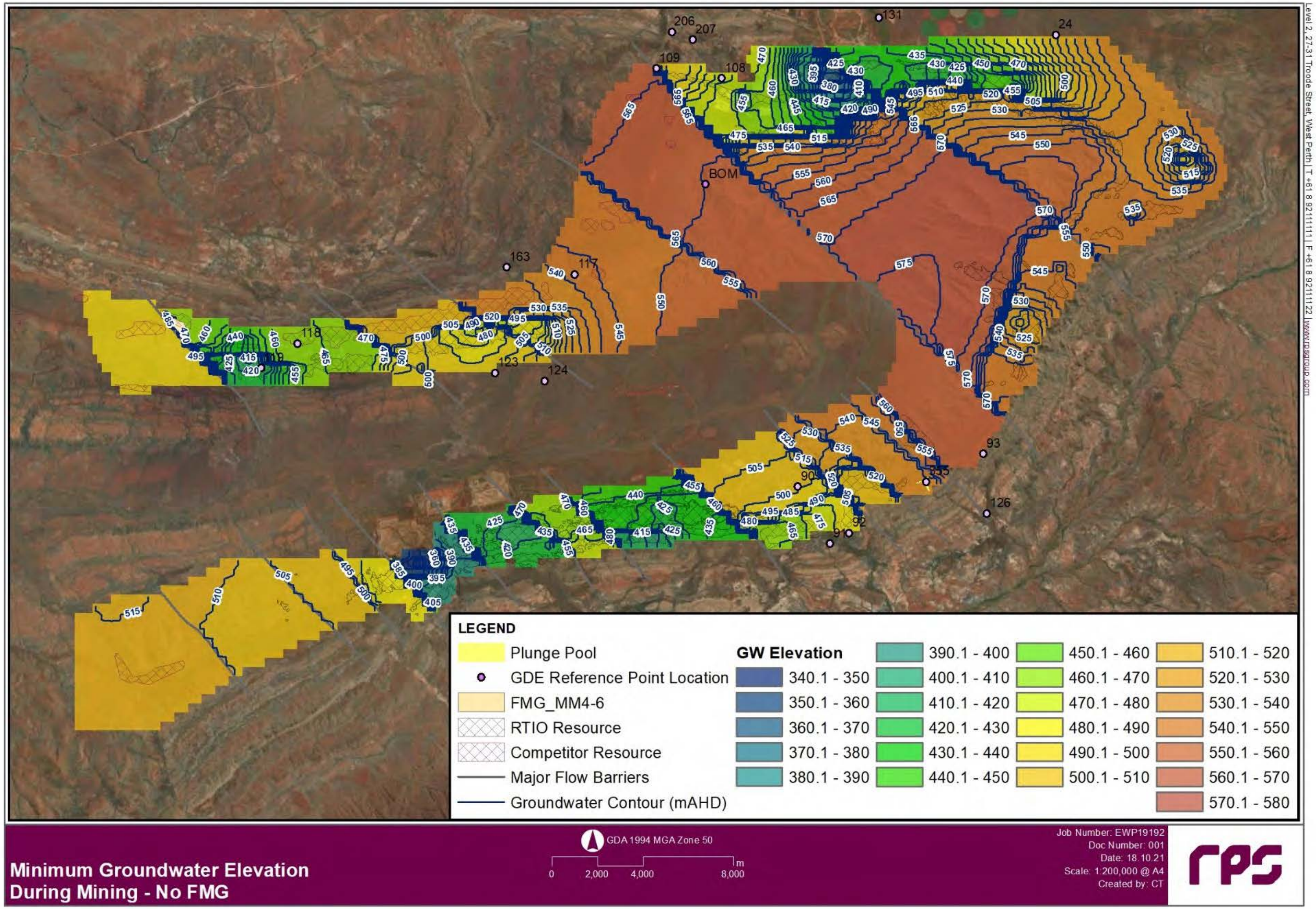

Figure 12 Minimum predicted groundwater level during mining without FMG (to 2050)

7.4 Post-Closure Recovery

Groundwater recovery was simulated for the proposed closure scenario outlined in Section 3.1.2. It is important to reiterate that the recovery groundwater levels simulated within the pit extent under the open void condition *do not* represent a potential pit lake surface, rather the model can only be used in this regard to obtain an estimate of the rate of groundwater inflow into each pit at a given lake stage, taking into consideration the interaction of drawdown between nearby pits. Additional work is required to develop a pit lake water balance model that includes components of lake evaporation, direct rainfall, pit wall runoff, surface water runoff etc. Groundwater levels simulated within the backfilled pits are considered appropriate to represent the likely recovery of groundwater within the pit footprint post-mining, with the assumption that appropriate closure bunding is in place to prevent significant influx of surface water runoff to the pit.

Regional groundwater levels predicted at 2350 under the proposed closure scenario with FMG mining are presented in Figure 13, and without FMG in Figure 14. Groundwater recovery hydrographs are presented in Appendix D for pits that a proposed to remain as open voids and Appendix E for those proposed to be backfilled. None of the pits are expected to recover to pre-mining groundwater levels by 2350 due to the very low rate of groundwater recharge within the Brockman Syncline.

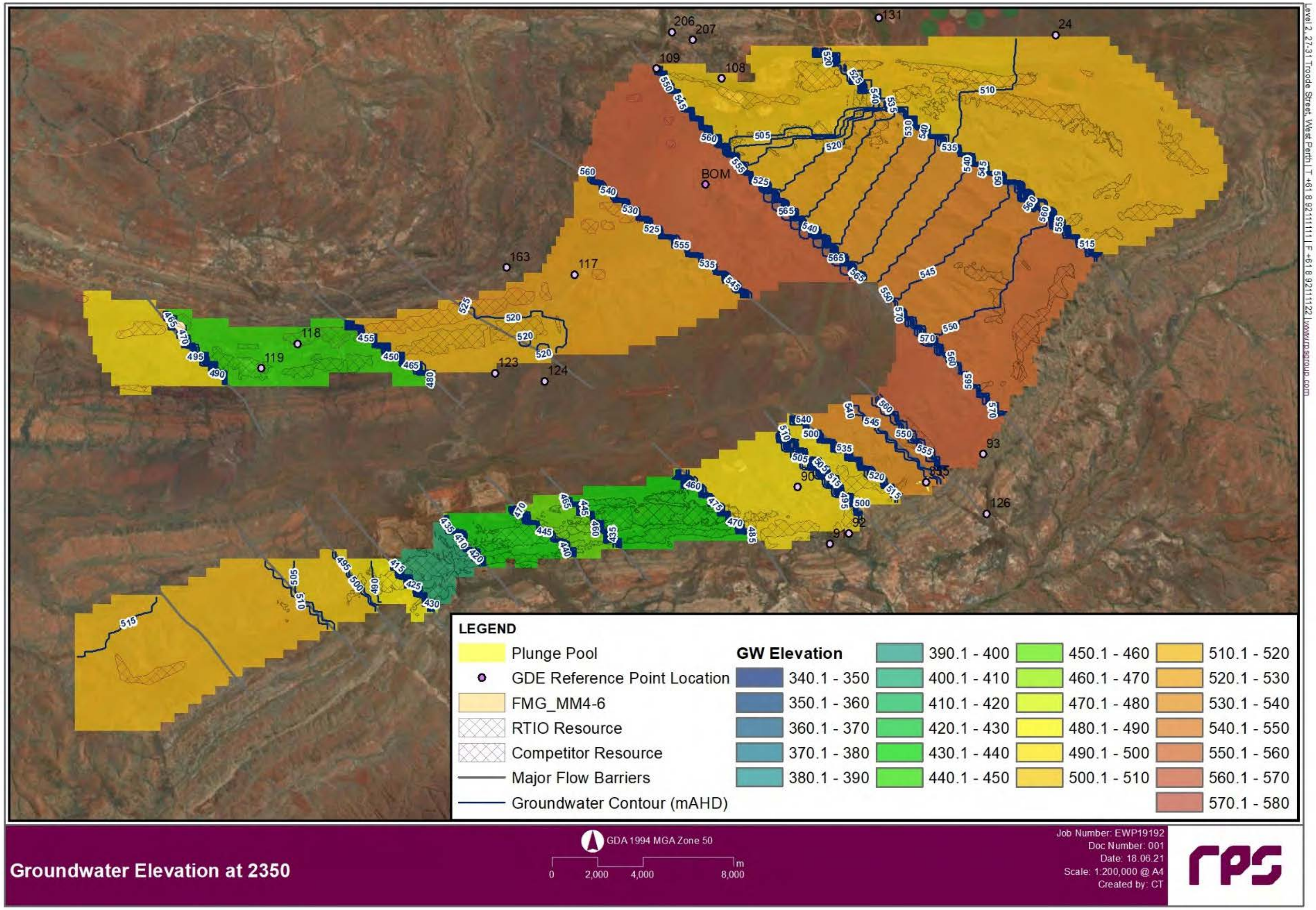

Figure 13 Recovered groundwater level at 2350 with FMG

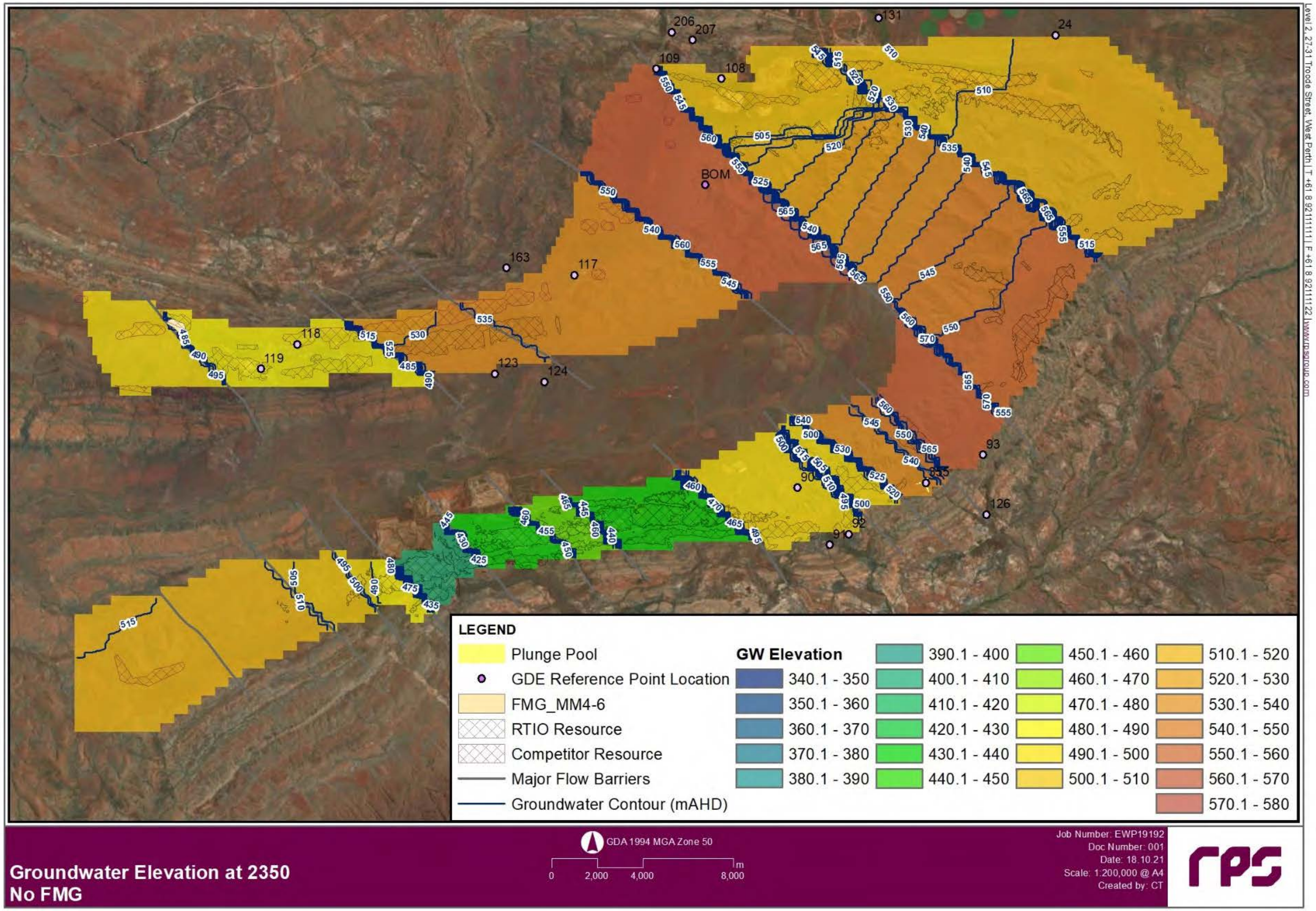

Figure 14 Recovered groundwater level at 2350 without FMG

8 POTENTIAL IMPACTS ON THE GROUNDWATER RESOURCE

This assessment of potential impacts to the groundwater resources of the Brockman Syncline focuses on the following criteria:

- Licensable takes of water for the purpose of dewatering.
- Water table drawdown.
- Impacts to other groundwater users.
- Impacts to water quality.

8.1 Licensable Takes of Water

Rio Tinto currently holds groundwater extraction licenses within the Brockman Syncline:

Nammuldi/BS2/Silvergrass East - GWL107421 55GL/annum

Brockman 4 – GWL164398 13GL/annum

Maximum predicted dewatering volumes

Table 8 Maximum predicted annual dewatering volume by hub

Hub	Maximum Predicted Dewatering Volume (GL/yr)	Year of Maximum
Nammuldi/BS2[1]	22.7	2024
BS4	8.6	2025

[1] Does not include Silvergrass East

Based on the predictive modelling, Rio Tinto currently hold sufficient licence entitlement to cover the modelled groundwater abstraction at BS4 and Nammuldi/BS2 (assuming dewatering at Silvergrass East does not exceed 32GL/year).

8.2 Groundwater Drawdown

As mining progresses, the dewatering of open cut pits will result in a cone of depression and cause a reversal of groundwater flow direction towards the pits. In the long term (post mining) open voids will continue to act as groundwater sinks, resulting in continued propagation of the cone of depression away from the pits. Pits that are backfilled will result in less long-term drawdown than open voids due to limited evaporation. However, due to the low rainfall recharge and lack of throughflow from neighbouring aquifers the time taken for the groundwater levels to return to circa pre-mining levels is expected to be several hundreds of years.

Drawdowns are naturally restricted from developing to a regional extent as a result of low permeability barriers in the form of dykes, and aquitard units (Jeerinah FM at the outer syncline extent, Weeli Wolli Fm at the inner extent, as well as internal low permeability units (Mt McRae Shale and Mt Sylvia Fm). The maximum regional drawdown due to mining at the end of mine life (2050) is shown in Figure 15 with FMG and Figure 16 without FMG. It is important to note that this does not represent an individual snapshot in time, rather the maximum drawdown that occurs in any given location for the duration of mining (up to 2050). Predicted long term drawdown (at 2350) for the with and without FMG scenarios are shown in Figure 17 and Figure 18 respectively. The extent of long-term drawdown exceeds that at the end of operations due to the pit voids continuing to act as sinks. If significant recharge occurs though high permeability channel sediments or major surface runoff events occurs (e.g. a major cyclone event) there is potential for the short-term level in pit voids to exceed that of the surrounding groundwater, whereby pits may become localised throughflow systems.

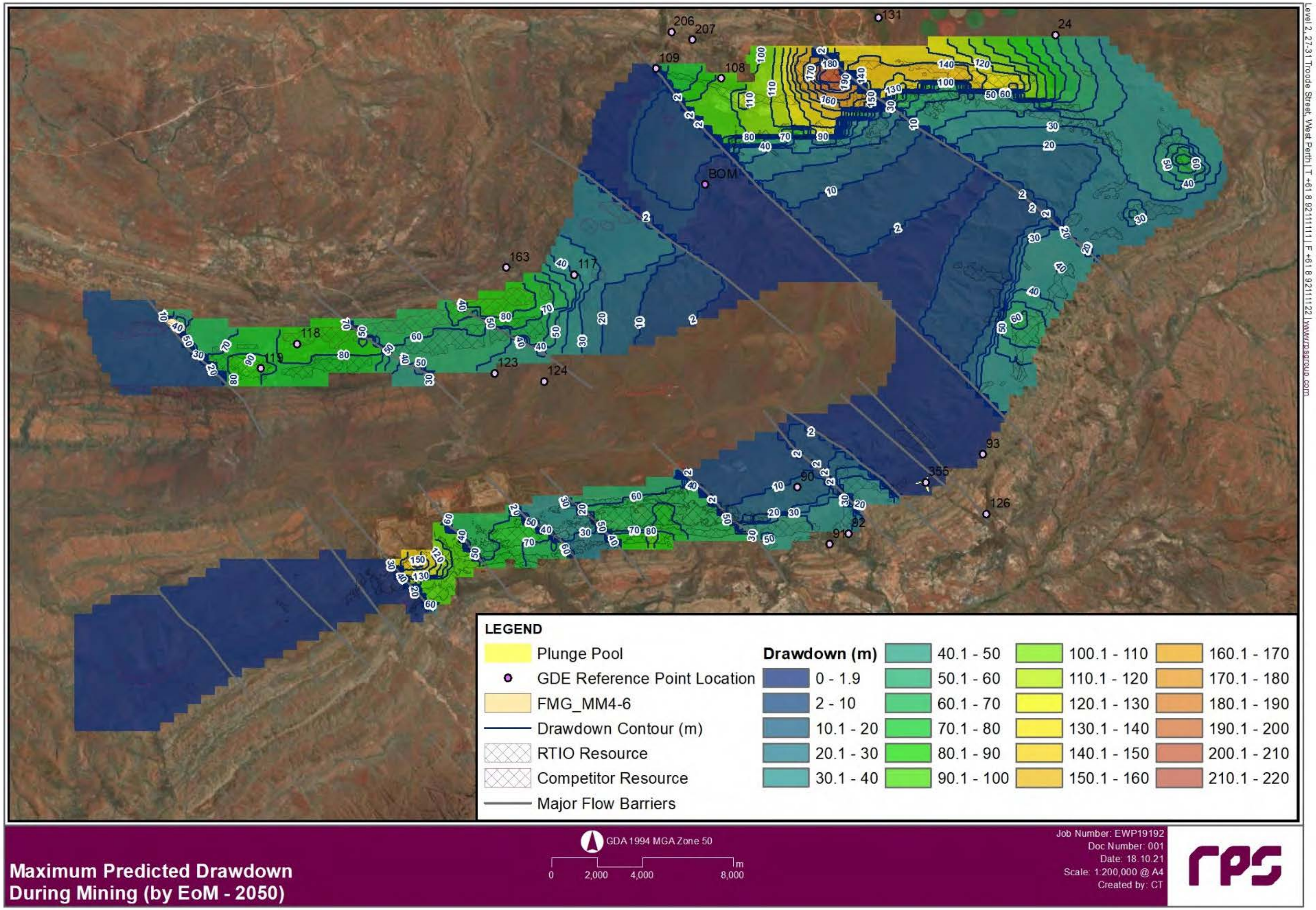

Figure 15 **Predicted maximum drawdown at end of mining with FMG**

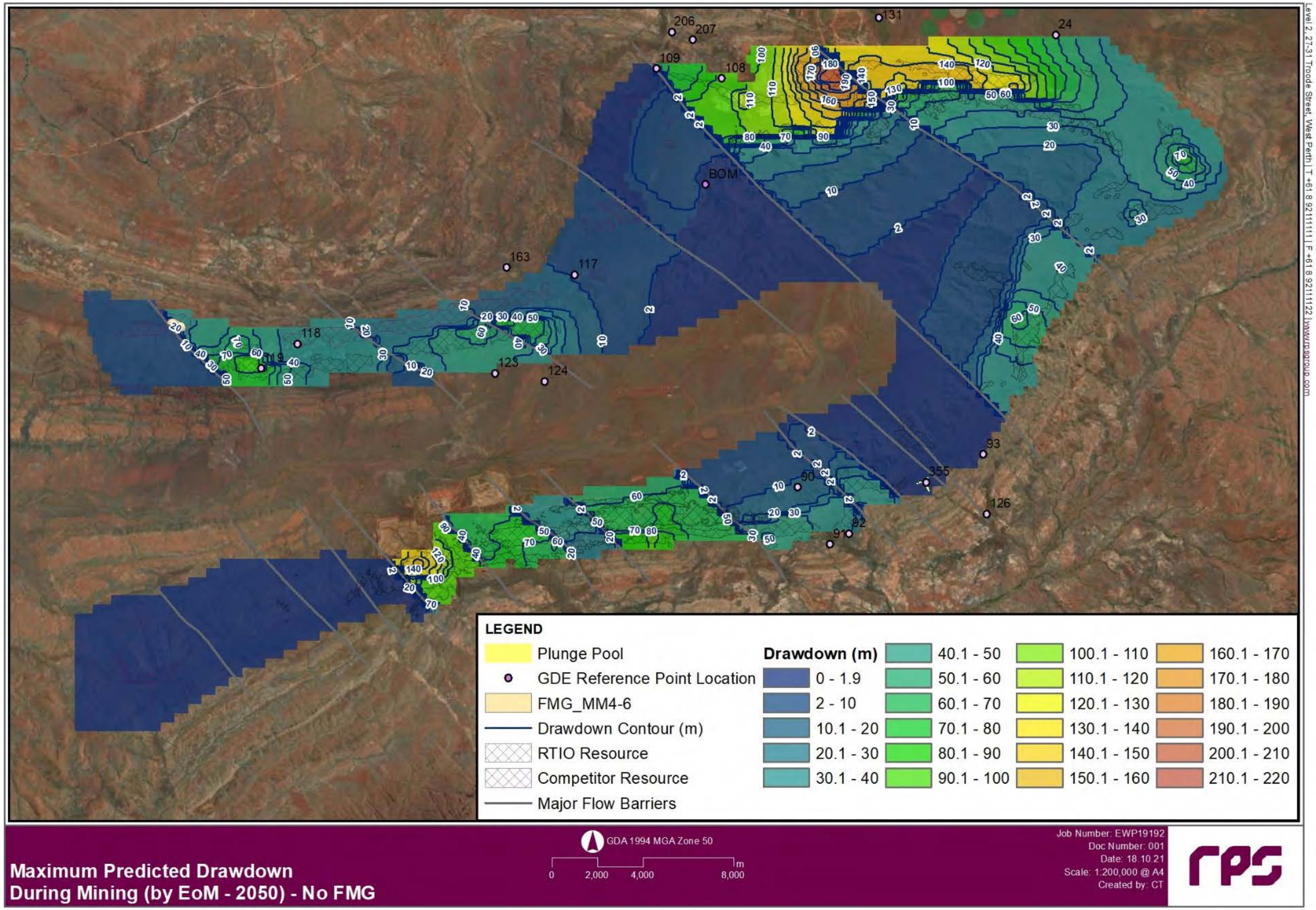

Figure 16 Predicted maximum drawdown at end of mining without FMG

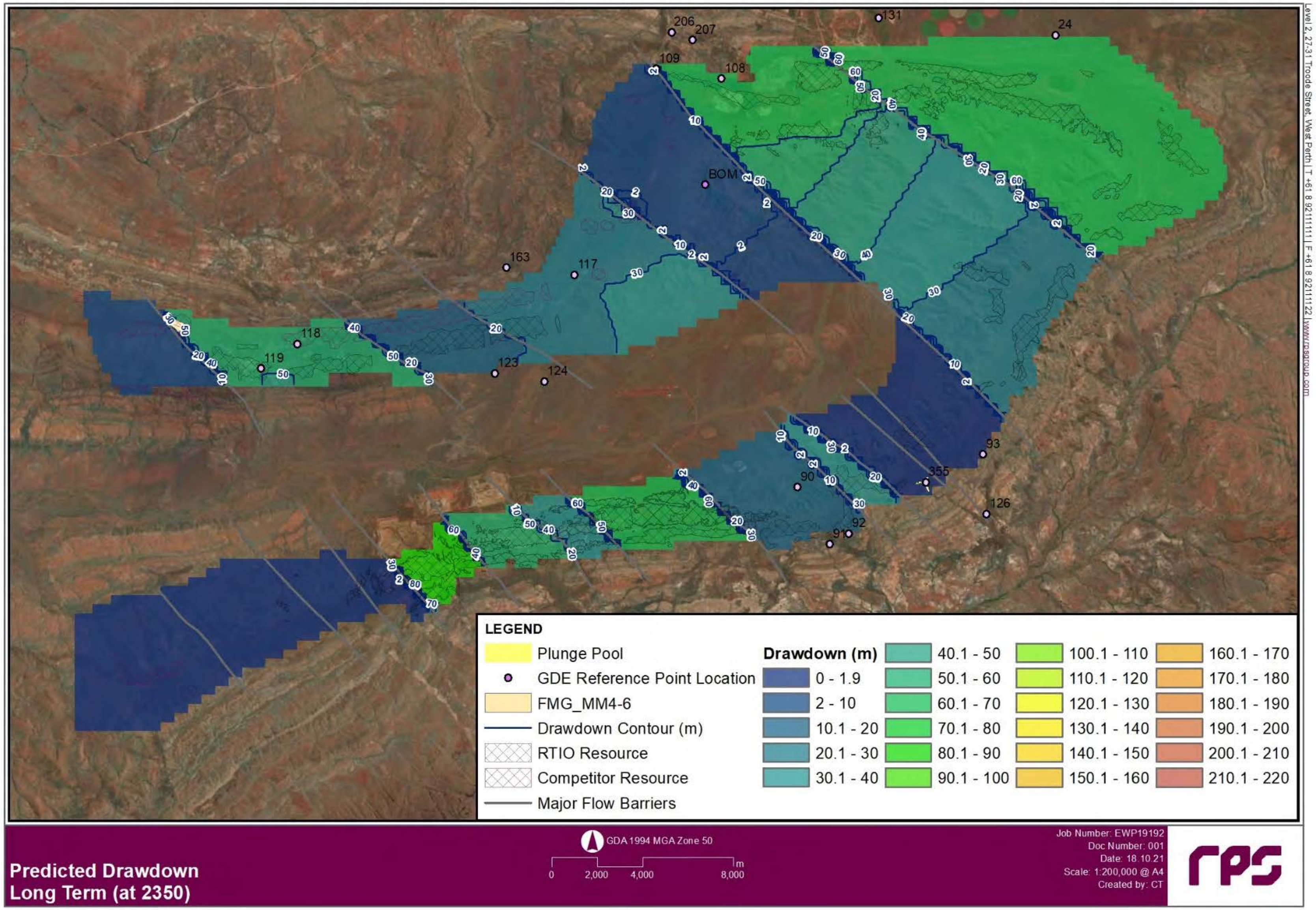

Figure 17 Predicted long term drawdown with FMG

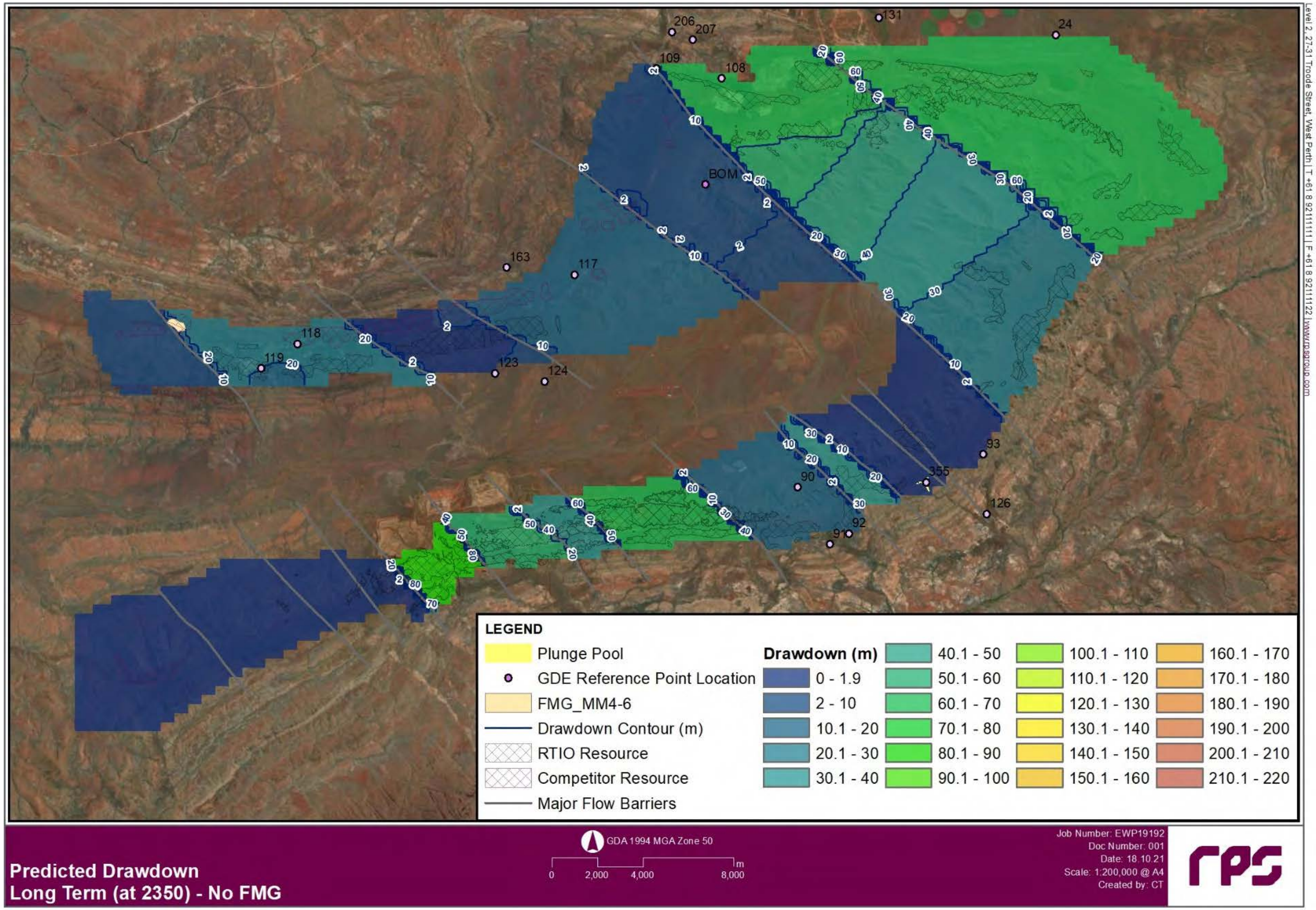

Figure 18 Predicted long term drawdown without FMG

8.3 Other Groundwater Users

According to the DWER Groundwater Register there are no registered water supply bores within the Brockman Syncline that are not operated by Rio Tinto. However, FMG also holds several groundwater licenses within the north-western limb of the syncline. Drawdown from the FMG and Rio Tinto operations have the potential to overlap at the BS1 mining area which may affect the pit inflow and/or bore abstraction rates at both operations. This model simulates the cumulative drawdown inclusive of the potential water supply borefield at FMG's Flying Fish deposit and mining of the MM4-6 deposit north of BS1 but does not assess the impact of Rio Tinto operations on the likely inflow or abstraction volumes at FMG.

Several potential GDE's occur within the syncline, with the primary GDE of concern being Plunge Pool (as outlined in Section 3). Plunge Pool is conceptually separated from mine dewatering activities by the presence of low permeability dykes. With a simulated dyke permeability of $1x10^{-7}$m/day, drawdown predicted at Plunge Pool is 0.1m by the end of mining (2050). Long term drawdown (by 2350) is predicted to be 0.8m. This drawdown is likely to be attributed to the dewatering from upgradient mining activities resulting in reduced volumes of groundwater overtopping the dykes via shallow alluvial sediments after recharge events. The simulated mining activities at FMG have no effect on the amount of drawdown at Plunge Pool (i.e. modelled drawdown at this location is due to Rio Tinto mining only). This is true for all GDEs with the exception of those that are located within the conceptual dyke-bound "compartments" where FMG mining and/or water supply abstraction is proposed to take place (notably GDEs 117, 118, 119 and 123). Predicted drawdowns at the other potential GDE locations are listed in Table 9 and hydrographs presented in Appendix F.

Table 9 Simulated drawdown at GDEs

	Drawdown (m) at 2050		Drawdown (m) at 2350	
GDE	With FMG	Without FMG	With FMG	Without FMG
90	11.8	11.8	19.4	19.4
92	28.5	28.5	19.2	19.1
108	92.4	92.4	77.4	77.2
109	23.0	23.0	27.8	27.8
117	35.5	9.1	30.1	13.9
118	73.8	38.4	58.9	29.9
119	78.6	66.2	57.7	29.4
123	47.3	41.2	25.1	3.0
355/Plunge Pool	0.1	0.1	0.8	0.8
BOM	1.2	1.2	2.0	2.0

8.4 Changes in Groundwater Quality

Changes in groundwater quality during and post mining have not been assessed in this study. However, consideration should be given to the management of potentially acidic waters that may develop as the result of oxidation of pyrite within the McRae Shale, as well as the potential long-term degradation of water quality in pit lakes due to solution of pit wall materials and evapoconcentration.

9 UNCERTAINTY

Broadly, sensitivity is defined as the change in an output quantity as a result of the change in an input quantity. In groundwater modelling, sensitivity testing is done intrinsically during the calibration process by varying one model parameter to establish a closeness of fit to the calibration dataset. The model was calibrated with the objective of minimising the sum of squared residuals error, where the residuals are the difference between groundwater head observations and equivalent modelled outputs; therefore, the sensitivity of the objective function to the change in model parameters governs the calibration success. Due to model non-uniqueness, whereby multiple combinations of parameters may be equally good at fitting historical measurements, there is inherent uncertainty in the parameterisation of the groundwater model. This parameter uncertainty leads to an uncertainty in model predictions.

Due to the compartmentalisation of aquifers and low direct rainfall recharge, the majority of the volume of water to be removed by mining comes from existing aquifer storage, as indicated by the model mass balance presented in Section 5.2.1.Therefore the Sy of key aquifers (mineralised BIF, Wittenoom and Tertiary sediments) are considered to be the most significant drivers of modelled drawdown and pit inflows, with the extent of drawdown limited by hydraulic conductivity of the low permeability units (dykes and McRae Shale). Predictive uncertainty analysis using a simple parameter perturbation method has been undertaken to assess the likely changes to predicted mine inflows and drawdown where the Sy of the aforementioned key aquifers is increased to 0.1 and 0.15, McRae Shale conductivity is increased two orders of magnitude to 1m/day, and dyke permeability is increased to 0.02m/day to simulate potential leakage across the dykes.

9.1 Performance of Uncertainty Model Runs

Table 10 summarises the resulting impact on calibration statistics with the changed parameter values. Only the increase in the dyke hydraulic conductivity results in a model that is not suitably calibrated to be considered as reasonably possible based on available groundwater level data.

Table 10 Calibration statistics for uncertainty model runs

Statistics	Base model	Dykes K=0.02m/day	McRae Shale K=1m/day	Major aquifers Sy=0.1	Major aquifers Sy=0.15
Residual Mean (m)	3.1	15.9	2.8	1.9	1.3
RMS Error (m)	11.4	32.9	11.3	11.0	11.4
Min. Residual (m)	-53.1	-38.8	-53.9	-59.0	-62.3
Max. Residual (m)	55.2	88.6	55.2	55.2	55.2
Scaled RMS Error (%)	6.0	17.3	6.0	5.8	6.0

Predicted inflows for each of the uncertainty runs to reported dewatering volumes is presented in Table 11. The closest overall match to total historical inflow volumes was obtained by the run where the McRae Shale was not simulated as a major barrier to flow and the Sy = 10% model.

Table 11 Actual vs modelled inflows for uncertainty model runs

Year	NAM/ BS4 Hubs	Base model		Dykes K=0.02m/day		McRae Shale K=1m/day		Major aquifers Sy=0.1		Major aquifers Sy=0.15	
	Total GL	Modelled GL	*% of actual*	Modelled GL	*% of actual*	Modelled GL	*% of actual*	Modelled GL	*% of actual*	Modelled GL	*% of actual*
2016	19	15	*80*	15	*77*	17	*87*	20	*104*	23	*122*
2017	20	17	*84*	16	*81*	18	*92*	21	*105*	25	*125*
2018	22	20	*91*	19	*87*	21	*98*	25	*112*	28	*130*
Total	61	52	*85*	50	*82*	56	*93*	65	*107*	77	*126*

On the basis of predicted vs actual dewatering volumes all of the simulated uncertainty scenarios are possible, although a dyke hydraulic conductivity of 0.02m/day is unlikely based on poor calibration performance.

9.2 Predicted Inflows

Predicted future dewatering requirements for each hub for each uncertainty run are presented in Table 12. The uncertainty models mostly suggest future inflows may be greater than predicted by the base model, with inflows predicted to double for the Sy=0.15 scenario. The remaining uncertainty runs suggest inflows are likely to be 95% to 150% of the base flow predictions.

Table 12 Predicted inflows for uncertainty model runs

	Base model		Dykes K=0.02m/day		McRae Shale K=1m/day		Major aquifers Sy=0.1		Major aquifers Sy=0.15	
Year	NAM/BS2	BS4	NAM/BS2	BS4	NAM/BS2	BS4	NAM/BS2	BS4	NAM/BS2	BS4
2020	14.2	2.9	13.1	3.4	16.5	3.8	17	3.3	18.3	3.6
2021	13.2	2.8	12.7	3.2	16.3	3.4	18.1	3	21.7	3.4
2022	16.3	3	15.4	3.5	18.9	4.2	22.3	3.4	27.6	4.9
2023	18.5	5.5	18.9	8.5	23.5	7.7	27.8	7.6	37.0	9.1
2024	22.7	7	22.8	9.9	28.5	9.8	31.9	11.5	39.2	16.7
2025	17.6	8.6	17.3	11.9	21.5	9.2	23.8	14.1	29.4	18.2
2026	16.4	5.2	16.4	7.3	20.6	6.2	23.5	7.8	27.4	9.5
2027	15.3	5.8	15.5	6.7	20.2	5	22	9.1	26.8	12.3
2028	12.6	7.5	13	10.6	17.2	8.1	19.4	11.3	22.9	13.7
2029	17.3	8.5	15.2	11	20.5	7.5	24.8	13.2	30.0	18.0
2030	12.9	5.7	11.3	7.4	15.6	5.1	19.1	9.3	24.2	13.2
2031	20.4	5.8	18.7	7	23.5	2.9	28.2	9.3	34.3	12.7
2032	18.2	6.8	17.2	8.2	21.5	4.7	24.4	11.5	29.7	16.1
2033	12.2	5.2	12.2	6.6	15.3	3.3	16.3	8.2	20.4	10.8
2034	11.6	5.6	11.6	6.2	15.3	5.6	16.1	8.2	21.8	10.7
2035	13.2	4.9	11.4	5.2	16.6	5	18.2	7.6	23.2	10.7
2036	9.1	5.8	8	7.1	13.3	5.9	13	10.5	17.1	14.6
2037	8.3	3.1	7.1	3.9	10.7	2.4	10.5	5	13.0	7.1
2038	8.5	2.1	7.5	3	10.9	2.3	10.5	3.4	12.8	5.0
2039	8.6	2.5	7.7	3.6	11	2.2	10.4	4.1	12.5	5.7
2040	8.8	3.4	8	4.5	11.4	3.7	10.9	5.1	13.2	6.8
2041	8.7	3.5	7.9	4.7	11.9	3.2	11.1	5.1	13.4	6.5
2042	5.1	3.7	4.7	4.2	7.2	3.1	6.2	5.1	7.6	6.3
2043	4.3	3.2	4	3.8	5.5	2.7	4.8	4.4	5.7	5.5
2044	4.8	2	4.5	2.5	7.2	1.2	5.8	3.1	7.5	4.2
2045	4.1	0.8	4	1.3	5.4	0.6	4.7	1.4	5.5	1.9
2046	4.1	0	4	0	5.5	0	4.7	0	5.6	0.0

	Base model		Dykes K=0.02m/day		McRae Shale K=1m/day		Major aquifers Sy=0.1		Major aquifers Sy=0.15	
2047	4	0	4	0	5.5	0	4.8	0	5.6	0.0
2048	4	0	4.1	0	5.5	0	4.8	0	5.6	0.0
2049	4	0	4.1	0	5.5	0	4.8	0	5.6	0.0
2050	0	0	0	0	0	0	0	0	0.0	0.0
Total	339	120.9	322.3	155.2	428	118.8	459.9	185.6	564.4	247.1
% of basecase			95%	128%	126%	98%	136%	154%	166%	204%

9.3 Predicted Drawdown

Maximum drawdown contours for the uncertainty runs are presented in Figure 19 for the end of mining, and Figure 20 for long-term. Changes in the specific yield of the major aquifers does not result in substantial variation in the depth or extent of predicted drawdown from the base model run. However, increasing the hydraulic conductivity of the McRae Shale does result in a significant change to the drawdown distribution, with drawdown extending much further from the proposed pits as its propagation is not laterally restricted by the shale. Drawdown predicted by uncertainty Dykes K=0.02m/day is significantly less than the other runs immediately within mining areas but the predicted inflows for the predicted drawdown are considered to not be representative of likely conditions during mining as the model is not adequately calibrated and simulated pre-mining water levels are too low (i.e. the magnitude of total drawdown is limited by simulated pre-mining water level minus pit floor depth). However, the uncertainty run does serve to demonstrate that a higher degree of regional drawdown is likely if the dykes do not act as effective hydraulic barriers.

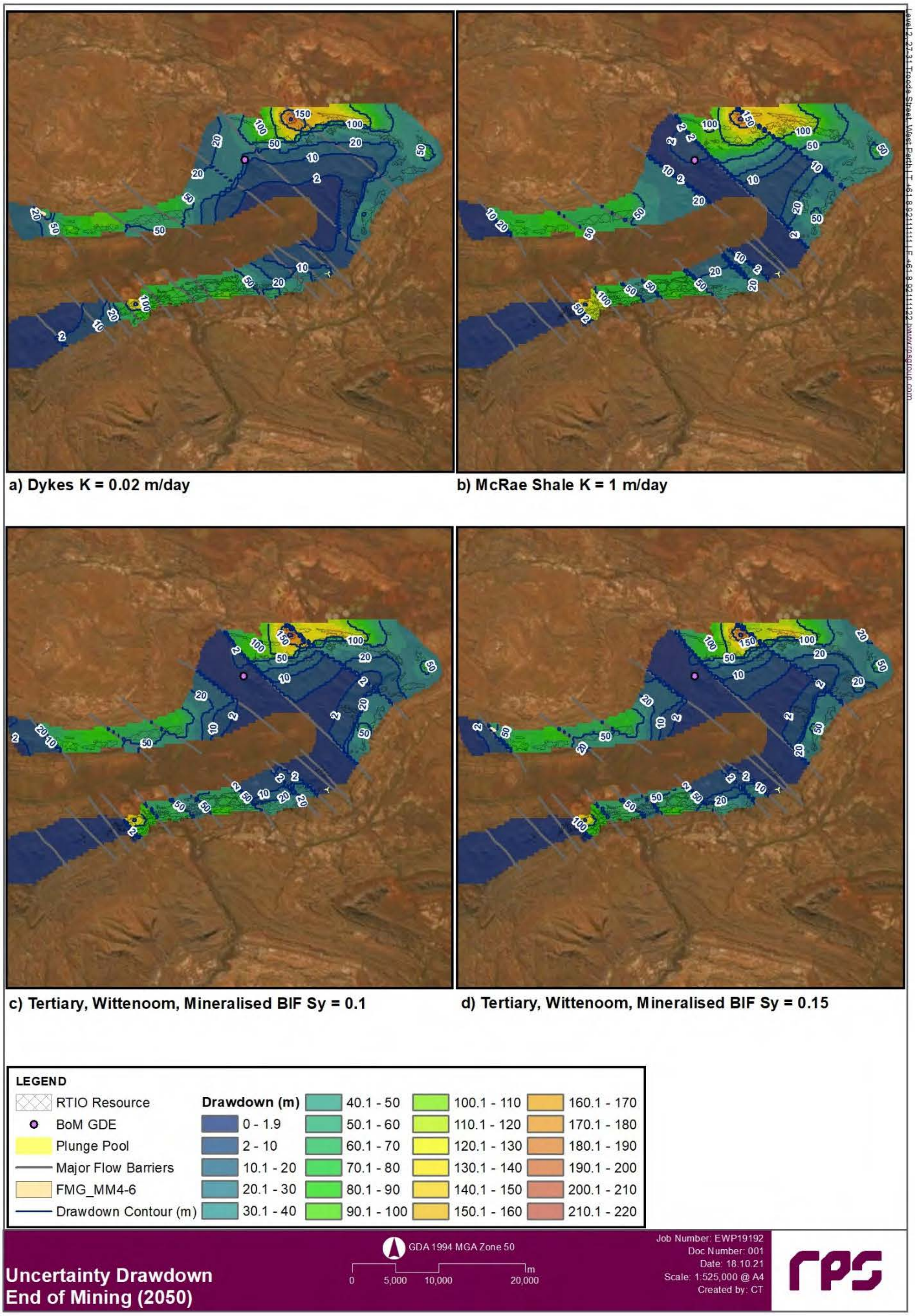

Figure 19 Maximum drawdown for uncertainty runs at the end of mining

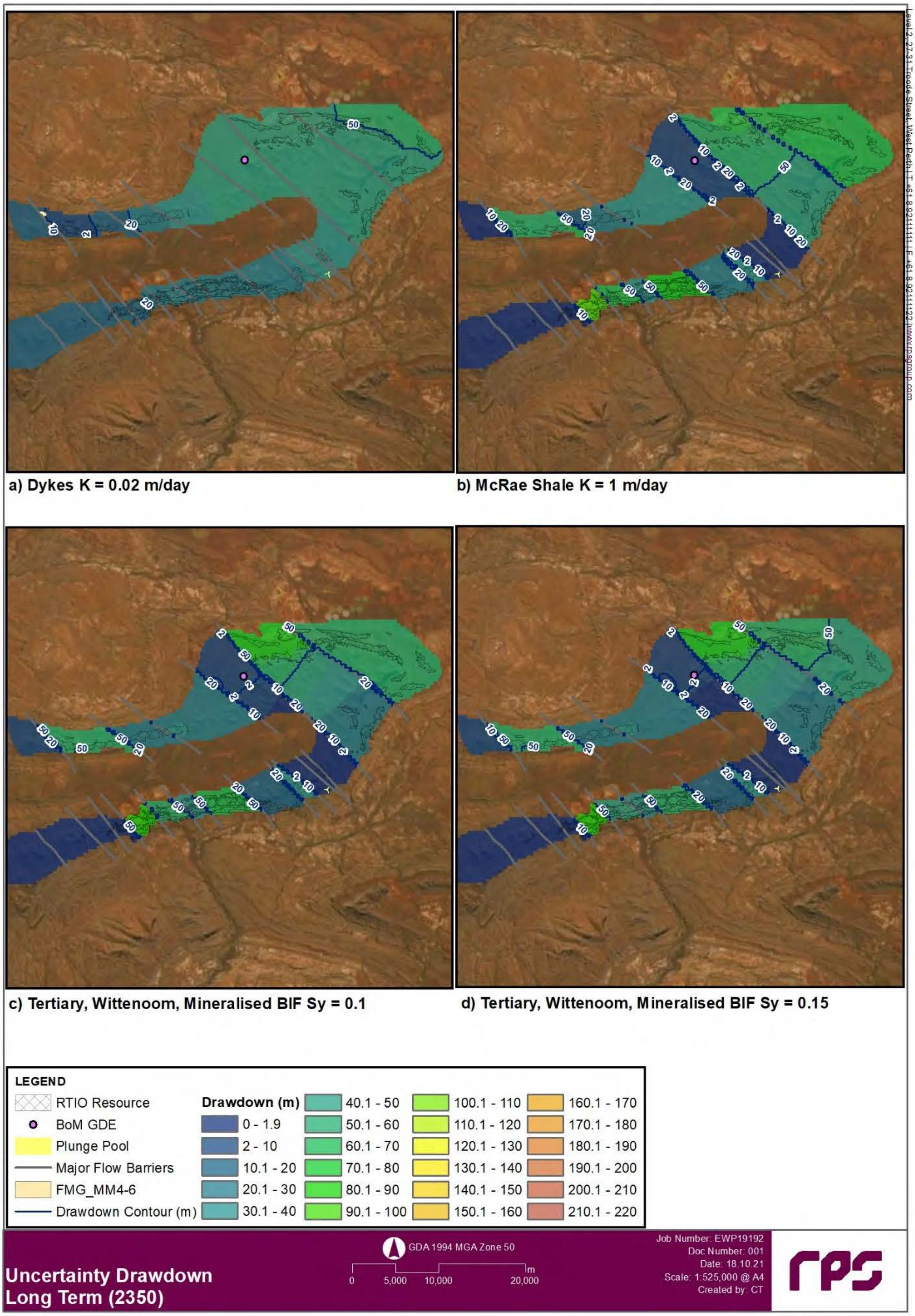

Figure 20 **Long-term drawdown for uncertainty runs**

The predicted drawdown at potential GDE locations is summarised in Table 13 for each of the uncertainty scenarios. At Plunge Pool, drawdown is predicted to range between 0.0m and 10.4m at the end of mining (2050) up to 0.3m to 29.6m by 2350. However, the predicted drawdown at Plunge Pool is less than or equal to that of the base model (0.1m and 0.9m at 2050 and 2350 respectively) for all uncertainty runs, except for the run with significantly increased dyke hydraulic conductivity (which as previously discussed is unlikely based on poor calibration to existing water level data).

Table 13 Predicted drawdown at GDEs for uncertainty model runs

GDE	Base model		Dykes K=0.02m/day		McRae Shale K=1m/day		Major aquifers Sy=0.1		Major aquifers Sy=0.15	
	2050	2350	2050	2350	2050	2350	2050	2350	2050	2350
90	11.8	19.4	15.8	29.3	24.4	22.9	11.0	19.5	10.6	19.1
92	28.5	19.2	32.1	27.9	26.3	22.8	26.3	19.2	24.1	18.9
108	92.4	77.4	63.1	50.3	84.9	67.0	79.2	81.0	69.2	81.1
109	23	27.8	28.7	49.0	21.4	24.0	19.0	29.0	16.3	28.9
117	35.5	30.1	30.2	39.9	35.8	35.4	32.1	28.7	29.5	27.0
118	73.8	58.9	70.6	15.6	76.5	63.9	72.4	57.4	70.2	54.9
119	78.6	57.7	76.0	14.4	74.8	63.0	77.8	56.0	75.9	53.3
123	47.3	25.1	49.1	30.8	63.0	31.2	43.2	28.9	40.5	30.0
355/Plunge Pool	0.1	0.8	10.4	29.6	0.0	0.3	0.0	0.8	0.0	0.7
BOM	1.2	2	13.7	43.6	2.0	2.6	0.9	1.9	0.7	1.8

As the most significant source of uncertainty surrounding the potential drawdown at Plunge Pool is related to the hydraulic conductivity of the dykes, additional uncertainty runs where undertaken to assess the potential drawdown for a rage of dyke conductivities. Results, displayed in Graph 9, suggest that there is minimal change to predicted drawdown if dyke permeability is less than $1x10^{-5}$m/day (2 orders of magnitude higher than the base model). It remains a possibility that some drawdown may propagate across the dykes with time, the degree to which is dependent on the dyke permeability which may be variable with strike and depth due to factors such as fractures and weathering, among other geological complexities which are not readily able to be quantified by field testing.

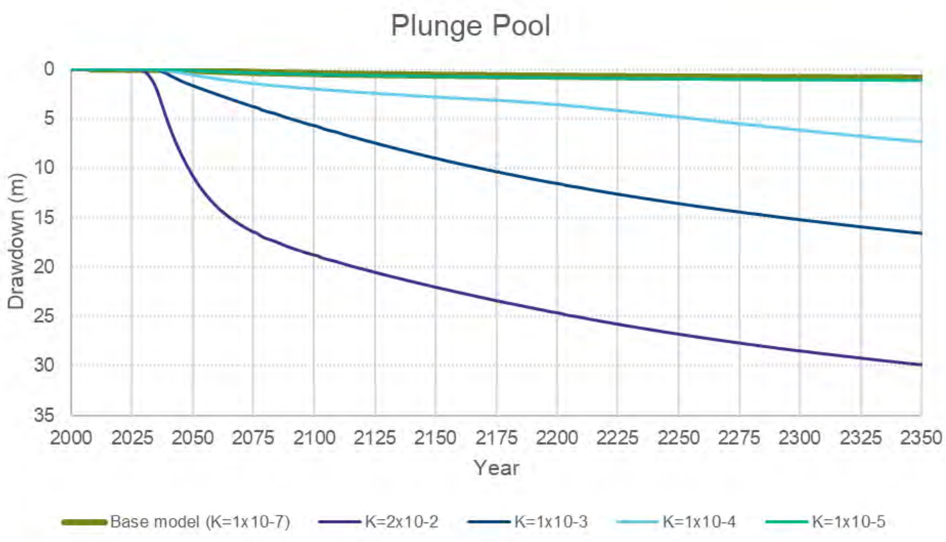

Graph 9 Effect of dyke hydraulic conductivity (m/day) on predicted drawdown at Plunge Pool

10 CONCLUSION

RPS has prepared a numerical model that incorporates all of Rio Tinto's existing and proposed below water table excavations within the Brockman Syncline, as well as FMG below water table mining where publicly available information exists. Results of the modelling will be used to provide input to the predicted cumulative impacts of mining within the Brockman Syncline and incorporated into Rio Tinto's Part IV submission to the EPA. The model also provides a preliminary guide to the requirements for dewatering management and mine water balance.

The model has been built consistent with methods outlined in the *Australian Groundwater Modelling Guidelines* (Barnett *et al.*, 2012) as well as the *MDBC Groundwater Flow Modelling Guideline* (MDBC 2001), and provides a Class 2 confidence level, which is considered to be suitable for its intended use of predicting the impacts of the proposed developments.

The key findings of this assessment are:

- Predicted annual dewatering volumes within the Nammuldi hubs are predicted to ramp-up to approximately 23 GL/year over the coming five to ten years, decreasing to around 4 GL/year towards the end of mine life. Life of mining dewatering across the Nammuldi hub is predicted to be in the order of 425 GL. Lens CD and Lens EF are expected to be the dominant contributors to total dewatering volume (totalling around 70% of cumulative inflow volumes).

- Within the Brockman 4 hub peak dewatering volumes of up to 9 GL/year are predicted, with the greatest dewatering volume currently forecast for the period 2024 to 2029. Cumulative inflows over the life of mining total approximately 145 GL. Approximately 60% of the overall dewatering volumes are predicted from BS4 main area (Pits 2 and 5 combined, Pits 3 and 4 combined, Pit 11and Pit 18), 20% from the BS1 area and the remainder from the BSMM and BSMN areas.

- Drawdown (to the 2m contour) caused by the Proposal is expected to propagate relatively rapidly away from the mine voids to the extent where dykes act as a barrier to further flow. The McRae Shale also acts to slow the propagation of drawdown in locations where it is not mined out.

- Rio Tinto is the primary groundwater user within the majority of the modelled area, with FMG also holding water licenses within the north-western limb of the syncline. Drawdown from the FMG and Rio Tinto operations have the potential to overlap at the BS1 mining area, which may affect the pit inflow and/or bore abstraction rates at both operations.

- Several potential GDEs occur, with the most significant being Plunge Pool on the southern arm of the syncline. Plunge Pool is conceptually separated from mine dewatering activities by the presence of low permeability dykes, however there is a possibility for drawdown to propagate across the dykes with time, the degree to which is dependent on the dyke permeability. With a simulated dyke permeability of $1x10^{-7}$m/day, drawdown predicted at Plunge Pool is 0.1m by the end of mining (2050) and 0.8m long term (by 2350) due to the dewatering and drawdown at upgradient mine areas reducing the shallow groundwater flow that overtops the dykes. Potential impacts to riparian vegetation have not been assessed here.

- All below water table pit voids are predicted to remain as groundwater sinks post mining (assuming closure bunding minimised surface water ingress), and as a result drawdown continues in some locations for several decades after pit completion as the cone of depression induced by nearby deeper pits continues to propagate. Groundwater recovery is expected to be greater if pits are backfilled as opposed to left as open voids, however, no locations are expected to recover to pre-mining water levels by 2350 under either open void or backfilled scenarios.

- Groundwater inflow to open voids has been simulated by this model but further work is required to undertake pit lake water balance modelling to determine the likely equilibrium lake levels.

- Predictive uncertainty analysis was undertaken to assess the likely changes to predicted mine inflows and drawdown where the Sy of key aquifers is increased to 0.1 and 0.15, McRae Shale conductivity is increased two orders of magnitude to 1m/day, and dyke permeability is increased to 0.02m/day to simulate potential leakage across the dykes. Parameter modification as part of the sensitivity analysis results in a reasonably calibrated model in all instances bar a five order of magnitude increase in dyke hydraulic conductivity, which results in an SRMS ~17 %. Comparison of modelled vs measured inflows suggests that all uncertainty scenarios may be producing meaningful results.

- Uncertainty runs suggest that predicted inflows may be 95 to 205% of those suggested by the base model. Drawdown has the potential to propagate to a further regional extent across the syncline where the dykes and/or McRae Shale are less restrictive to lateral groundwater flow.

- The increase in dyke permeability has the most significant effect on predicted drawdown at Plunge Pool, therefore additional uncertainty runs where undertaken to assess the potential drawdown for a range of dyke conductivities. Uncertainty results suggest that there is minimal change to predicted drawdown if dyke permeability is less than $1x10^{-5}$m/day (2 orders of magnitude higher than the base model), however permeabilities greater than this may result in a much greater degree of drawdown than predicted by the base model.

11 REFERENCES

Barnett, B, Townley, L.R., Post, V., Evans, R.E., Hunt, R.J., Peeters, L., Richardson, S., Werner, A.D., Knapton, A. and Boronkay, A., 2012, Australian Groundwater Modelling Guidelines. Waterlines report 82, National Water Commission, Canberra

BoM [Bureau of Meteorology], 2019. Groundwater Dependent Ecosystems Atlas. Available at: http://www.bom.gov.au/water/groundwater/gde/

Doherty, J., 2010, PEST: Model-Independent Parameter Estimation User Manual (5th ed.): Watermark Numerical Computing, Brisbane, Queensland, Australia.

Golder, 2018. Eliwana Mining Project Groundwater Impact Assessment. Prepared for Fortescue Metals Group Limited. Report 167 1484-007-R-Rev4

Murray Darling Basin Commission, 2001, Groundwater Flow Modelling Guideline. Prepared by Aquaterra Pty Ltd, November 2000, Project No. 125, Final guideline issued January 2001.

Niswonger, R.G., Panday, Sorab, and Ibaraki, Motomu, 2011, MODFLOW–NWT, A Newton formulation for MOD-FLOW–2005: U.S. Geological Survey Techniques and Methods, book 6, chap. A37, 44p.

Panday, Sorab, Langevin, C.D., Niswonger, R.G., Ibaraki, Motomu, and Hughes, J.D., 2013, MODFLOW–USG version 1: An unstructured grid version of MODFLOW for simulating groundwater flow and tightly coupled processes using a control volume finite-difference formulation: U.S. Geological Survey Techniques and Methods, book 6, chap. A45, 66 p

Rio Tinto, 2019a. Brockman 2 Nammuldi and Silvergrass East Triennial Aquifer Review 2016 – 2018.

Rio Tinto, 2019b. Brockman 4 Triennial Aquifer Review 2016 – 2018.

Rumbaugh, J. and Rumbaugh, D. 2017. Groundwater Vistas Version 7. Environmental Simulations Inc.

APPENDIX A - MINIMUM SCHEDULED DROP-CUT BY PIT

	2022	2023	2024	2025	2026	2027	2028	2029	2030	2031	2032	2033	2034	2035	2036	2037	2038	2039	2040	2041	2042	2043	2044	2045	2047	2049	2050
BS1				550	550	520	550	500	490	480	490	460	490	480	460	450	470	440	410	440	510	470	440	450			
BS1_e1_01				600	560	560	550		540					540		520				500							
BS1_e1_02				590	550	530		500	490	480		460															
BS1_e1_03				550	550	520		500						490													
BS1_e1_04				620	580	540																					
BS1_e1_05					570	570				560									530	520							
BS1_e1_06													560	520	480	470											
BS1_e2_01					600	570	570	550	510	480		460															
BS1_e2_02					620	590	550	540	530	530						520			520		510	490	480				
BS1_e2_03				640	600	590	560		550																		
BS1_e2_04					650	610	570			540										530							
BS1_e3_01												710	670	630	590												
BS1_e3_02															720	680											
BS1_e3_03																720	680	640	600	570	570						
BS1_w1_01										610	600	580	570	530	490	470											
BS1_w1_02									620	580	540	500															
BS1_w1_03										610		600			570		530	520	510								
BS1_w1_04										580	550	540		510													
BS1_w1_05																550		540					500	500			
BS1_w1_06																570					550	510	470				
BS1_w1_07																					510	470	440				
BS1_w2_01									570		530	500	490		460	450											
BS1_w2_02a																570	560				550	510	470	450			
BS1_w2_02b										520	490			480													
BS1_w2_03																520	480	440	410								
BS1_w2_04									710	680	650	620															
BS1_w2_05												650	610	570	530	490	470		450	440							
BS4 Main	410	400	390	370	360	350	330	330	460	430	510	520	500	490	450	510	490	490	450	440	410	400	400	440			
BS4 Main_Pit1_s3	520																										
BS4 Main_Pit1_s4	520	480	470																								
BS4 Main_Pit10			550	520							510								500	490			480				
BS4 Main_Pit11_s1	550	520	490	460																							
BS4 Main_Pit11_uf												570		560		550	530	490	450	440							
BS4 Main_Pit13																			640	610							
BS4 Main_Pit14		590	560	540					530																		
BS4 Main_Pit15		570	530	520																							
BS4 Main_Pit16				560	520		510	500																			
BS4 Main_Pit17_s1	570	530	520	510																							
BS4 Main_Pit17_uf			550	510	500			470	460	460											450						

BS4 Main_Pit18_s1	530	510	480																								
BS4 Main_Pit18_s2	560		520	490					490	460										460							
BS4 Main_Pit18_s4e	560	540	500	470																							
BS4 Main_Pit18_s4f																	530	490	450	440	410	400	400				
BS4 Main_Pit18_s4w													550	520		510											
BS4 Main_Pit18_s5a								550	530	490																	
BS4 Main_Pit18_s5b																560				520	500						
BS4 Main_Pit18_s5f												520	500	490	450												
BS4 Main_Pit18_s6	530	490	470						460											450							
BS4 Main_Pit18_s7	540	500	500																								
BS4 Main_Pit19					610												570	530	500								
BS4 Main_Pit2_s4	410	400	390	370	360	350	330	330																			
BS4 Main_Pit3_c	450	450	440																								
BS4 Main_Pit3_e	450	450																									
BS4 Main_Pit3_s3	490																										
BS4 Main_Pit3_s4		460																									
BS4 Main_Pit3_s5			520	480	460		450	440		430																	
BS4 Main_Pit3_s5i	490																										
BS4 Main_Pit3_s6		570	520	480	440			430																			
BS4 Main_Pit4_s1	510	490																									
BS4 Main_Pit4_s2	510	480																					470				
BS4 Main_Pit4_s3		550	510	490																							
BS4 Main_Pit5	410	410																									
BS4 Main_Pit6														540		530	520	510	500	470	450						
BS4 Main_Pit7	560	520	500											500			490			490	480	450	440	440			
BS4 Main_Pit8	580	540																						530			
BS4 Main_Pit9			600	590						570	550	530															
BS4 MM - MN						530	500	490	580	570	480	470	500	470	460	460	450	480	450								
BS4 MM - MN_M1						530	500	490			480	470															
BS4 MM - MN_M2									580		570	540	500	470													
BS4 MM - MN_M3_East						580	540	520																			
BS4 MM - MN_M3_West						610				570	530		520														
BS4 MM - MN_MP_BSMN_M													510	500		460	450										
BS4 MM - MN_MP_BSMN_N															510	500	490	480	450								
BS4 MM - MN_N1						540	500	490			480	480															
BS4 MM - MN_N2_S1						530	500	490			480																
BS4 MM - MN_N2_S2												550	530	490	460												
BS4 MM - OST			520	490	510	470	510	460		490	470	460	420	420	460	450					400	400					
BS4 MM - OST_o1_s1				550	530	510																					
BS4 MM - OST_o2_s1					520	480																					
BS4 MM - OST_o3_s1					530	510																					
BS4 MM - OST_o4_s1			530	500		490																					
BS4 MM - OST_o5e_s1							540	500			490		450														
BS4 MM - OST_o5e_s2						550	510	490																			

BS4 MM - OST_o5e_uf													530	490	460	450											
BS4 MM - OST_o5w_s1				530	520	490																					
BS4 MM - OST_o5w_s2			520	490																							
BS4 MM - OST_o5w_s3			550	530	510	470		460																			
BS4 MM - OST_o5w_uf								530		490	470	460	420	420							400	400					
BS4 MM - QR	500	500	460	430	490	420	460	440			400	500	490	430	420	520	410	510	420	480		540	500	490			
BS4 MM - QR_q1_s1		520	480	460																							
BS4 MM - QR_q1_s2												500	490	460	420		410										
BS4 MM - QR_q2_s1			530	490																							
BS4 MM - QR_q2_s2				520	490	460	460	440						430					420								
BS4 MM - QR_q3_s1	540	500	470																								
BS4 MM - QR_q3_s2				520	490	470	460																				
BS4 MM - QR_q4_s1																						540	500	490			
BS4 MM - QR_r_s1			460																								
BS4 MM - QR_r_s2																520		510		480							
BS4 MM - QR_r_s3	500	500	460	430		420					400																
Endeavour			550	510	500	540	480	560	520	480	590	470		500	460												
Endeavour_End1_e1			550	510	500		480																				
Endeavour_End1_e2							590	560	520	480		470															
Endeavour_End1_e3			680	640	600	560																					
Endeavour_End1_e4									610	570																	
Endeavour_End1_ef						660	620	580	540	510																	
Endeavour_End1_w1				620	580	540	500																				
Endeavour_End1_wf							590		550	510		500		500	460												
Endeavour_End2_ef											590			550													
Endeavour_End2_wf										630	590			550													
B2ED	580	480	460	680	640	640	760	760																			
B2ED_P10_S232	640	610	590																								
B2ED_P10_S232E	580	580	570																								
B2ED_P10_S401		700																									
B2ED_P10_S501				780	740																						
B2ED_P12_S302	580																										
B2ED_P13_S203B	580		570																								
B2ED_P13_S203c			720	680	640	640																					
B2ED_P8_S253		480	460																								
B2ED_P9_S200					850	800	760	760																			
BS2						600	560	620	770		740		730														
BS2_BS2_PIT1C						680	680																				
BS2_BS2_PIT1E								790	770				750														
BS2_BS2_PIT1W							660	660																			
BS2_BS2_PIT2E								620																			
BS2_BS2_PIT2S											760		730														
BS2_BS2_PIT2W						600	560																				
BS2_BS2_PIT3C							670	650																			

BS2_BS2_PIT3N						620	610																				
BS2_BS2_PIT3S								750			740																
EXT	670			630	620	600	570	550	570	530	520	580	570	560	550	540	530	520	510	500	600						
EXT_BROKENWOOD						790	750	730	720			720		710	710	700	650	610	610		600						
EXT_CREEKSIDE						630	610	570	570	540	530																
EXT_diesel				630	620	600	570	550		530	520																
EXT_MMJ							680	630	620	610	590	580	570	560	550	540	530	520	510	500							
EXT_sandelford	670					660		620																			
LAB		580	540	500	480	460	500	500	460	420																	
LAB_PIT_1_S2								640																			
LAB_PIT_2_S1		600	590																								
LAB_PIT_2_S2		600	580																								
LAB_PIT_3_S1		580	570																								
LAB_PIT_3_S2		580	540																								
LAB_PIT_4_S1		560	540	500																							
LAB_PIT_4_S2		580			560	540	500	490																			
LAB_PIT_5_S1		580	540	520	480	460				450																	
LAB_PIT_5_S2				580	560	540	520	500	460	420																	
LAB_PIT_6_S1		580	560																								
LAB_PIT_6_S2			580	560	540	520	510																				
LCD	510	470	430	430	410	370		370				570	360	500	480												
LCD_LCD_S303	510	470	430	430																							
LCD_LCDBWT_S1003												570	540	500	480												
LCD_LCDBWT_S802		540	500	450	410	370		370					360														
LEF		520	500	540	500	480	460	480				480	620	580	560	540	520	520	500	500	480	480			480		
LEF_CS123		520	500																								
LEF_CS223		560	540	540	500	480	460																				
LEF_CS323		600	560	540																							
LEF_CS423		620	600	580	560	520	500	480				480															
LEF_CS523													620	580	560	540	520	520	500	500	480	480			480		
LG			620	600	590	600	590	580	560	540	530	510	500	490													
LG_lg_s1			620	600	590																						
LG_lg_s2			640	630	620	600	590	580	560	540	530	510	500	490													

APPENDIX B – CALIBRATION HYDROGRAPHS

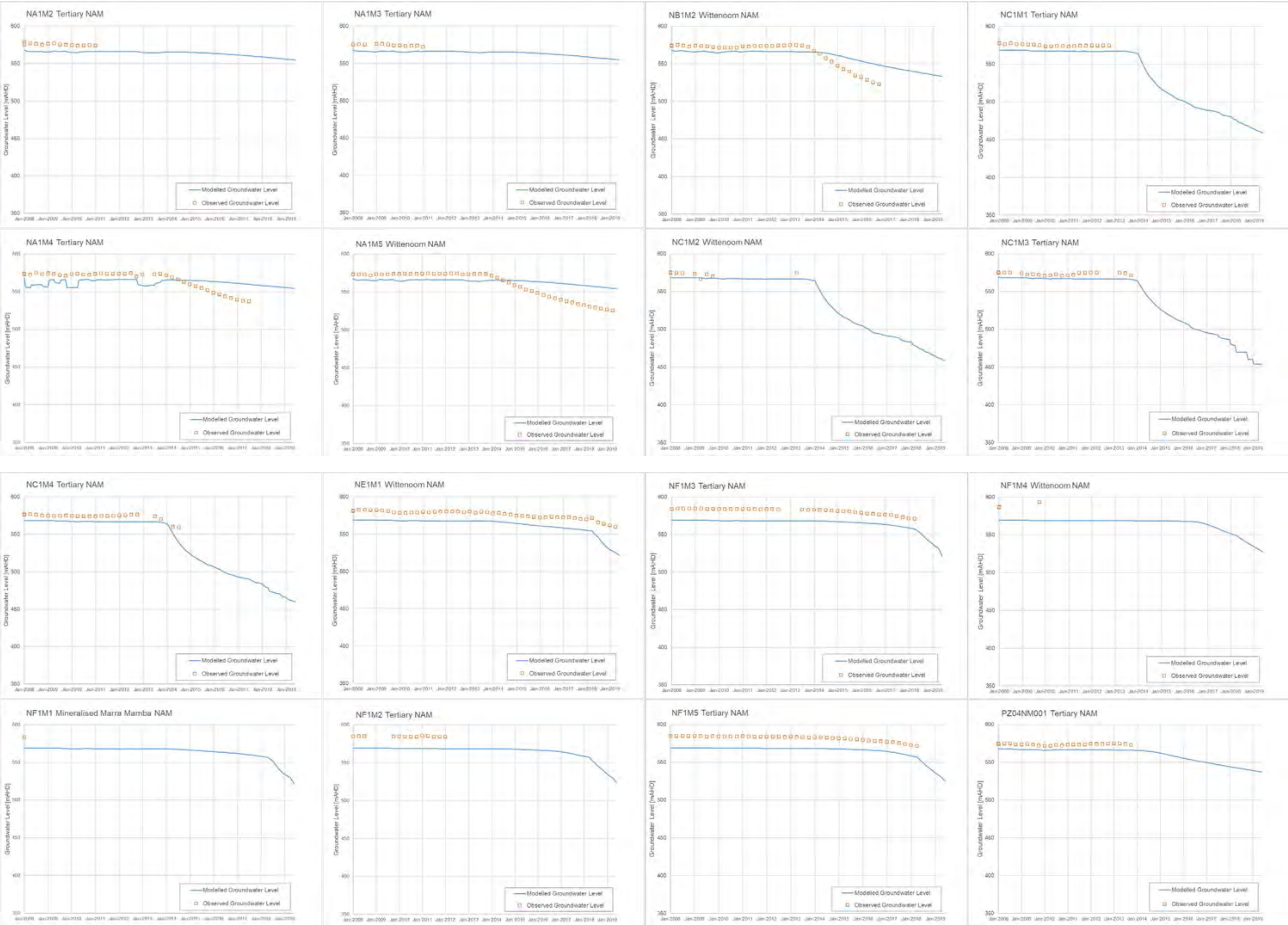
NA1M2 Tertiary NAM
NA1M3 Tertiary NAM
NB1M2 Wittenoom NAM
NC1M1 Tertiary NAM
NA1M4 Tertiary NAM
NA1M5 Wittenoom NAM
NC1M2 Wittenoom NAM
NC1M3 Tertiary NAM
NC1M4 Tertiary NAM
NE1M1 Wittenoom NAM
NF1M3 Tertiary NAM
NF1M4 Wittenoom NAM
NF1M1 Mineralised Marra Mamba NAM
NF1M2 Tertiary NAM
NF1M5 Tertiary NAM
PZ04NM001 Tertiary NAM
Groundwater Level [mAHD]
Modelled Groundwater Level
Observed Groundwater Level

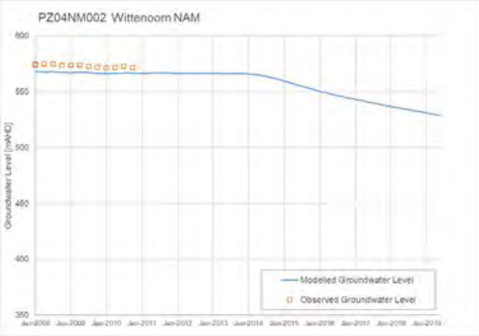
PZ04NM002 Wittenoom NAM
Groundwater Level [mAHD]
Modelled Groundwater Level
Observed Groundwater Level

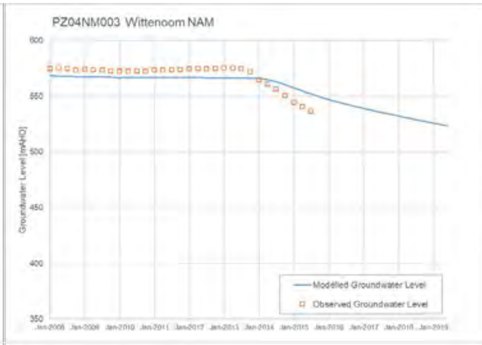
PZ04NM003 Wittenoom NAM
Groundwater Level [mAHD]
Modelled Groundwater Level
Observed Groundwater Level

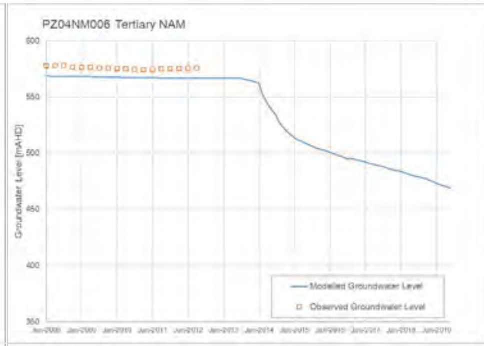
PZ04NM006 Tertiary NAM
Groundwater Level [mAHD]
Modelled Groundwater Level
Observed Groundwater Level

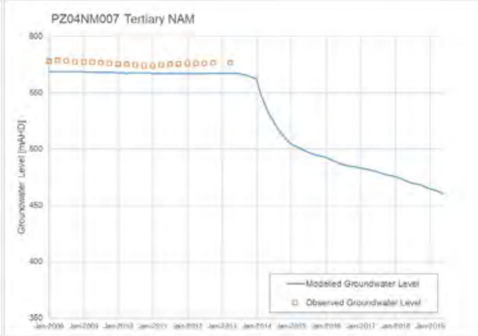
PZ04NM007 Tertiary NAM
Groundwater Level [mAHD]
Modelled Groundwater Level
Observed Groundwater Level

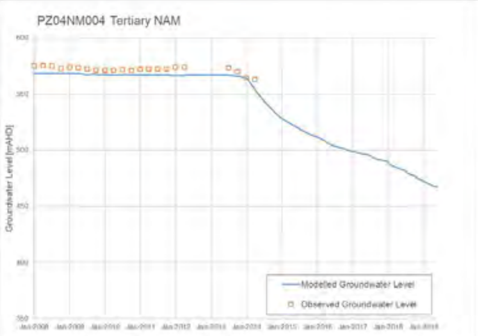
PZ04NM004 Tertiary NAM
Groundwater Level [mAHD]
Modelled Groundwater Level
Observed Groundwater Level

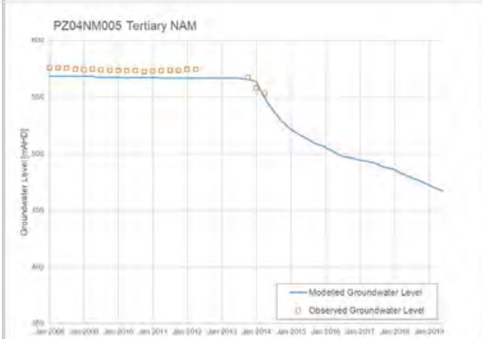
PZ04NM005 Tertiary NAM
Groundwater Level [mAHD]
Modelled Groundwater Level
Observed Groundwater Level

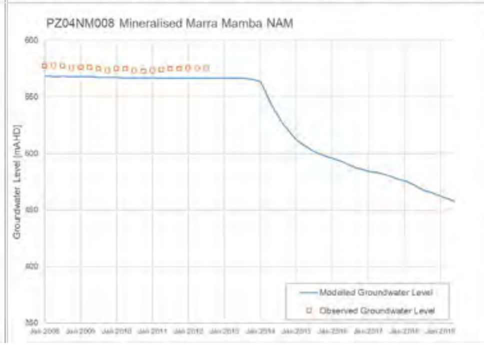
PZ04NM008 Mineralised Marra Mamba NAM
Groundwater Level [mAHD]
Modelled Groundwater Level
Observed Groundwater Level

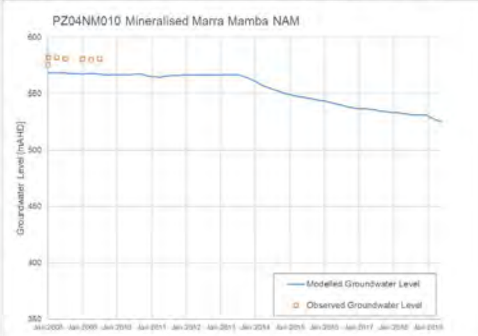
PZ04NM010 Mineralised Marra Mamba NAM
Groundwater Level [mAHD]
Modelled Groundwater Level
Observed Groundwater Level

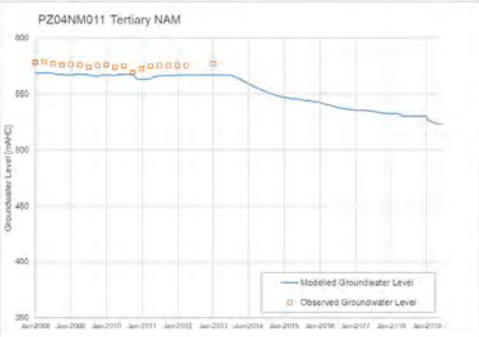
PZ04NM011 Tertiary NAM
Groundwater Level [mAHD]
Modelled Groundwater Level
Observed Groundwater Level

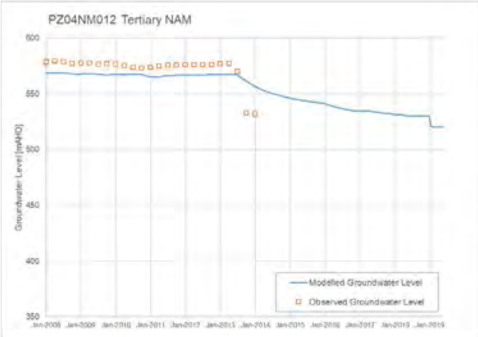
PZ04NM012 Tertiary NAM
Groundwater Level [mAHD]
Modelled Groundwater Level
Observed Groundwater Level

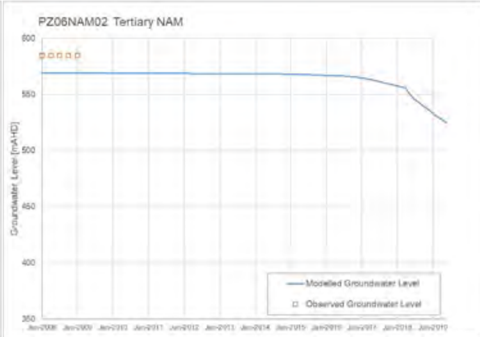
PZ06NAM02 Tertiary NAM
Groundwater Level [mAHD]
Modelled Groundwater Level
Observed Groundwater Level

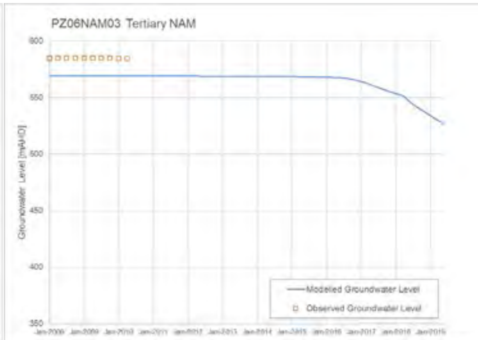
PZ06NAM03 Tertiary NAM
Groundwater Level [mAHD]
Modelled Groundwater Level
Observed Groundwater Level

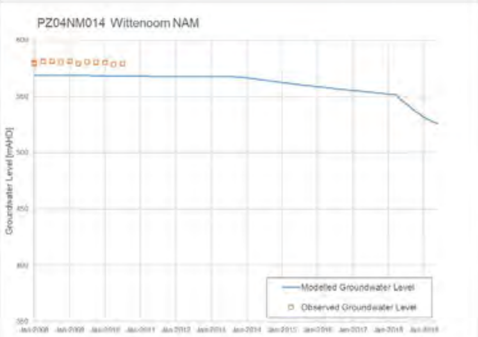
PZ04NM014 Wittenoom NAM
Groundwater Level [mAHD]
Modelled Groundwater Level
Observed Groundwater Level

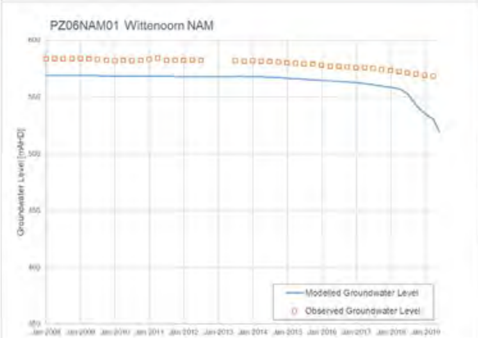
PZ06NAM01 Wittenoom NAM
Groundwater Level [mAHD]
Modelled Groundwater Level
Observed Groundwater Level

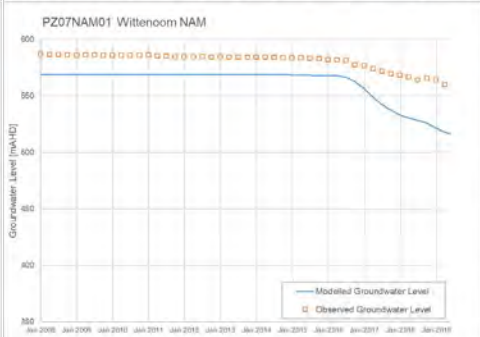
PZ07NAM01 Wittenoom NAM
Groundwater Level [mAHD]
Modelled Groundwater Level
Observed Groundwater Level

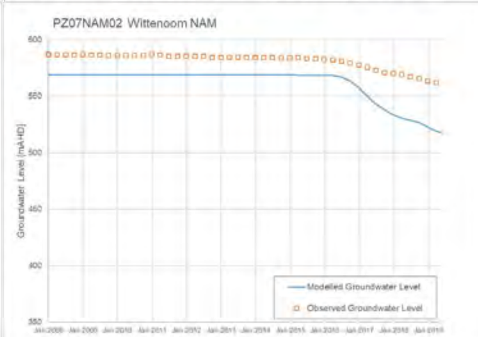
PZ07NAM02 Wittenoom NAM
Groundwater Level [mAHD]
Modelled Groundwater Level
Observed Groundwater Level

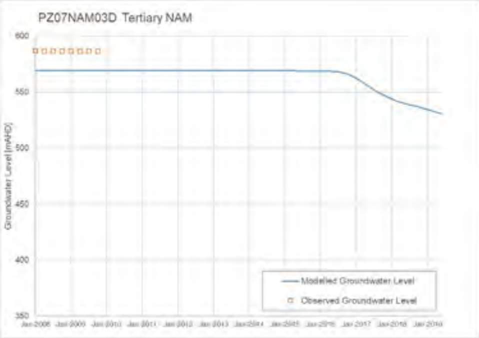
PZ07NAM03D Tertiary NAM
Groundwater Level [mAHD]
Modelled Groundwater Level
Observed Groundwater Level

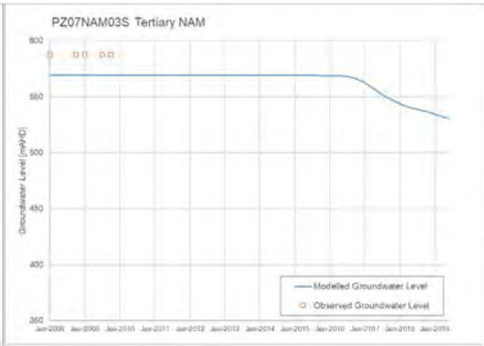
PZ07NAM03S Tertiary NAM
Groundwater Level [mAHD]
Modelled Groundwater Level
Observed Groundwater Level

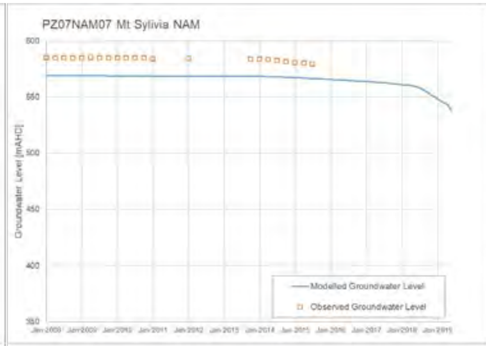
PZ07NAM07 Mt Sylivia NAM
Groundwater Level [mAHD]
Modelled Groundwater Level
Observed Groundwater Level

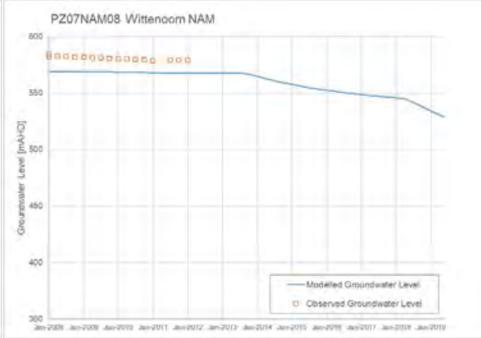
PZ07NAM08 Wittenoom NAM
Groundwater Level [mAHD]
Modelled Groundwater Level
Observed Groundwater Level

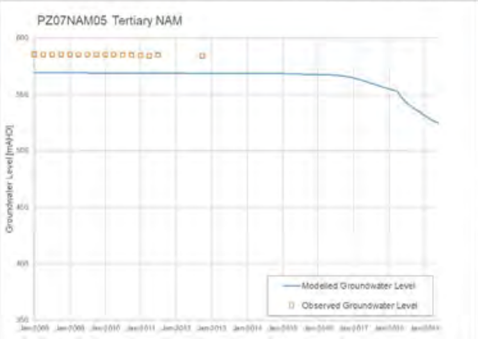
PZ07NAM05 Tertiary NAM
Groundwater Level [mAHD]
Modelled Groundwater Level
Observed Groundwater Level

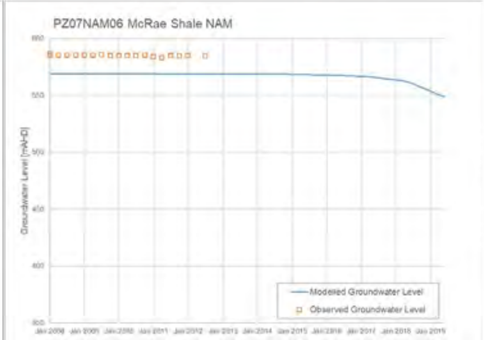
PZ07NAM06 McRae Shale NAM
Groundwater Level [mAHD]
Modelled Groundwater Level
Observed Groundwater Level

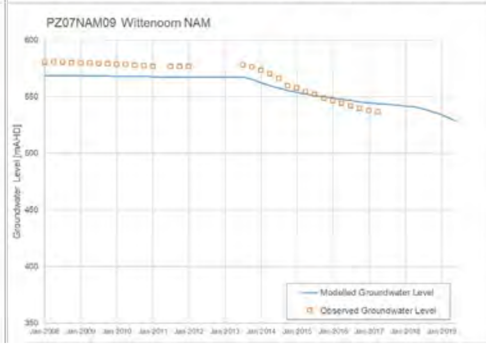
PZ07NAM09 Wittenoom NAM
Groundwater Level [mAHD]
Modelled Groundwater Level
Observed Groundwater Level

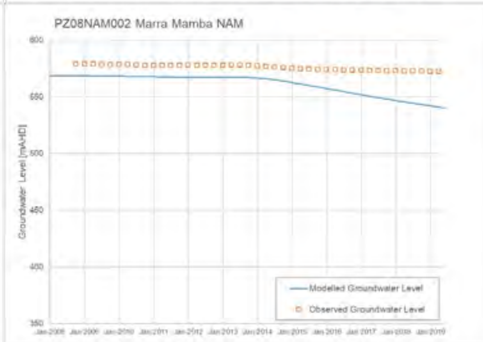
PZ08NAM002 Marra Mamba NAM
Groundwater Level [mAHD]
Modelled Groundwater Level
Observed Groundwater Level

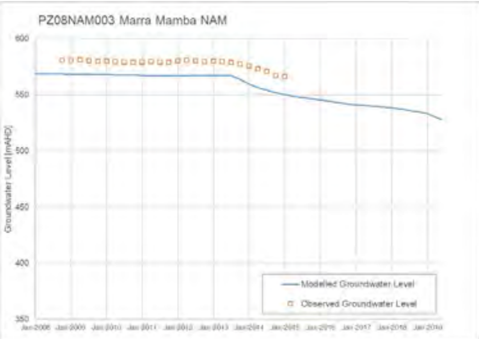
PZ08NAM003 Marra Mamba NAM
Groundwater Level [mAHD]
Modelled Groundwater Level
Observed Groundwater Level

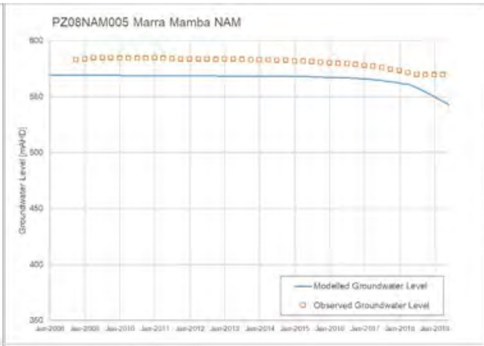
PZ08NAM005 Marra Mamba NAM
Groundwater Level [mAHD]
Modelled Groundwater Level
Observed Groundwater Level

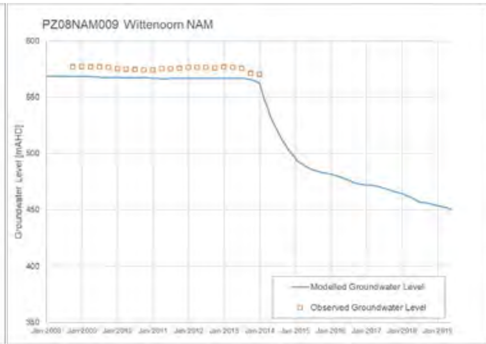
PZ08NAM009 Wittenoom NAM
Groundwater Level [mAHD]
Modelled Groundwater Level
Observed Groundwater Level

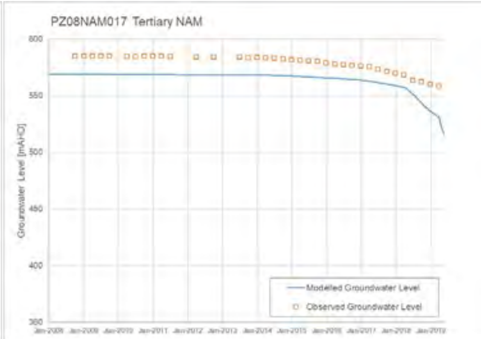
PZ08NAM017 Tertiary NAM
Groundwater Level [mAHD]
Modelled Groundwater Level
Observed Groundwater Level

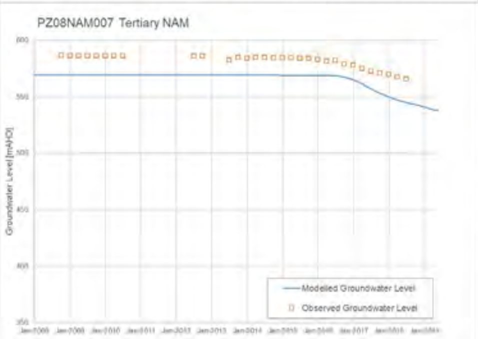
PZ08NAM007 Tertiary NAM
Groundwater Level [mAHD]
Modelled Groundwater Level
Observed Groundwater Level

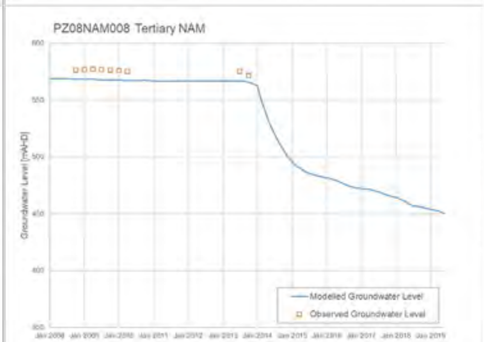
PZ08NAM008 Tertiary NAM
Groundwater Level [mAHD]
Modelled Groundwater Level
Observed Groundwater Level

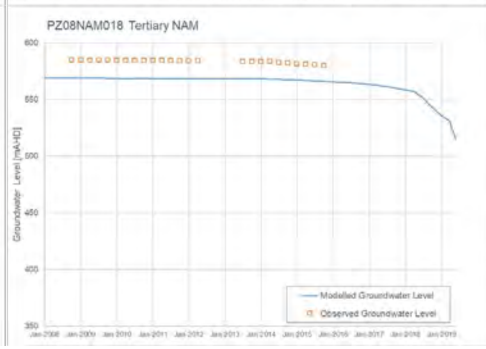
PZ08NAM018 Tertiary NAM
Groundwater Level [mAHD]
Modelled Groundwater Level
Observed Groundwater Level

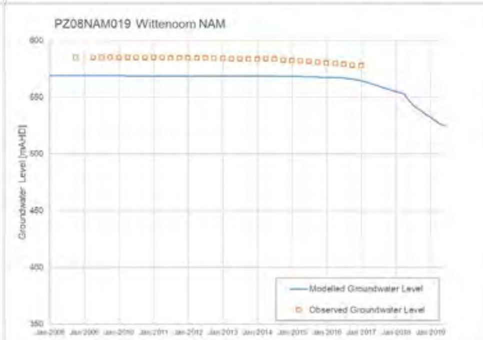
PZ08NAM019 Wittenoom NAM
Groundwater Level [mAHD]
Modelled Groundwater Level
Observed Groundwater Level

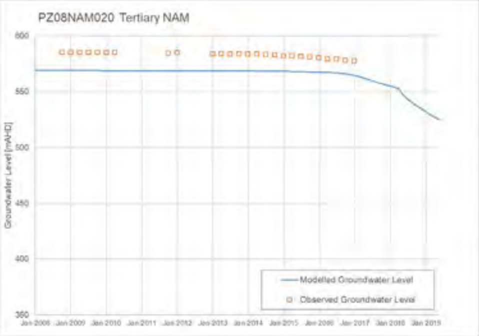
PZ08NAM020 Tertiary NAM
Modelled Groundwater Level
Observed Groundwater Level

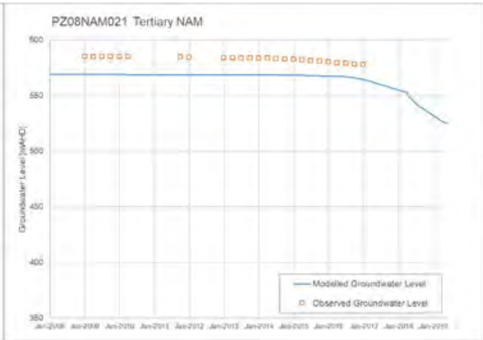
PZ08NAM021 Tertiary NAM
Modelled Groundwater Level
Observed Groundwater Level

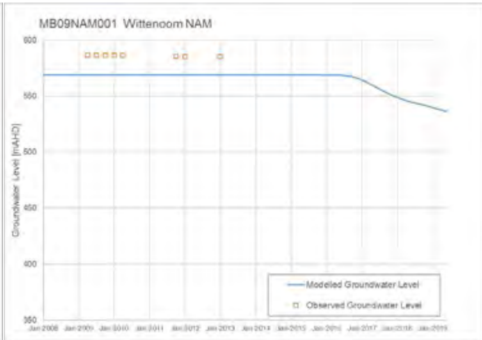
MB09NAM001 Wittenoom NAM
Modelled Groundwater Level
Observed Groundwater Level

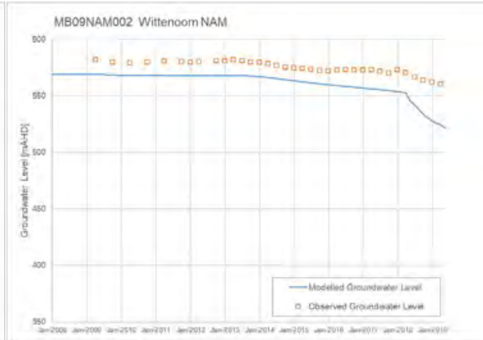
MB09NAM002 Wittenoom NAM
Modelled Groundwater Level
Observed Groundwater Level

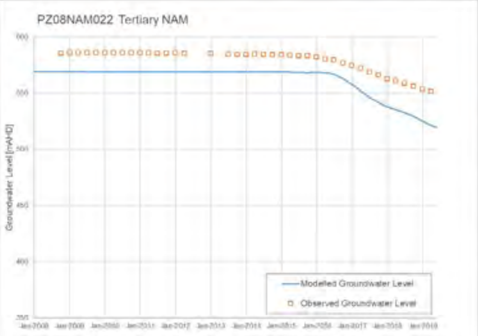
PZ08NAM022 Tertiary NAM
Modelled Groundwater Level
Observed Groundwater Level

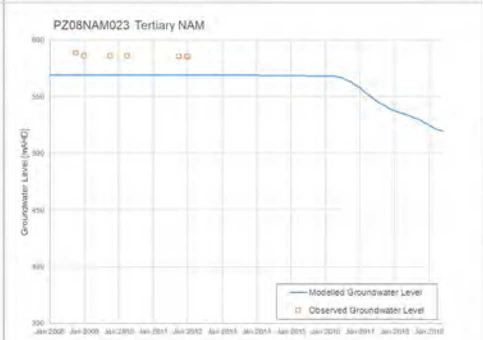
PZ08NAM023 Tertiary NAM
Modelled Groundwater Level
Observed Groundwater Level

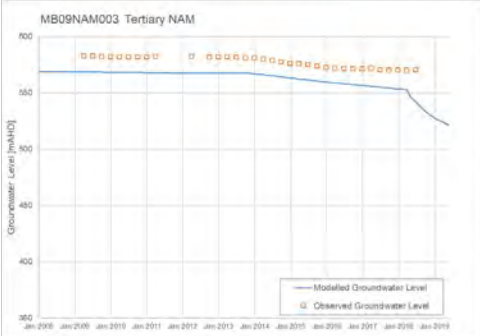
MB09NAM003 Tertiary NAM
Modelled Groundwater Level
Observed Groundwater Level

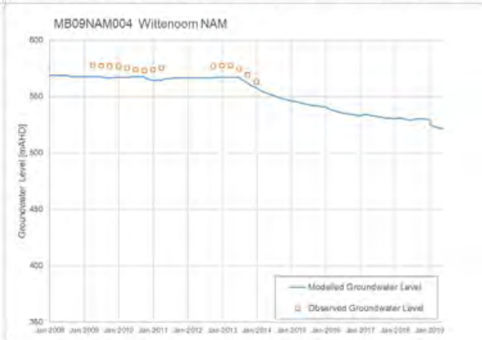
MB09NAM004 Wittenoom NAM
Modelled Groundwater Level
Observed Groundwater Level

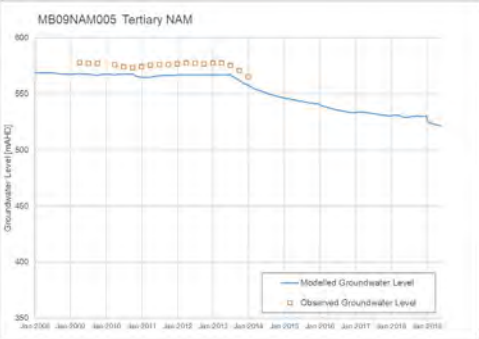
MB09NAM005 Tertiary NAM
Modelled Groundwater Level
Observed Groundwater Level

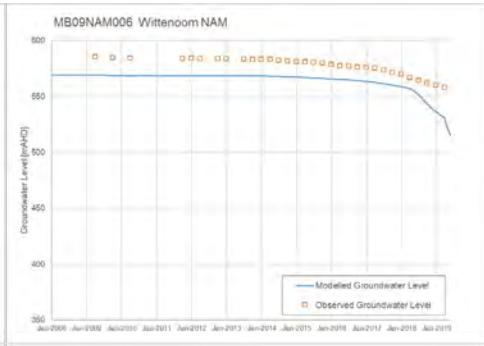
MB09NAM006 Wittenoom NAM
Modelled Groundwater Level
Observed Groundwater Level

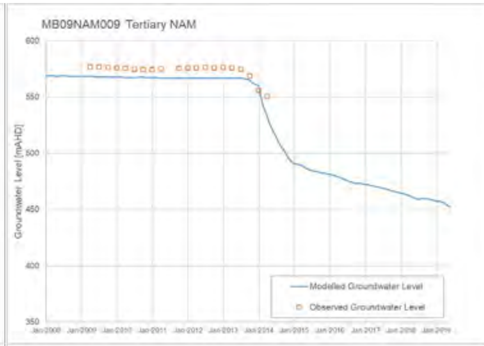
MB09NAM009 Tertiary NAM
Modelled Groundwater Level
Observed Groundwater Level

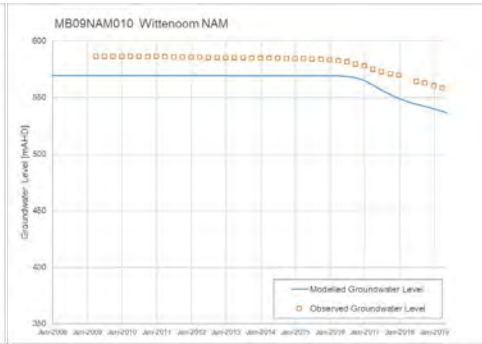
MB09NAM010 Wittenoom NAM
Modelled Groundwater Level
Observed Groundwater Level

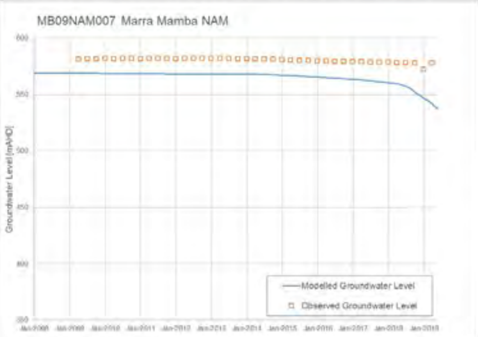
MB09NAM007 Marra Mamba NAM
Modelled Groundwater Level
Observed Groundwater Level

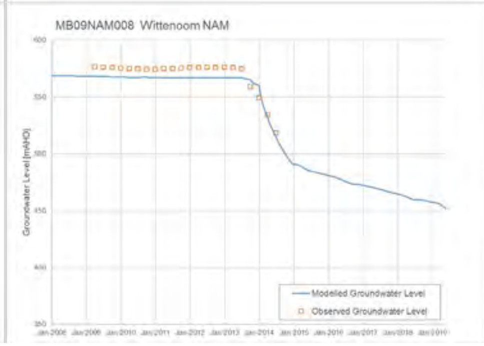
MB09NAM008 Wittenoom NAM
Modelled Groundwater Level
Observed Groundwater Level

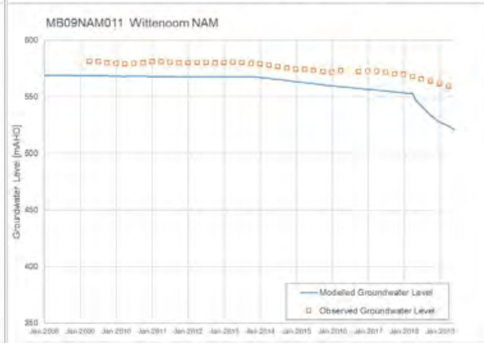
MB09NAM011 Wittenoom NAM
Modelled Groundwater Level
Observed Groundwater Level

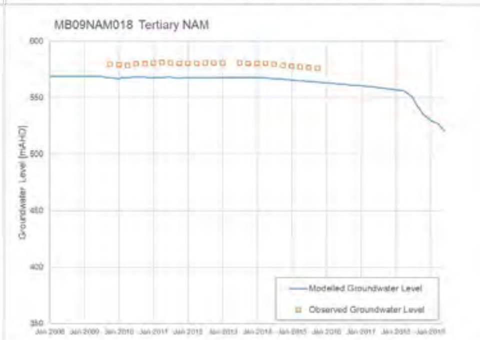
MB09NAM018 Tertiary NAM
Modelled Groundwater Level
Observed Groundwater Level

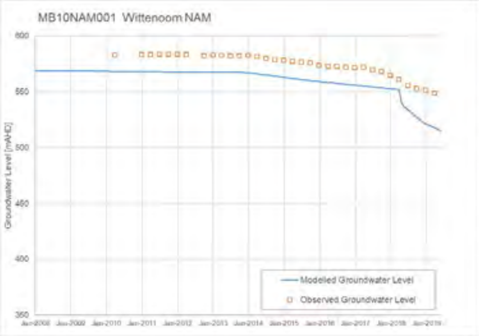
MB10NAM001 Wittenoom NAM
Modelled Groundwater Level
Observed Groundwater Level

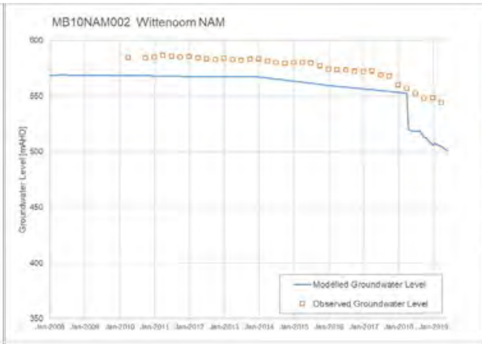
MB10NAM002 Wittenoom NAM
Modelled Groundwater Level
Observed Groundwater Level

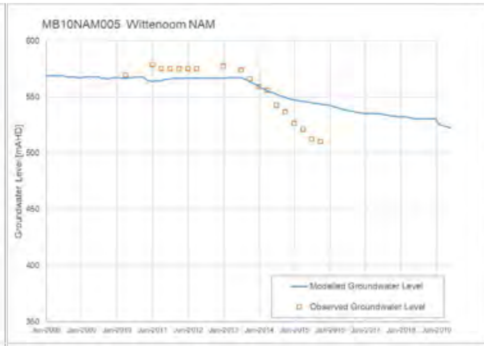
MB10NAM005 Wittenoom NAM
Modelled Groundwater Level
Observed Groundwater Level

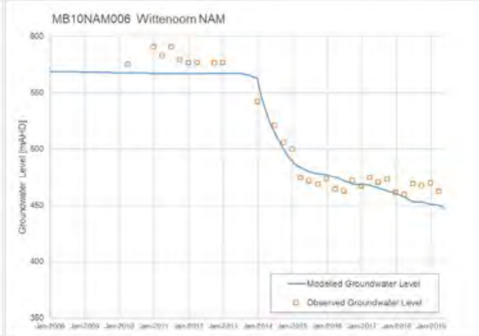
MB10NAM006 Wittenoom NAM
Modelled Groundwater Level
Observed Groundwater Level

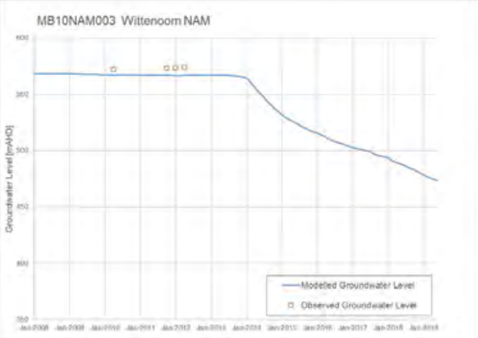
MB10NAM003 Wittenoom NAM
Modelled Groundwater Level
Observed Groundwater Level

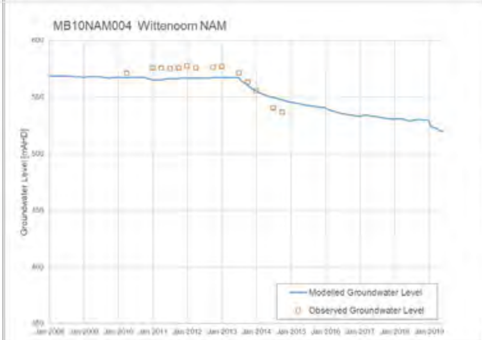
MB10NAM004 Wittenoom NAM
Modelled Groundwater Level
Observed Groundwater Level

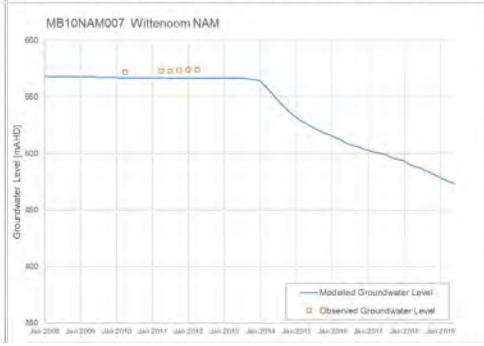
MB10NAM007 Wittenoom NAM
Modelled Groundwater Level
Observed Groundwater Level

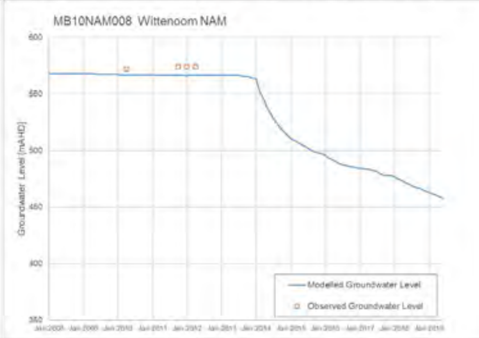
MB10NAM008 Wittenoom NAM
Modelled Groundwater Level
Observed Groundwater Level

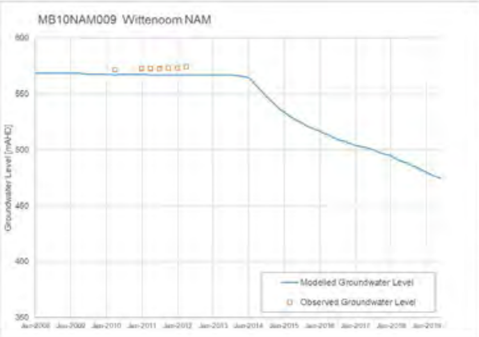
MB10NAM009 Wittenoom NAM
Modelled Groundwater Level
Observed Groundwater Level

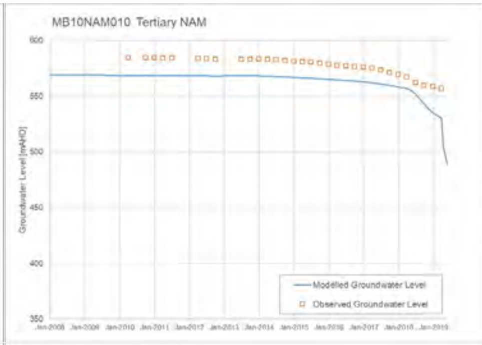
MB10NAM010 Tertiary NAM
Modelled Groundwater Level
Observed Groundwater Level

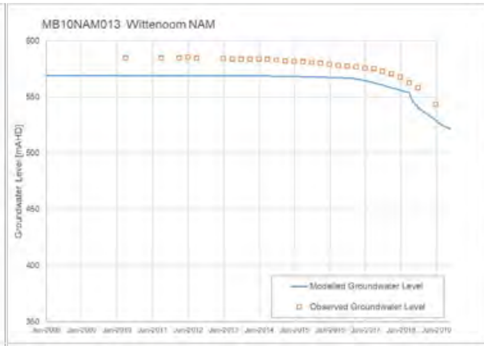
MB10NAM013 Wittenoom NAM
Modelled Groundwater Level
Observed Groundwater Level

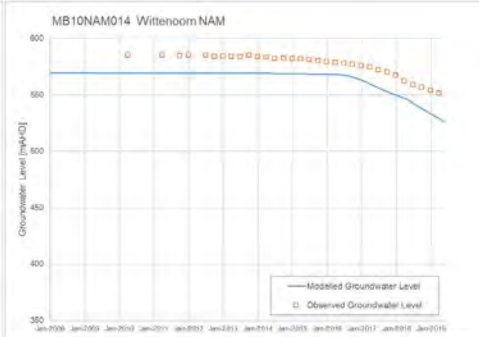
MB10NAM014 Wittenoom NAM
Modelled Groundwater Level
Observed Groundwater Level

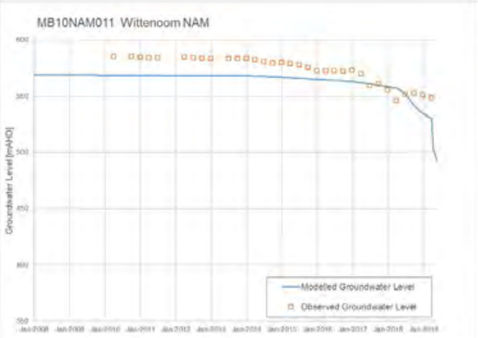
MB10NAM011 Wittenoom NAM
Modelled Groundwater Level
Observed Groundwater Level

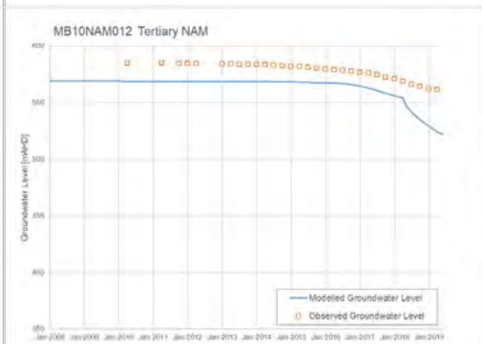
MB10NAM012 Tertiary NAM
Modelled Groundwater Level
Observed Groundwater Level

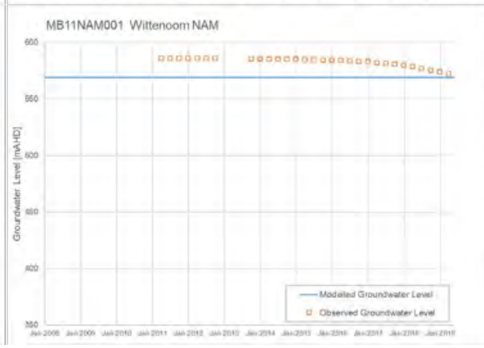
MB11NAM001 Wittenoom NAM
Modelled Groundwater Level
Observed Groundwater Level

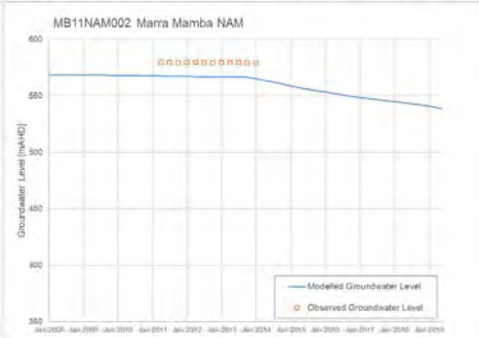
MB11NAM002 Marra Mamba NAM
Modelled Groundwater Level
Observed Groundwater Level

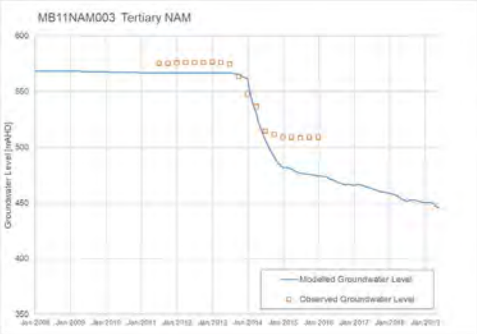
MB11NAM003 Tertiary NAM
Groundwater Level [mAHD]
Modelled Groundwater Level
Observed Groundwater Level

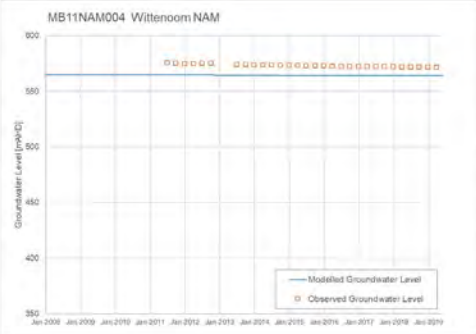
MB11NAM004 Wittenoom NAM
Groundwater Level [mAHD]
Modelled Groundwater Level
Observed Groundwater Level

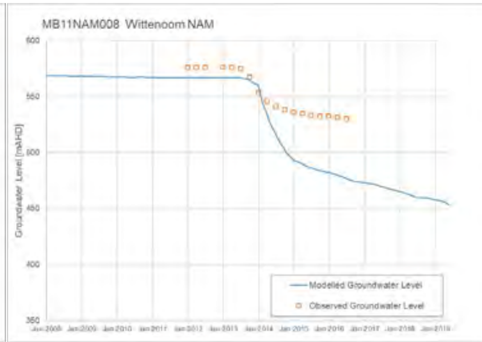
MB11NAM008 Wittenoom NAM
Groundwater Level [mAHD]
Modelled Groundwater Level
Observed Groundwater Level

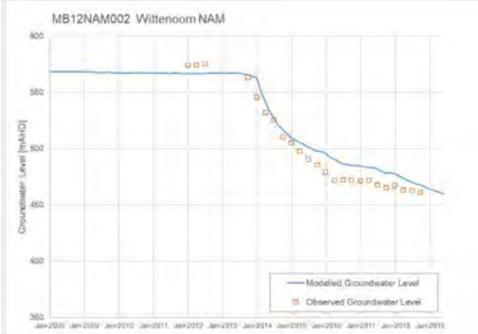
MB12NAM002 Wittenoom NAM
Groundwater Level [mAHD]
Modelled Groundwater Level
Observed Groundwater Level

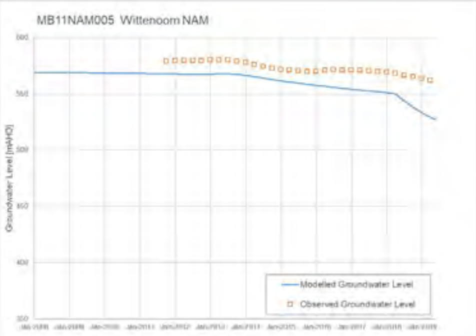
MB11NAM005 Wittenoom NAM
Groundwater Level [mAHD]
Modelled Groundwater Level
Observed Groundwater Level

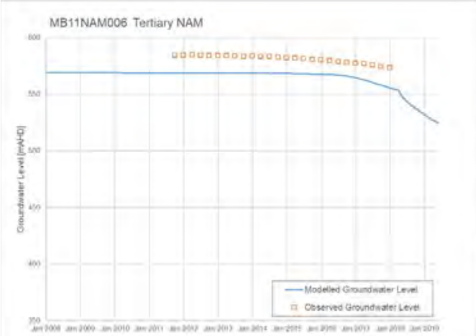
MB11NAM006 Tertiary NAM
Groundwater Level [mAHD]
Modelled Groundwater Level
Observed Groundwater Level

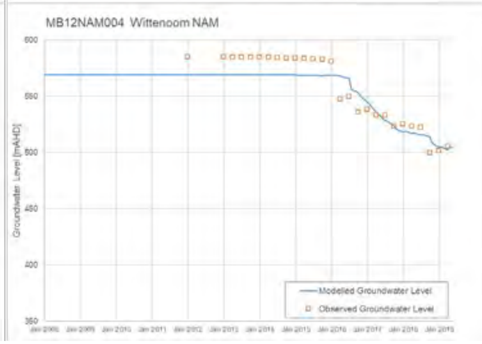
MB12NAM004 Wittenoom NAM
Groundwater Level [mAHD]
Modelled Groundwater Level
Observed Groundwater Level

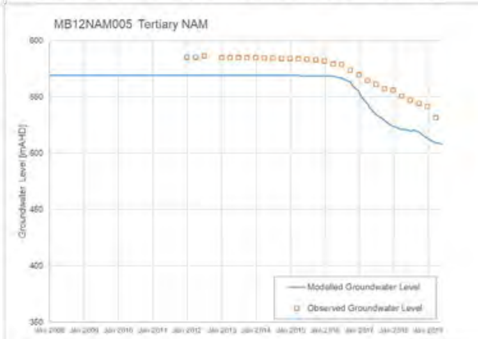
MB12NAM005 Tertiary NAM
Groundwater Level [mAHD]
Modelled Groundwater Level
Observed Groundwater Level

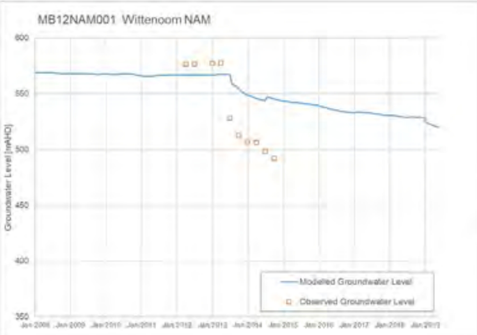
MB12NAM001 Wittenoom NAM
Groundwater Level [mAHD]
Modelled Groundwater Level
Observed Groundwater Level

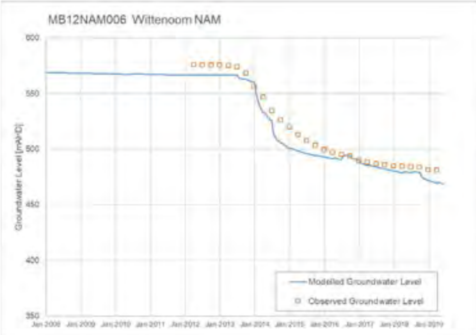
MB12NAM006 Wittenoom NAM
Groundwater Level [mAHD]
Modelled Groundwater Level
Observed Groundwater Level

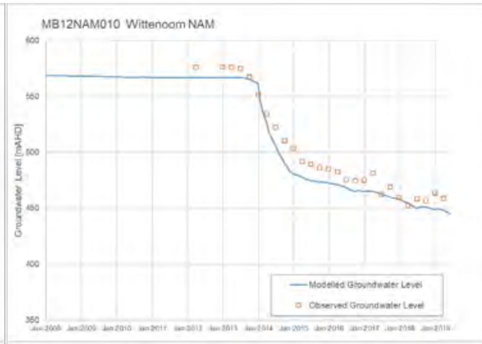
MB12NAM010 Wittenoom NAM
Groundwater Level [mAHD]
Modelled Groundwater Level
Observed Groundwater Level

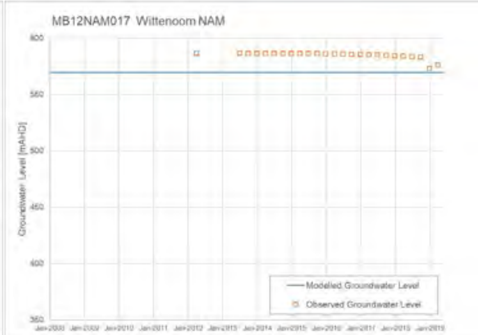
MB12NAM017 Wittenoom NAM
Groundwater Level [mAHD]
Modelled Groundwater Level
Observed Groundwater Level

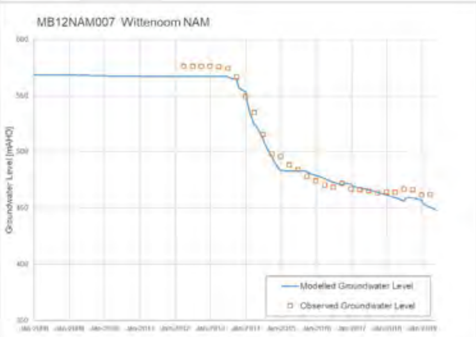
MB12NAM007 Wittenoom NAM
Groundwater Level [mAHD]
Modelled Groundwater Level
Observed Groundwater Level

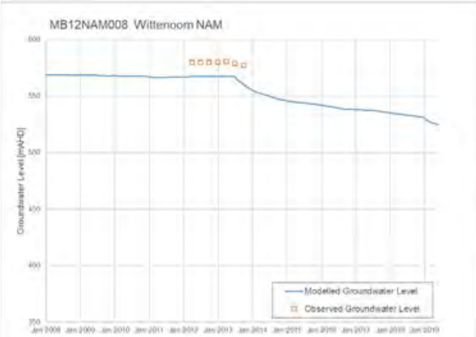
MB12NAM008 Wittenoom NAM
Groundwater Level [mAHD]
Modelled Groundwater Level
Observed Groundwater Level

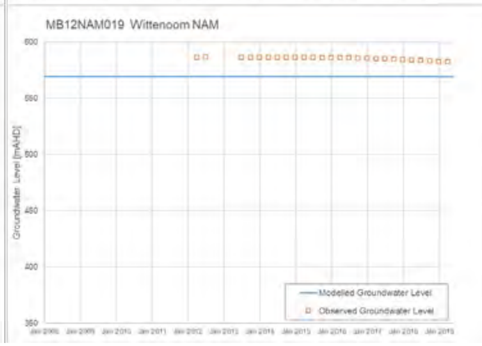
MB12NAM019 Wittenoom NAM
Groundwater Level [mAHD]
Modelled Groundwater Level
Observed Groundwater Level

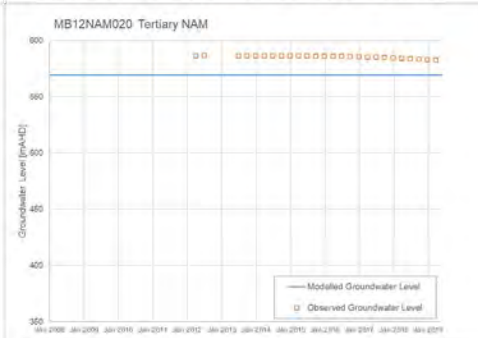
MB12NAM020 Tertiary NAM
Groundwater Level [mAHD]
Modelled Groundwater Level
Observed Groundwater Level

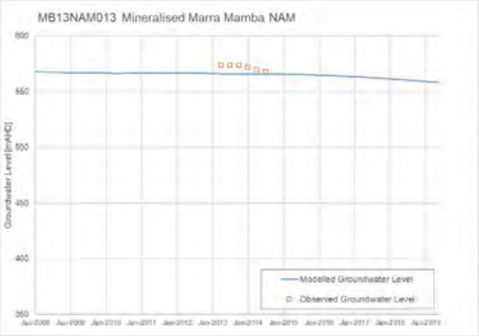
MB13NAM013 Mineralised Marra Mamba NAM
Modelled Groundwater Level
Observed Groundwater Level

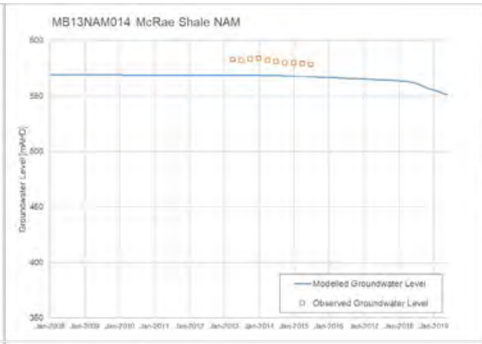
MB13NAM014 McRae Shale NAM
Modelled Groundwater Level
Observed Groundwater Level

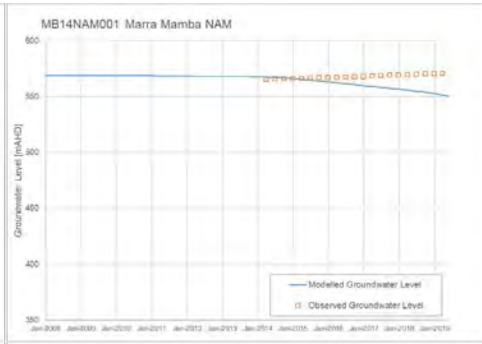
MB14NAM001 Marra Mamba NAM
Modelled Groundwater Level
Observed Groundwater Level

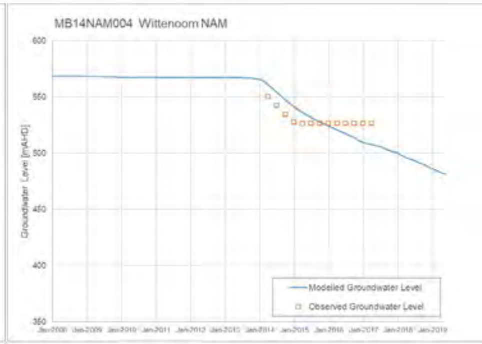
MB14NAM004 Wittenoom NAM
Modelled Groundwater Level
Observed Groundwater Level

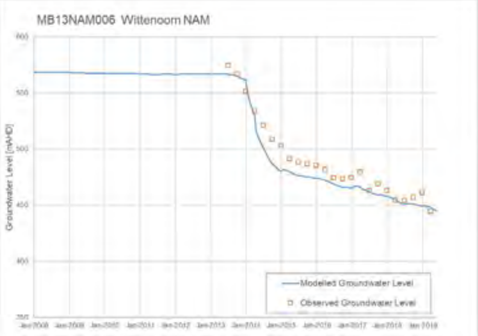
MB13NAM006 Wittenoom NAM
Modelled Groundwater Level
Observed Groundwater Level

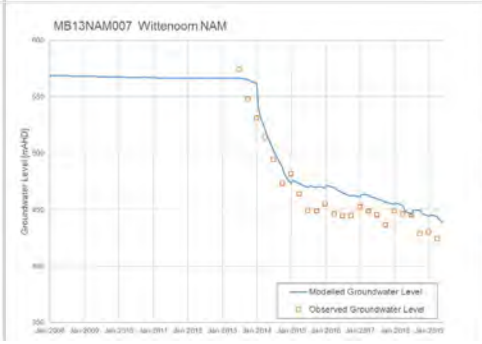
MB13NAM007 Wittenoom NAM
Modelled Groundwater Level
Observed Groundwater Level

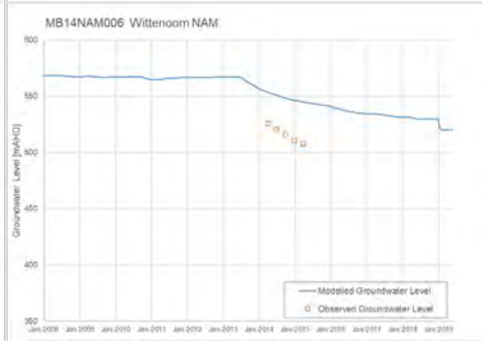
MB14NAM006 Wittenoom NAM
Modelled Groundwater Level
Observed Groundwater Level

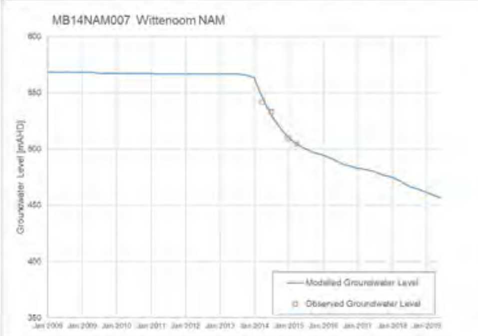
MB14NAM007 Wittenoom NAM
Modelled Groundwater Level
Observed Groundwater Level

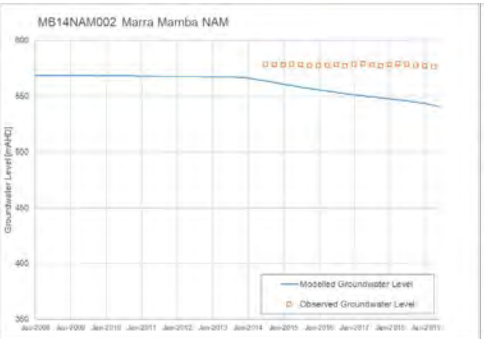
MB14NAM002 Marra Mamba NAM
Modelled Groundwater Level
Observed Groundwater Level

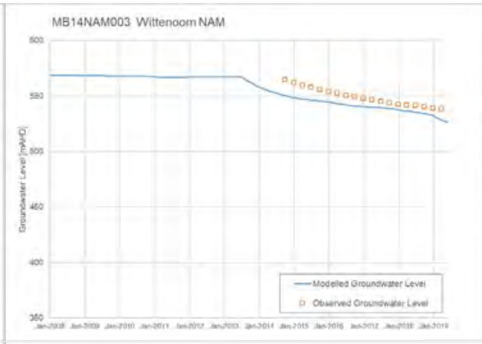
MB14NAM003 Wittenoom NAM
Modelled Groundwater Level
Observed Groundwater Level

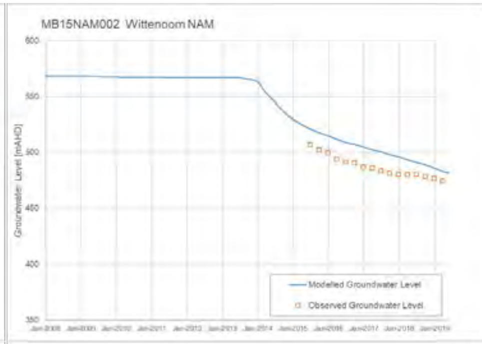
MB15NAM002 Wittenoom NAM
Modelled Groundwater Level
Observed Groundwater Level

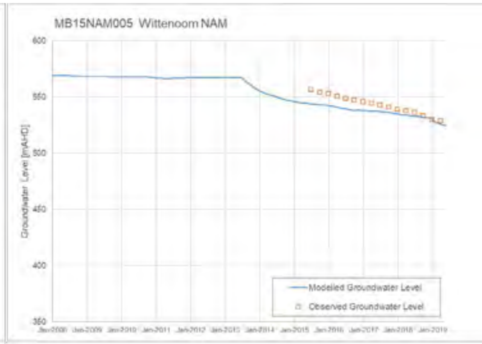
MB15NAM005 Wittenoom NAM
Modelled Groundwater Level
Observed Groundwater Level

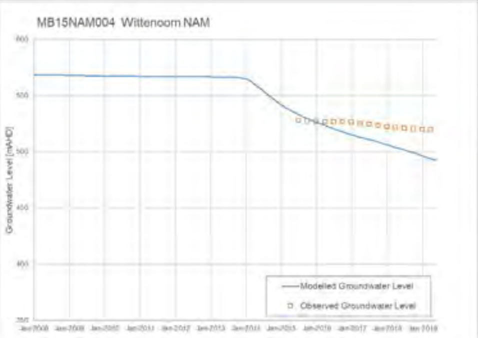
MB15NAM004 Wittenoom NAM
Modelled Groundwater Level
Observed Groundwater Level

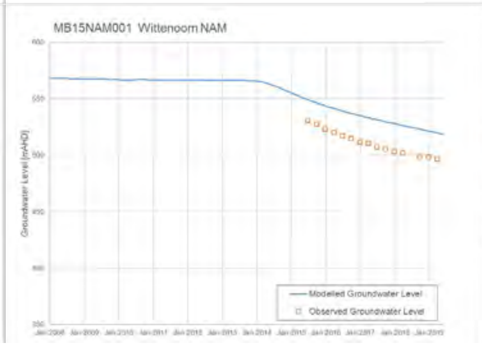
MB15NAM001 Wittenoom NAM
Modelled Groundwater Level
Observed Groundwater Level

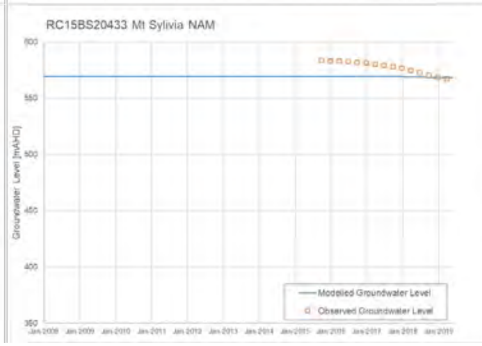
RC15BS20433 Mt Sylvia NAM
Modelled Groundwater Level
Observed Groundwater Level

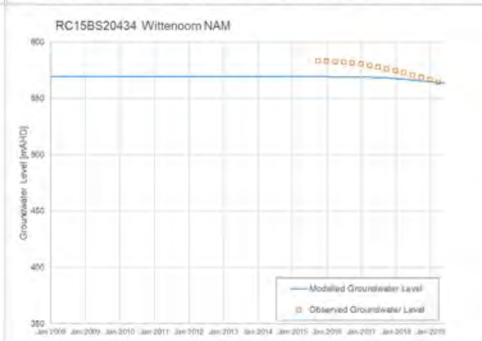
RC15BS20434 Wittenoom NAM
Modelled Groundwater Level
Observed Groundwater Level

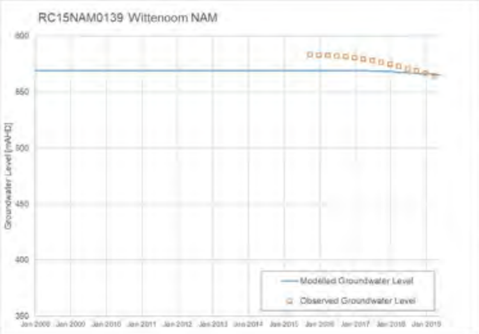
RC15NAM0139 Wittenoom NAM
Groundwater Level [mAHD]
Modelled Groundwater Level
Observed Groundwater Level

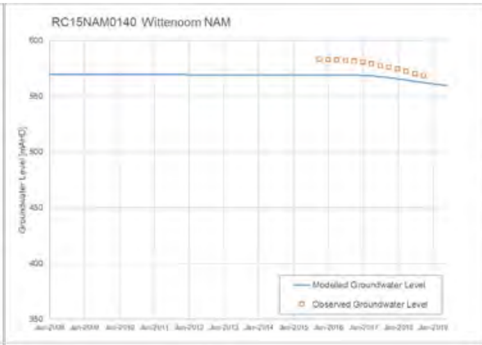
RC15NAM0140 Wittenoom NAM
Groundwater Level [mAHD]
Modelled Groundwater Level
Observed Groundwater Level

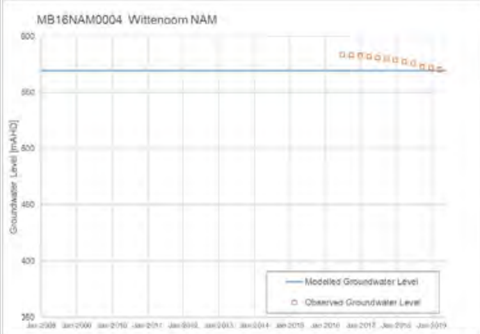
MB16NAM0004 Wittenoom NAM
Groundwater Level [mAHD]
Modelled Groundwater Level
Observed Groundwater Level

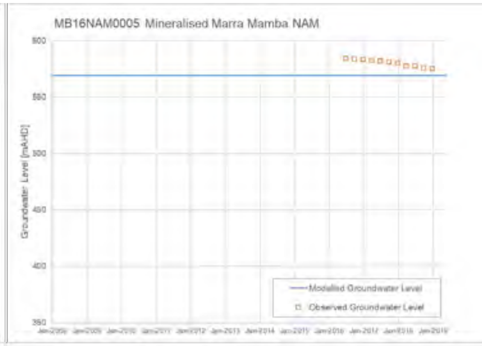
MB16NAM0005 Mineralised Marra Mamba NAM
Groundwater Level [mAHD]
Modelled Groundwater Level
Observed Groundwater Level

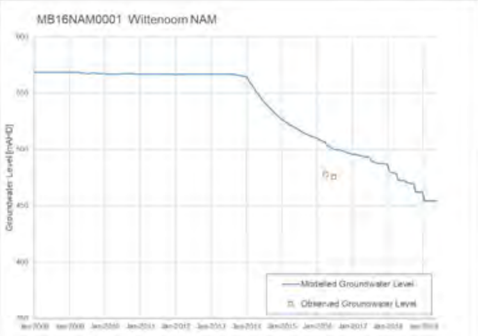
MB16NAM0001 Wittenoom NAM
Groundwater Level [mAHD]
Modelled Groundwater Level
Observed Groundwater Level

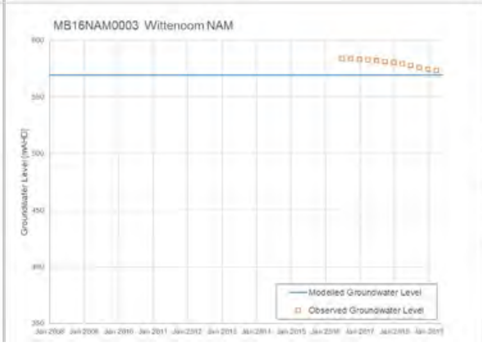
MB16NAM0003 Wittenoom NAM
Groundwater Level [mAHD]
Modelled Groundwater Level
Observed Groundwater Level

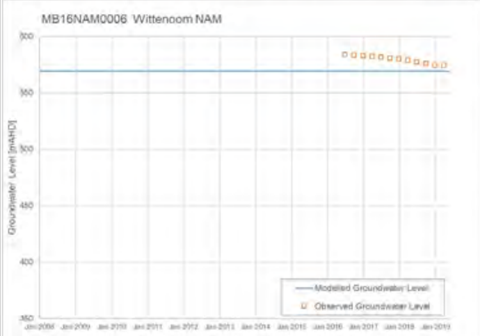
MB16NAM0006 Wittenoom NAM
Groundwater Level [mAHD]
Modelled Groundwater Level
Observed Groundwater Level

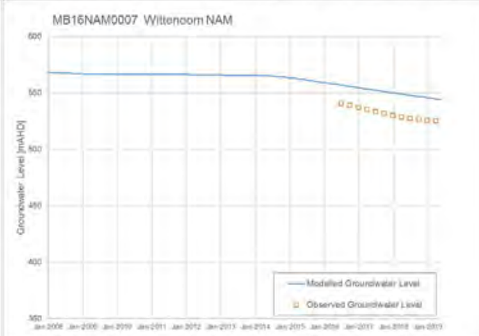
MB16NAM0007 Wittenoom NAM
Groundwater Level [mAHD]
Modelled Groundwater Level
Observed Groundwater Level

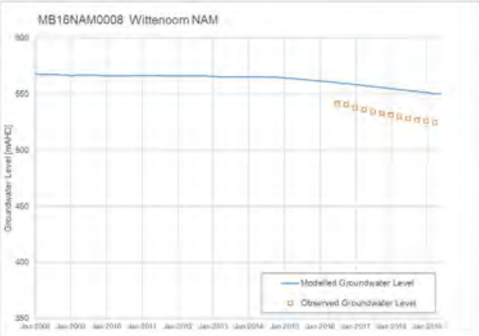
MB16NAM0008 Wittenoom NAM
Groundwater Level [mAHD]
Modelled Groundwater Level
Observed Groundwater Level

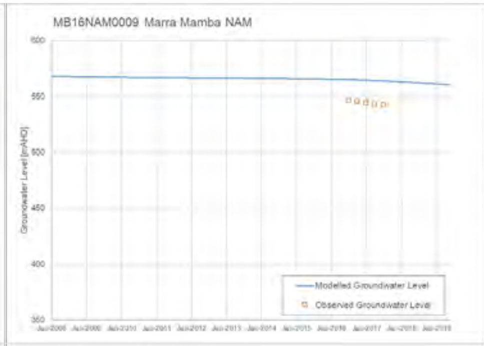
MB16NAM0009 Marra Mamba NAM
Groundwater Level [mAHD]
Modelled Groundwater Level
Observed Groundwater Level

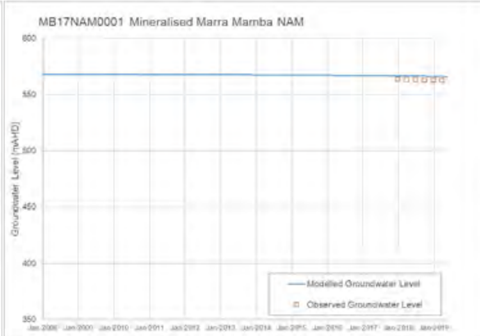
MB17NAM0001 Mineralised Marra Mamba NAM
Groundwater Level [mAHD]
Modelled Groundwater Level
Observed Groundwater Level

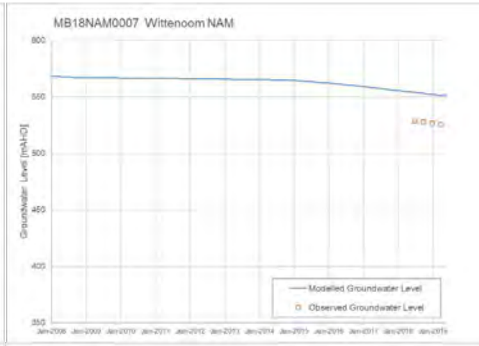
MB18NAM0007 Wittenoom NAM
Groundwater Level [mAHD]
Modelled Groundwater Level
Observed Groundwater Level

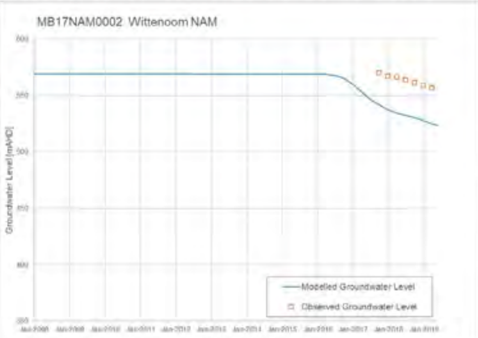
MB17NAM0002 Wittenoom NAM
Groundwater Level [mAHD]
Modelled Groundwater Level
Observed Groundwater Level

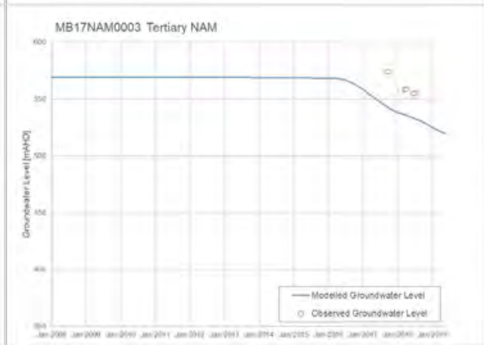
MB17NAM0003 Tertiary NAM
Groundwater Level [mAHD]
Modelled Groundwater Level
Observed Groundwater Level

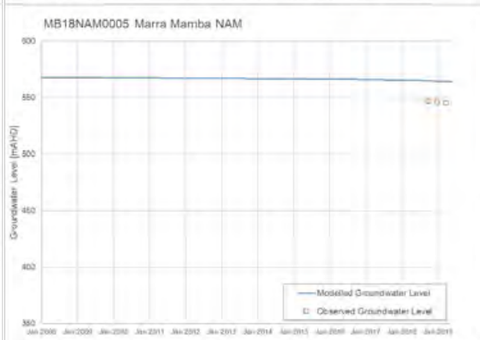
MB18NAM0005 Marra Mamba NAM
Groundwater Level [mAHD]
Modelled Groundwater Level
Observed Groundwater Level

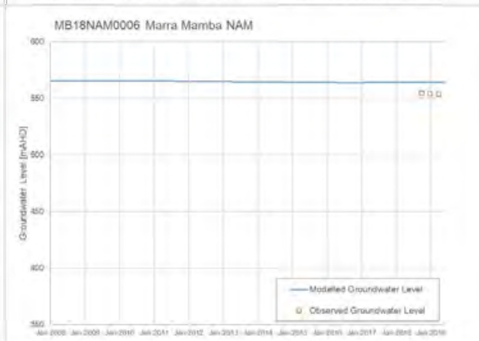
MB18NAM0006 Marra Mamba NAM
Groundwater Level [mAHD]
Modelled Groundwater Level
Observed Groundwater Level

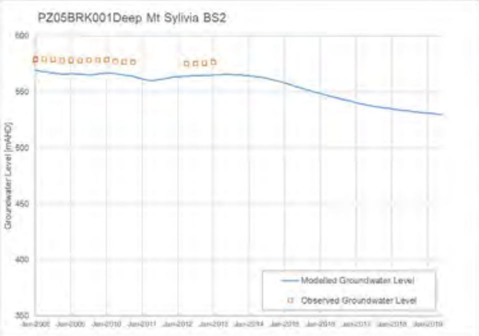
PZ05BRK001Deep Mt Sylivia BS2
Modelled Groundwater Level
Observed Groundwater Level

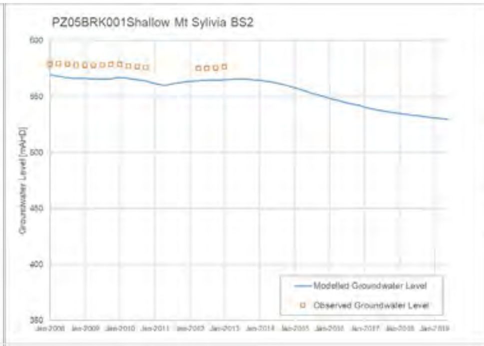
PZ05BRK001Shallow Mt Sylivia BS2
Modelled Groundwater Level
Observed Groundwater Level

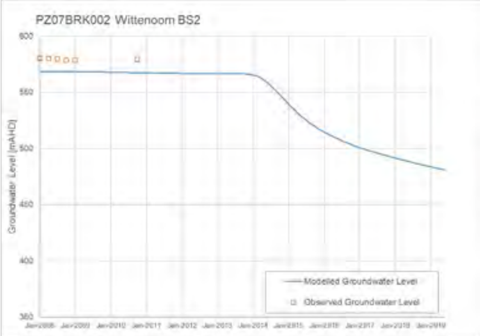
PZ07BRK002 Wittenoom BS2
Modelled Groundwater Level
Observed Groundwater Level

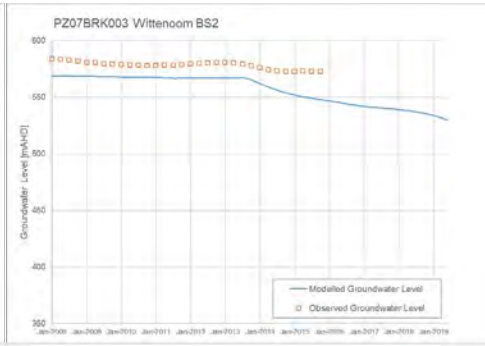
PZ07BRK003 Wittenoom BS2
Modelled Groundwater Level
Observed Groundwater Level

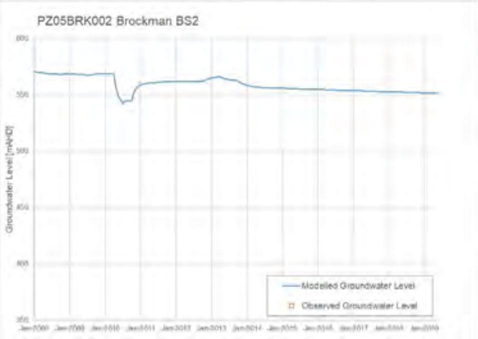
PZ05BRK002 Brockman BS2
Modelled Groundwater Level
Observed Groundwater Level

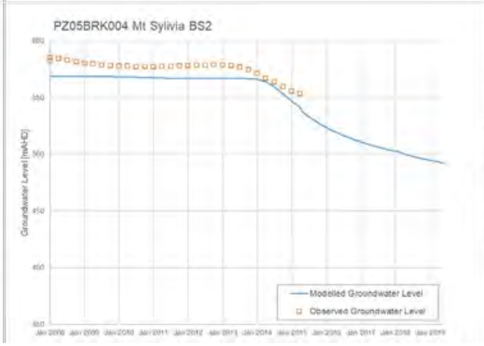
PZ05BRK004 Mt Sylivia BS2
Modelled Groundwater Level
Observed Groundwater Level

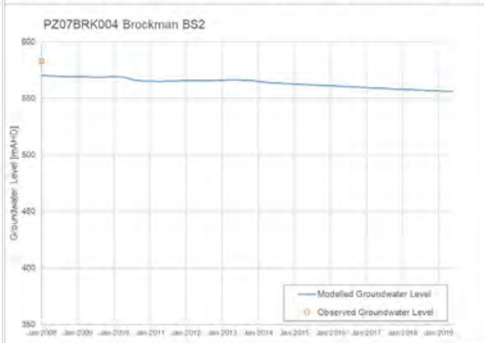
PZ07BRK004 Brockman BS2
Modelled Groundwater Level
Observed Groundwater Level

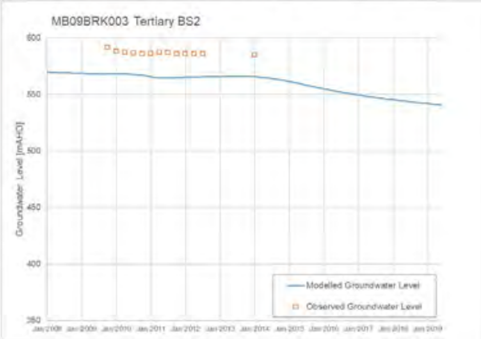
MB09BRK003 Tertiary BS2
Modelled Groundwater Level
Observed Groundwater Level

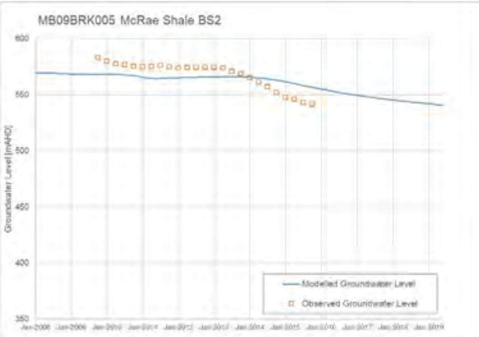
MB09BRK005 McRae Shale BS2
Modelled Groundwater Level
Observed Groundwater Level

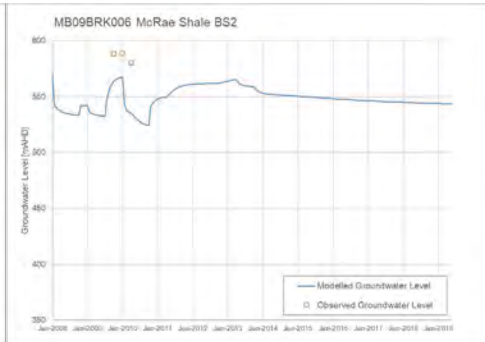
MB09BRK006 McRae Shale BS2
Modelled Groundwater Level
Observed Groundwater Level


MB09BRK011 Wittenoom BS2
Modelled Groundwater Level
Observed Groundwater Level

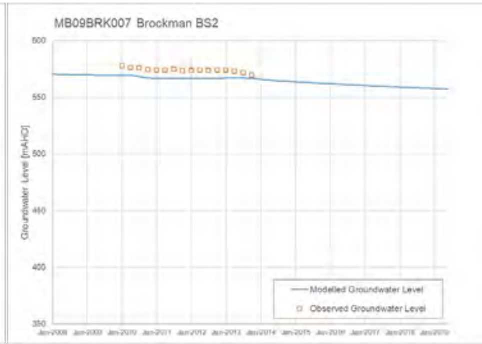
MB09BRK007 Brockman BS2
Modelled Groundwater Level
Observed Groundwater Level

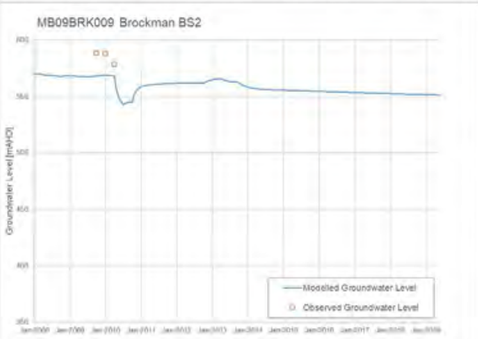
MB09BRK009 Brockman BS2
Modelled Groundwater Level
Observed Groundwater Level

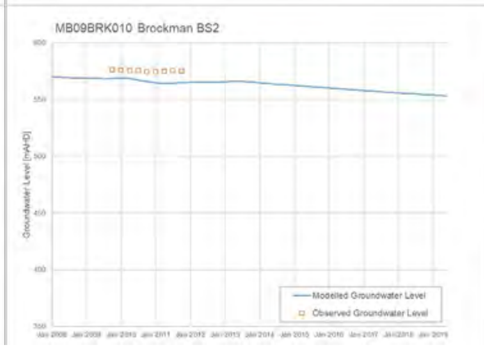
MB09BRK010 Brockman BS2
Modelled Groundwater Level
Observed Groundwater Level

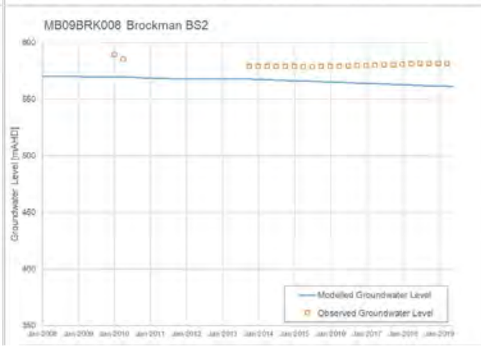
MB09BRK008 Brockman BS2
Modelled Groundwater Level
Observed Groundwater Level

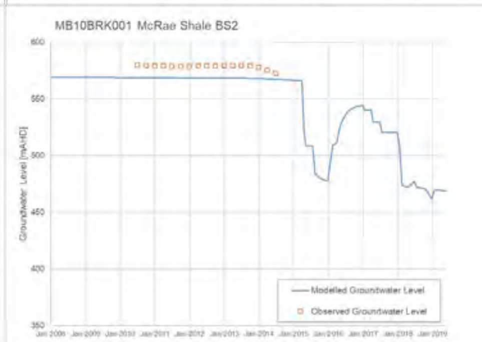
MB10BRK001 McRae Shale BS2
Modelled Groundwater Level
Observed Groundwater Level

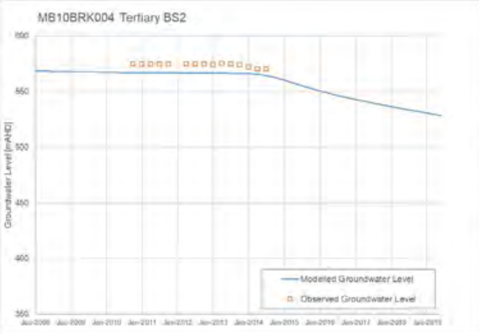
MB10BRK004 Tertiary BS2
Groundwater Level [mAHD]
Modelled Groundwater Level
Observed Groundwater Level

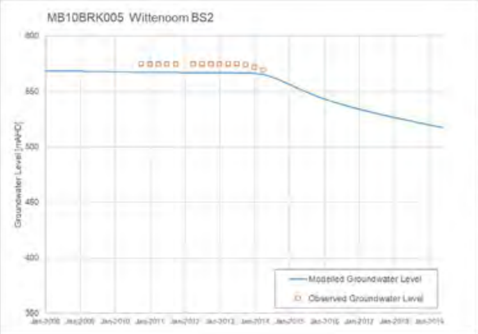
MB10BRK005 Wittenoom BS2
Groundwater Level [mAHD]
Modelled Groundwater Level
Observed Groundwater Level

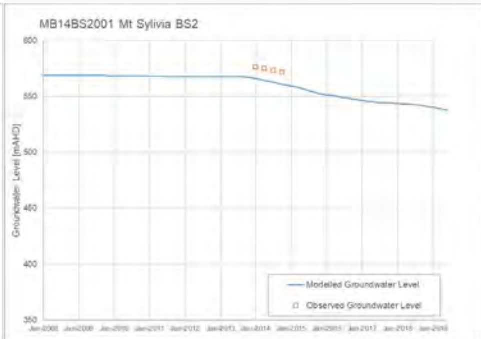
MB14BS2001 Mt Sylivia BS2
Groundwater Level [mAHD]
Modelled Groundwater Level
Observed Groundwater Level

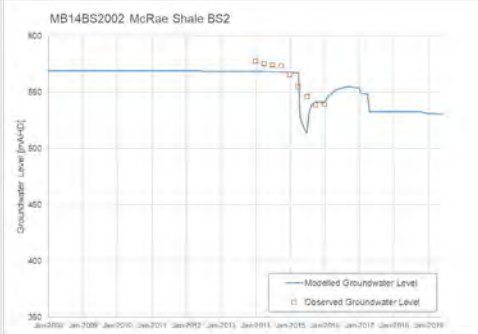
MB14BS2002 McRae Shale BS2
Groundwater Level [mAHD]
Modelled Groundwater Level
Observed Groundwater Level

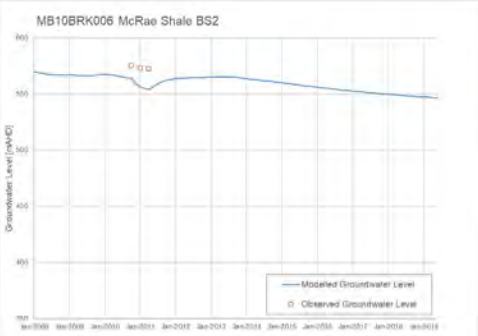
MB10BRK006 McRae Shale BS2
Groundwater Level [mAHD]
Modelled Groundwater Level
Observed Groundwater Level

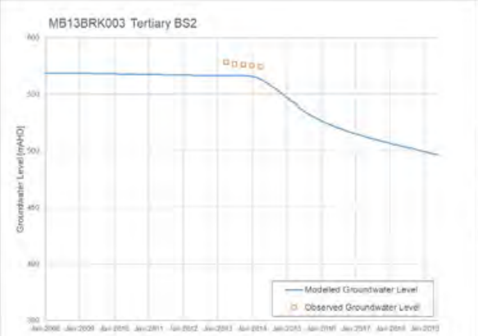
MB13BRK003 Tertiary BS2
Groundwater Level [mAHD]
Modelled Groundwater Level
Observed Groundwater Level

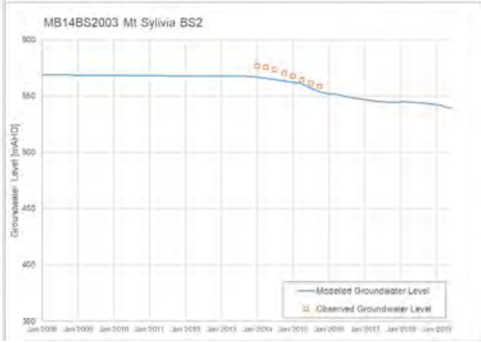
MB14BS2003 Mt Sylivia BS2
Groundwater Level [mAHD]
Modelled Groundwater Level
Observed Groundwater Level

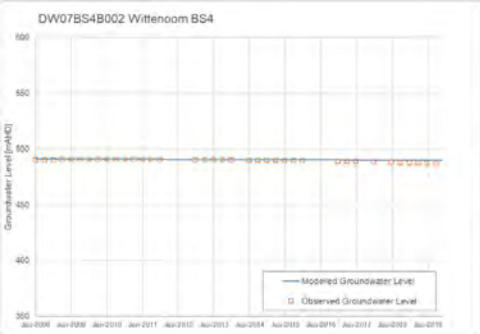
DW07BS4B002 Wittenoom BS4
Groundwater Level [mAHD]
Modelled Groundwater Level
Observed Groundwater Level

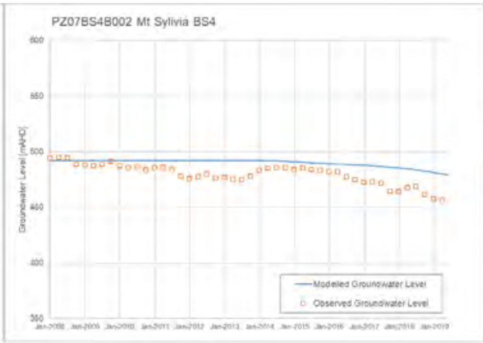
PZ07BS4B002 Mt Sylivia BS4
Groundwater Level [mAHD]
Modelled Groundwater Level
Observed Groundwater Level

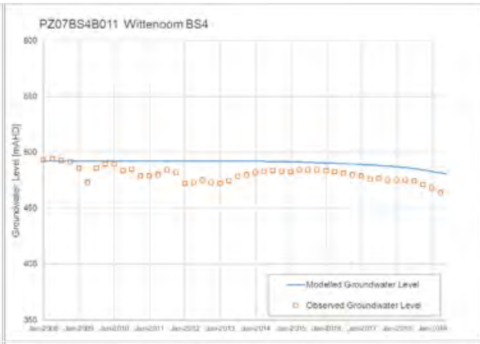
PZ07BS4B011 Wittenoom BS4
Groundwater Level [mAHD]
Modelled Groundwater Level
Observed Groundwater Level

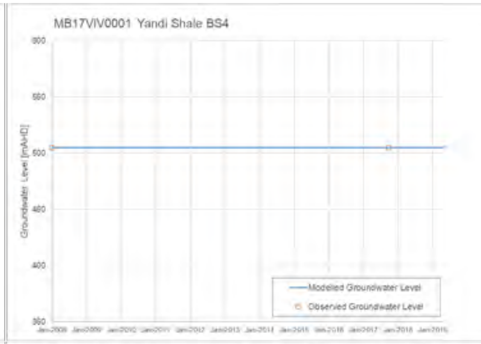
MB17VIV0001 Yandi Shale BS4
Groundwater Level [mAHD]
Modelled Groundwater Level
Observed Groundwater Level

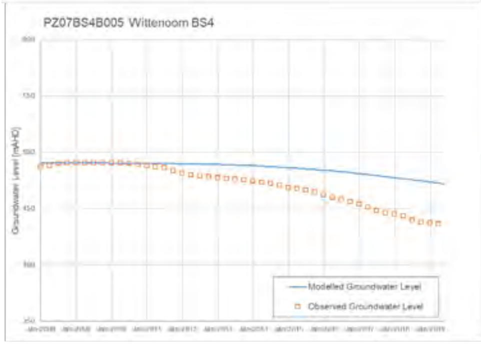
PZ07BS4B005 Wittenoom BS4
Groundwater Level [mAHD]
Modelled Groundwater Level
Observed Groundwater Level

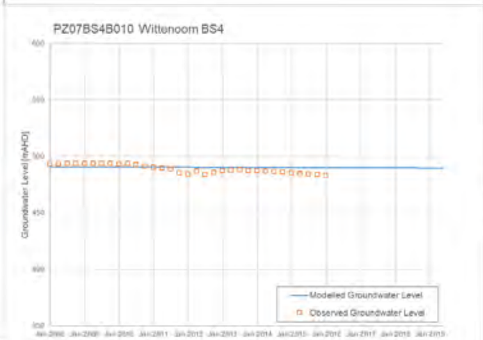
PZ07BS4B010 Wittenoom BS4
Groundwater Level [mAHD]
Modelled Groundwater Level
Observed Groundwater Level

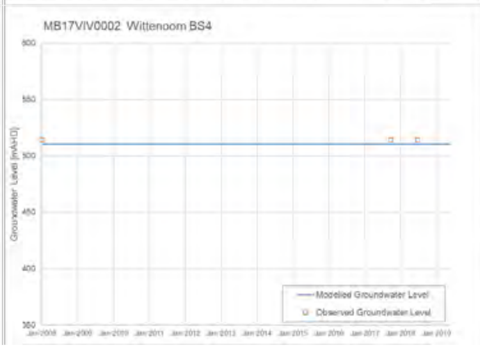
MB17VIV0002 Wittenoom BS4
Groundwater Level [mAHD]
Modelled Groundwater Level
Observed Groundwater Level

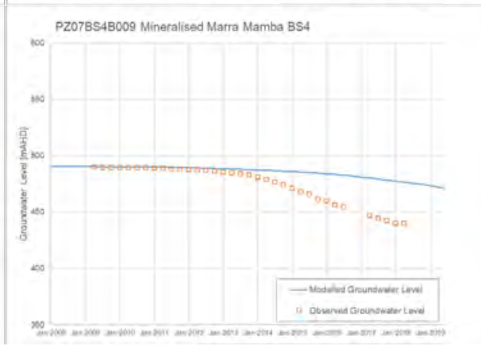
PZ07BS4B009 Mineralised Marra Mamba BS4
Groundwater Level [mAHD]
Modelled Groundwater Level
Observed Groundwater Level

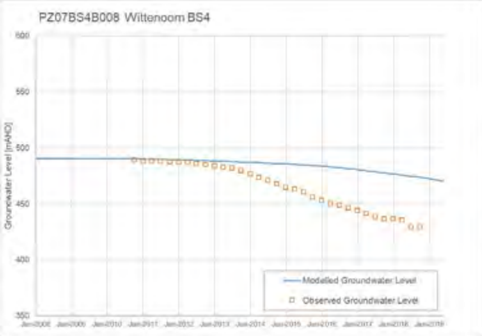
PZ07BS4B008 Wittenoom BS4
Groundwater Level [mAHD]
Modelled Groundwater Level
Observed Groundwater Level

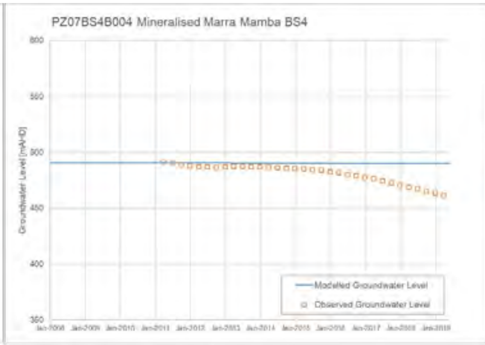
PZ07BS4B004 Mineralised Marra Mamba BS4
Groundwater Level [mAHD]
Modelled Groundwater Level
Observed Groundwater Level

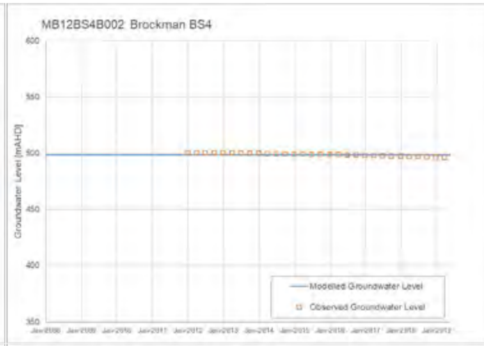
MB12BS4B002 Brockman BS4
Groundwater Level [mAHD]
Modelled Groundwater Level
Observed Groundwater Level

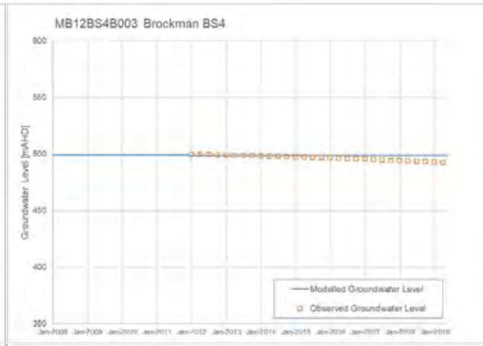
MB12BS4B003 Brockman BS4
Groundwater Level [mAHD]
Modelled Groundwater Level
Observed Groundwater Level

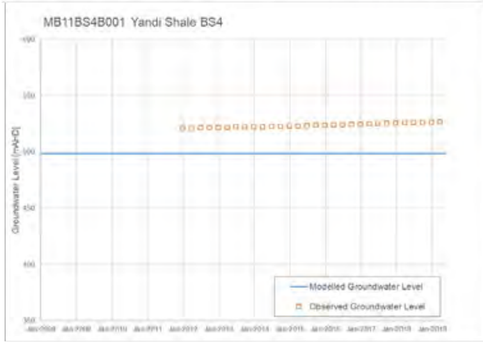
MB11BS4B001 Yandi Shale BS4
Groundwater Level [mAHD]
Modelled Groundwater Level
Observed Groundwater Level

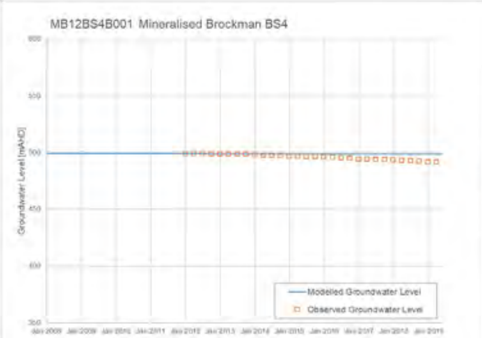
MB12BS4B001 Mineralised Brockman BS4
Groundwater Level [mAHD]
Modelled Groundwater Level
Observed Groundwater Level

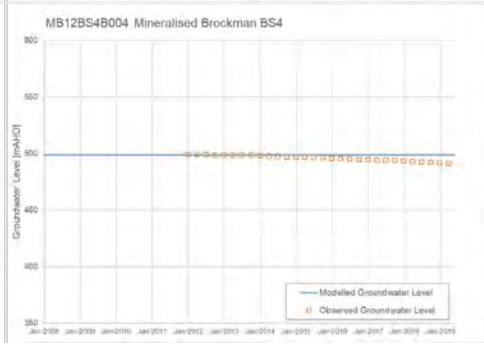
MB12BS4B004 Mineralised Brockman BS4
Groundwater Level [mAHD]
Modelled Groundwater Level
Observed Groundwater Level

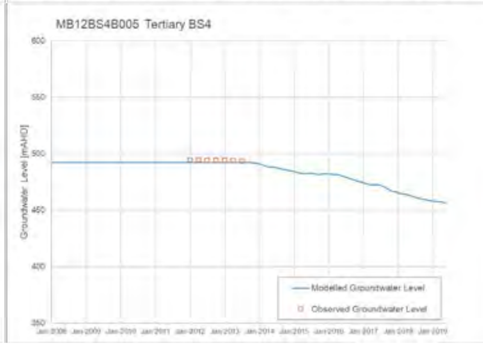
MB12BS4B005 Tertiary BS4
Groundwater Level [mAHD]
Modelled Groundwater Level
Observed Groundwater Level

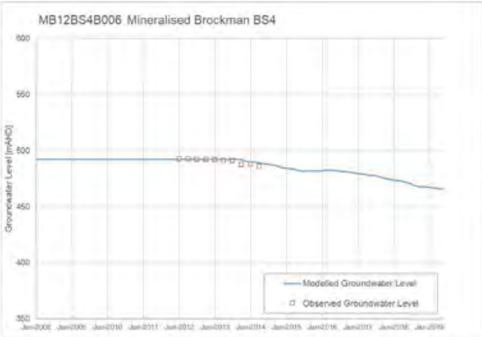
MB12BS4B006 Mineralised Brockman BS4
Groundwater Level [mAHD]
Modelled Groundwater Level
Observed Groundwater Level

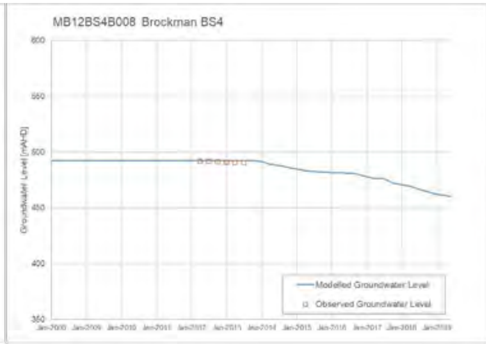
MB12BS4B008 Brockman BS4
Groundwater Level [mAHD]
Modelled Groundwater Level
Observed Groundwater Level

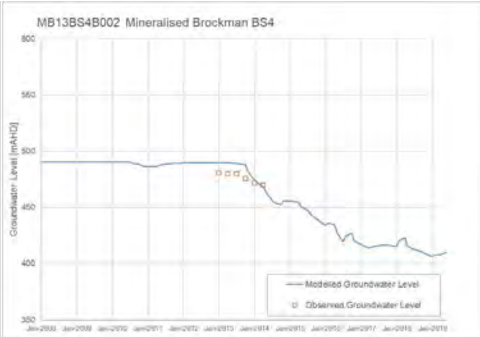
MB13BS4B002 Mineralised Brockman BS4
Groundwater Level [mAHD]
Modelled Groundwater Level
Observed Groundwater Level

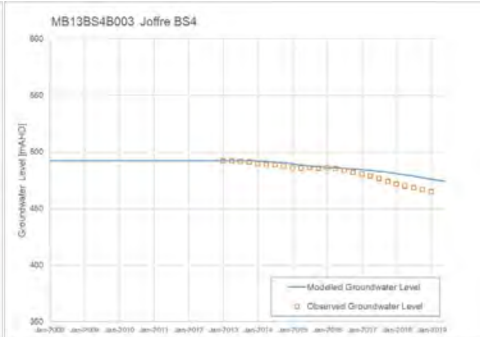
MB13BS4B003 Joffre BS4
Groundwater Level [mAHD]
Modelled Groundwater Level
Observed Groundwater Level

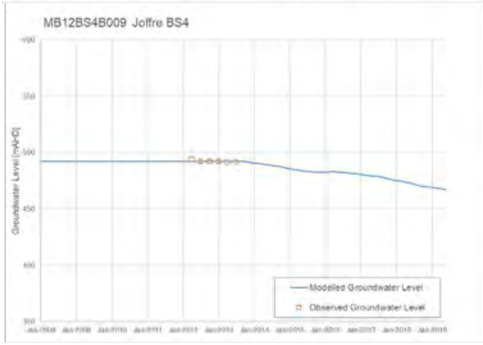
MB12BS4B009 Joffre BS4
Groundwater Level [mAHD]
Modelled Groundwater Level
Observed Groundwater Level

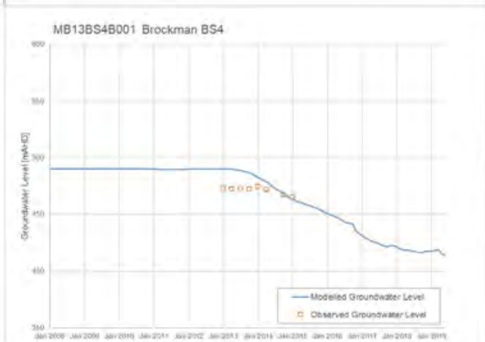
MB13BS4B001 Brockman BS4
Groundwater Level [mAHD]
Modelled Groundwater Level
Observed Groundwater Level

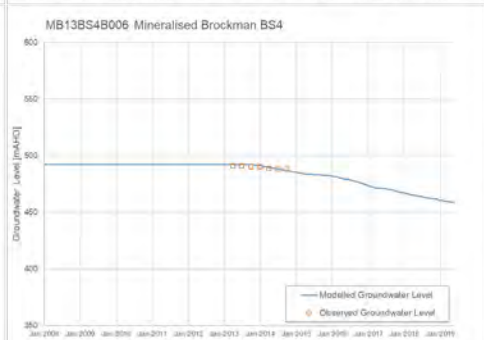
MB13BS4B006 Mineralised Brockman BS4
Groundwater Level [mAHD]
Modelled Groundwater Level
Observed Groundwater Level

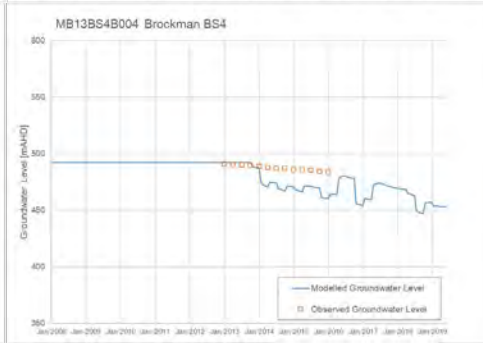
MB13BS4B004 Brockman BS4
Groundwater Level [mAHD]
Modelled Groundwater Level
Observed Groundwater Level

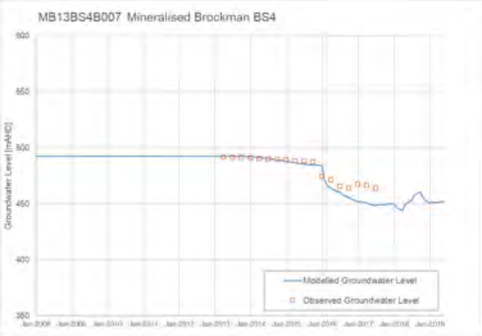
MB13BS4B007 Mineralised Brockman BS4
Groundwater Level [mAHD]
Modelled Groundwater Level
Observed Groundwater Level

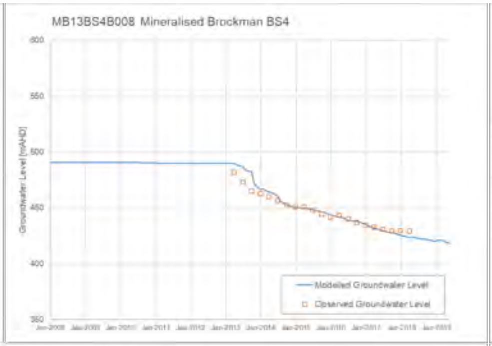
MB13BS4B008 Mineralised Brockman BS4
Groundwater Level [mAHD]
Modelled Groundwater Level
Observed Groundwater Level

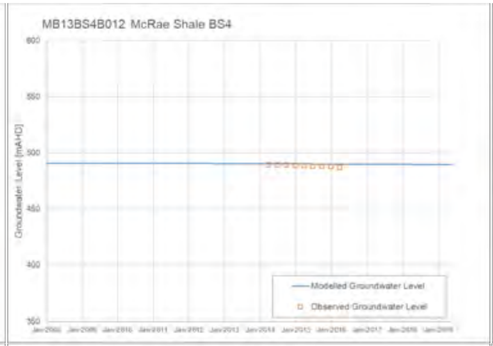
MB13BS4B012 McRae Shale BS4
Groundwater Level [mAHD]
Modelled Groundwater Level
Observed Groundwater Level

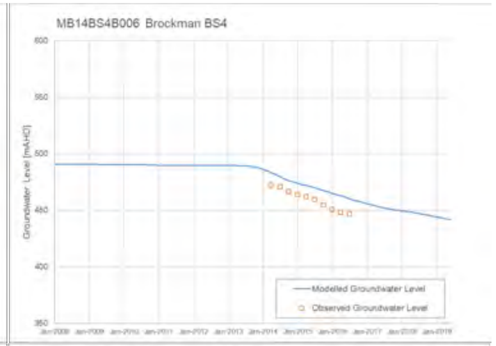
MB14BS4B006 Brockman BS4
Groundwater Level [mAHD]
Modelled Groundwater Level
Observed Groundwater Level

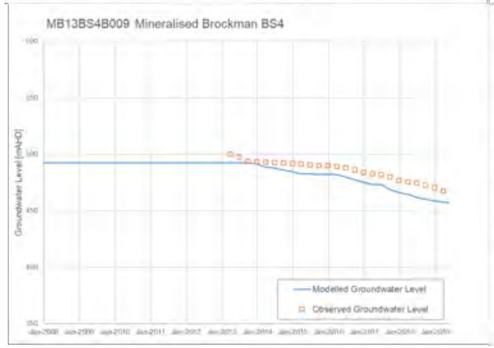
MB13BS4B009 Mineralised Brockman BS4
Groundwater Level [mAHD]
Modelled Groundwater Level
Observed Groundwater Level

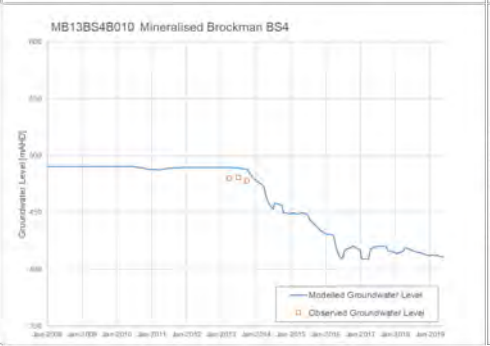
MB13BS4B010 Mineralised Brockman BS4
Groundwater Level [mAHD]
Modelled Groundwater Level
Observed Groundwater Level

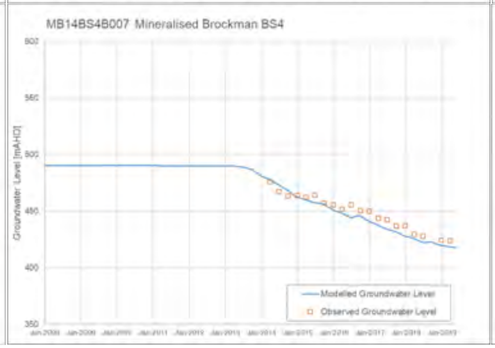
MB14BS4B007 Mineralised Brockman BS4
Groundwater Level [mAHD]
Modelled Groundwater Level
Observed Groundwater Level

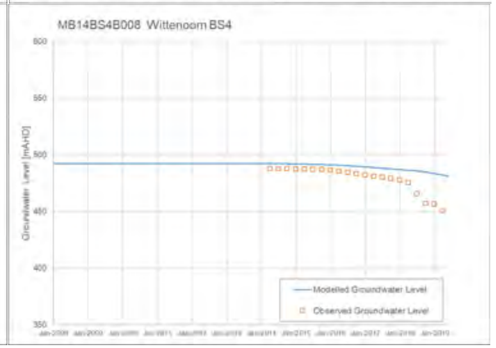
MB14BS4B008 Wittenoom BS4
Groundwater Level [mAHD]
Modelled Groundwater Level
Observed Groundwater Level

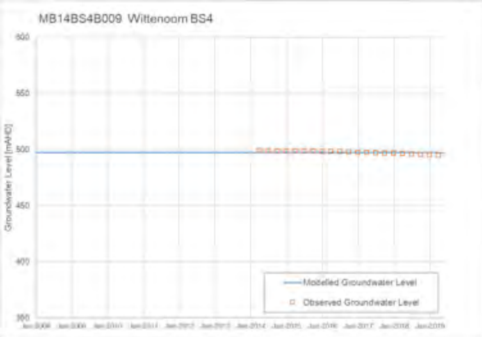
MB14BS4B009 Wittenoom BS4
Groundwater Level [mAHD]
Modelled Groundwater Level
Observed Groundwater Level

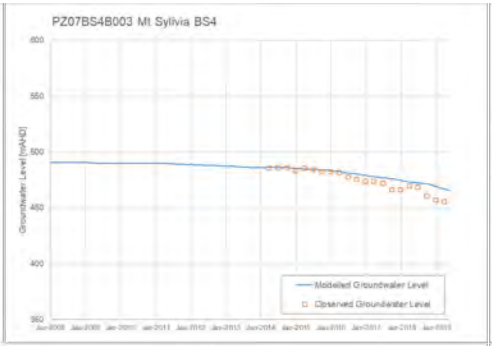
PZ07BS4B003 Mt Sylivia BS4
Groundwater Level [mAHD]
Modelled Groundwater Level
Observed Groundwater Level

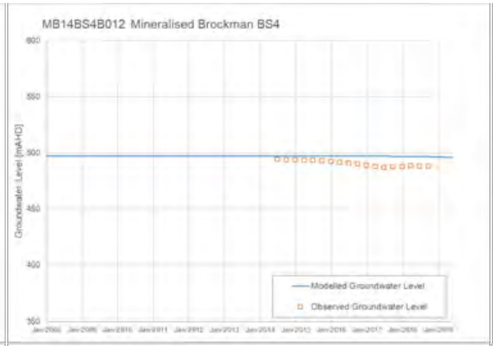
MB14BS4B012 Mineralised Brockman BS4
Groundwater Level [mAHD]
Modelled Groundwater Level
Observed Groundwater Level

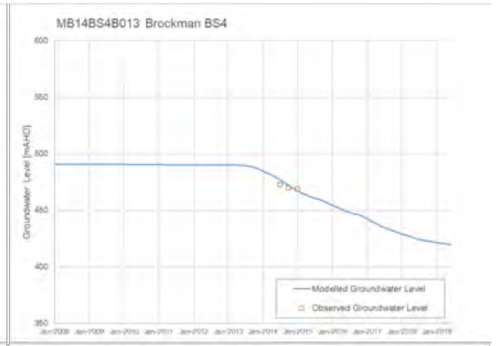
MB14BS4B013 Brockman BS4
Groundwater Level [mAHD]
Modelled Groundwater Level
Observed Groundwater Level

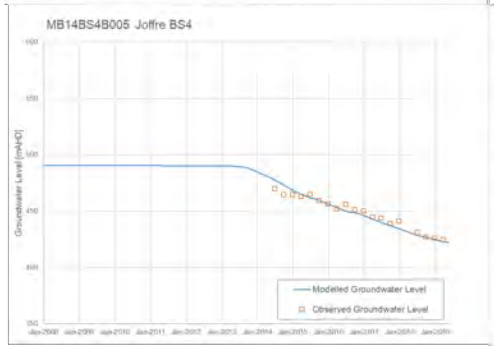
MB14BS4B005 Joffre BS4
Groundwater Level [mAHD]
Modelled Groundwater Level
Observed Groundwater Level

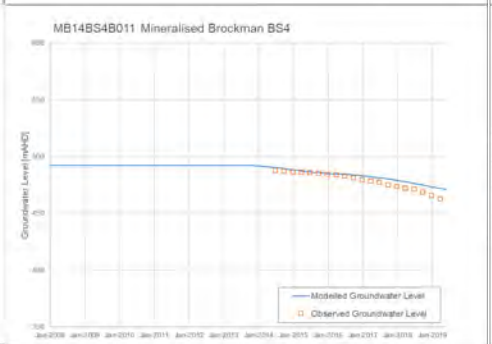
MB14BS4B011 Mineralised Brockman BS4
Groundwater Level [mAHD]
Modelled Groundwater Level
Observed Groundwater Level

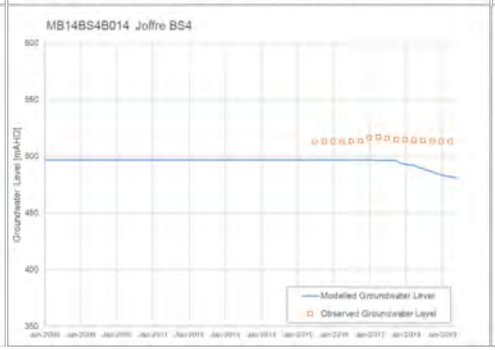
MB14BS4B014 Joffre BS4
Groundwater Level [mAHD]
Modelled Groundwater Level
Observed Groundwater Level

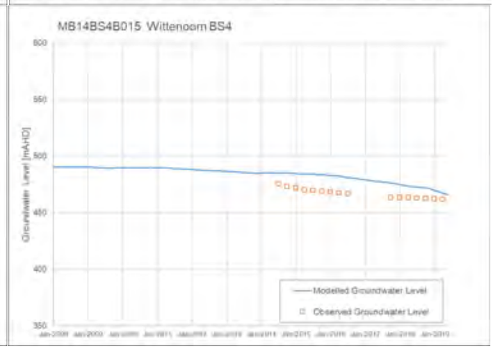
MB14BS4B015 Wittenoom BS4
Groundwater Level [mAHD]
Modelled Groundwater Level
Observed Groundwater Level

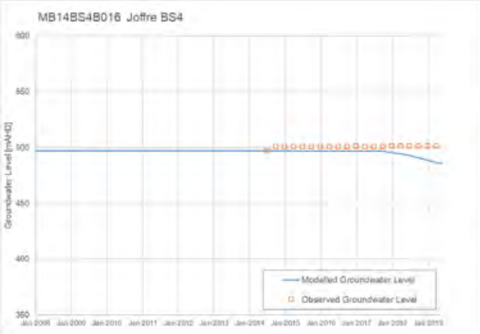
MB14BS4B016 Joffre BS4
Modelled Groundwater Level
Observed Groundwater Level

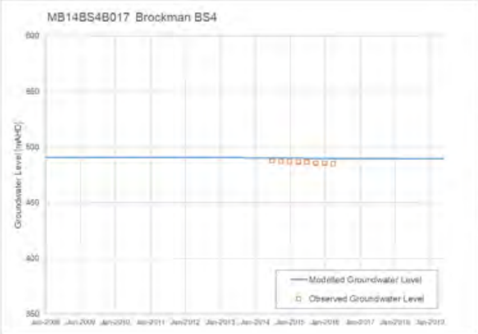
MB14BS4B017 Brockman BS4
Modelled Groundwater Level
Observed Groundwater Level

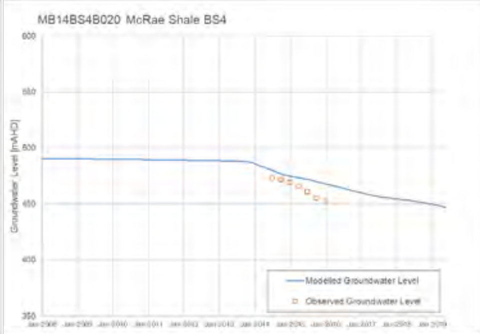
MB14BS4B020 McRae Shale BS4
Modelled Groundwater Level
Observed Groundwater Level

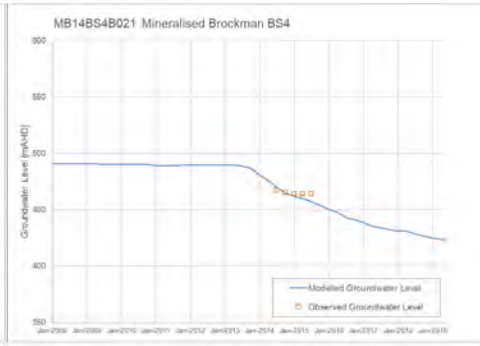
MB14BS4B021 Mineralised Brockman BS4
Modelled Groundwater Level
Observed Groundwater Level

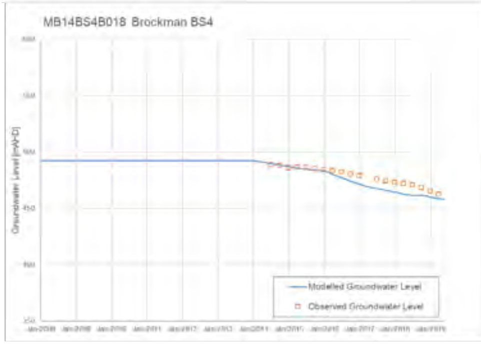
MB14BS4B018 Brockman BS4
Modelled Groundwater Level
Observed Groundwater Level

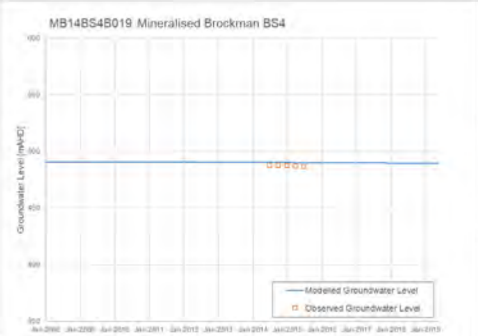
MB14BS4B019 Mineralised Brockman BS4
Modelled Groundwater Level
Observed Groundwater Level

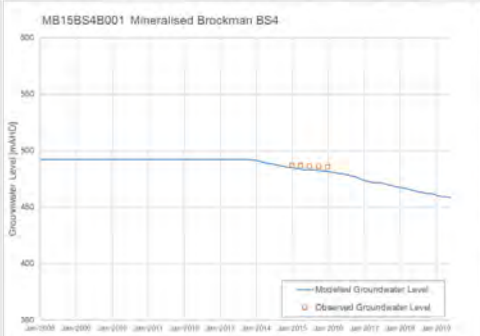
MB15BS4B001 Mineralised Brockman BS4
Modelled Groundwater Level
Observed Groundwater Level

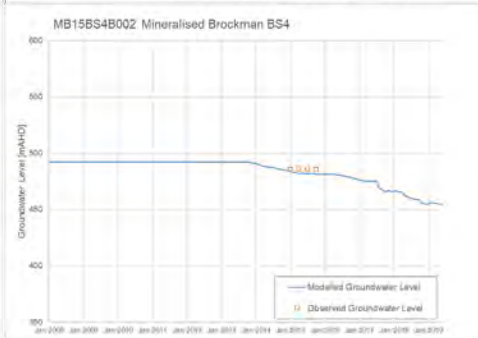
MB15BS4B002 Mineralised Brockman BS4
Modelled Groundwater Level
Observed Groundwater Level

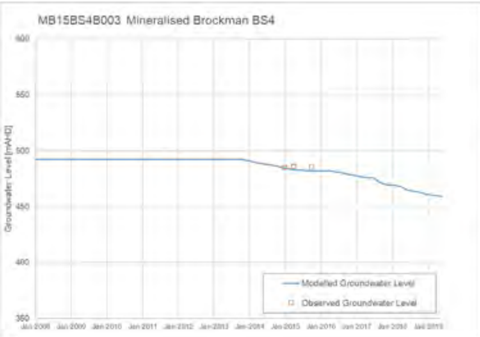
MB15BS4B003 Mineralised Brockman BS4
Modelled Groundwater Level
Observed Groundwater Level

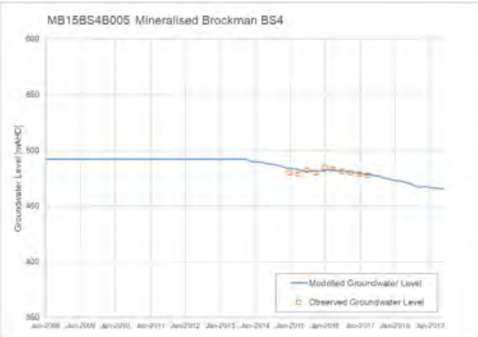
MB15BS4B005 Mineralised Brockman BS4
Modelled Groundwater Level
Observed Groundwater Level


MB15BS4B009 Joffre BS4
Modelled Groundwater Level
Observed Groundwater Level

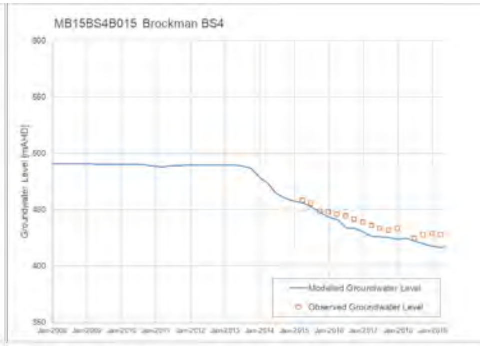
MB15BS4B015 Brockman BS4
Modelled Groundwater Level
Observed Groundwater Level

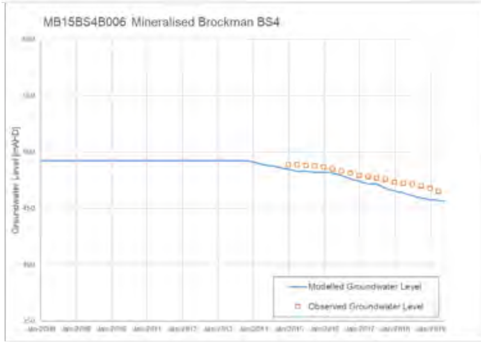
MB15BS4B006 Mineralised Brockman BS4
Modelled Groundwater Level
Observed Groundwater Level

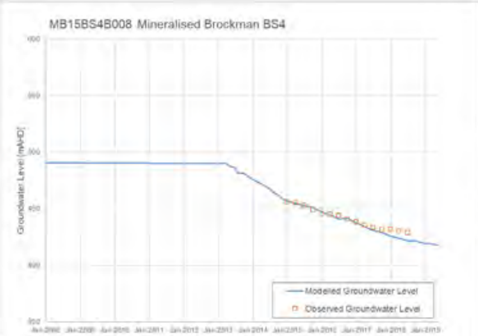
MB15BS4B008 Mineralised Brockman BS4
Modelled Groundwater Level
Observed Groundwater Level

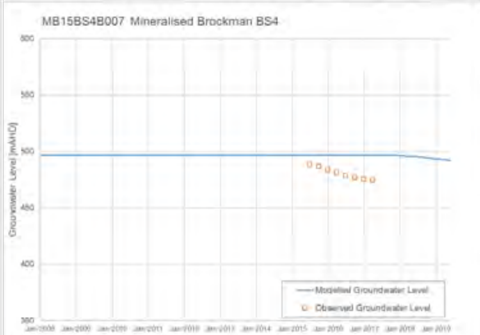
MB15BS4B007 Mineralised Brockman BS4
Modelled Groundwater Level
Observed Groundwater Level

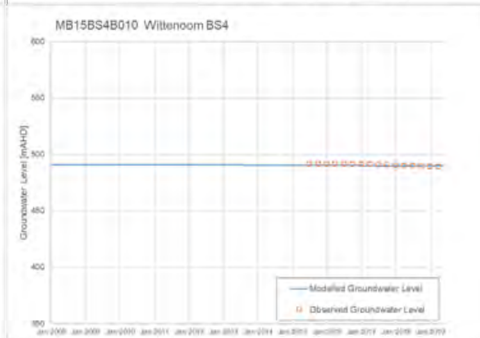
MB15BS4B010 Wittenoom BS4
Modelled Groundwater Level
Observed Groundwater Level

MB15BS4B017 Joffre BS4

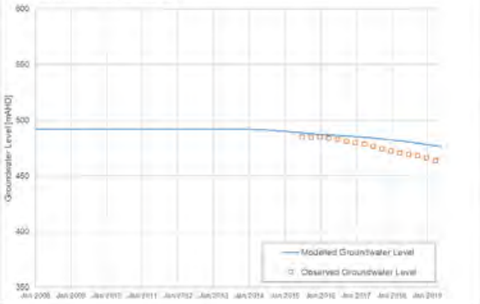

MB15BS4B018 Brockman BS4

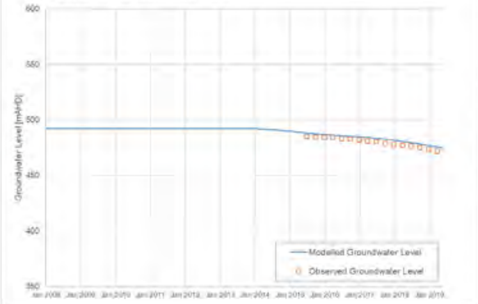

MB15BFH003 Tertiary BS4

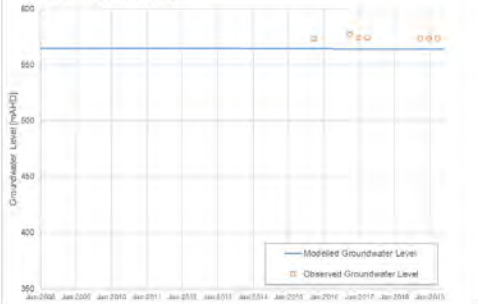

MB15BS4B016 Tertiary BS4

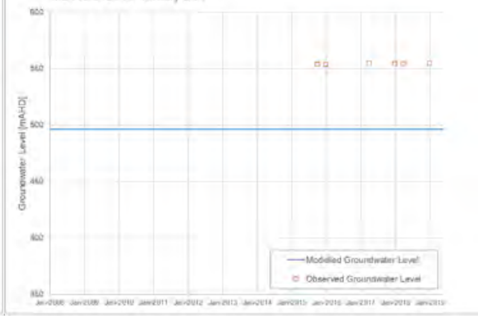

MB15BS4B019 Brockman BS4

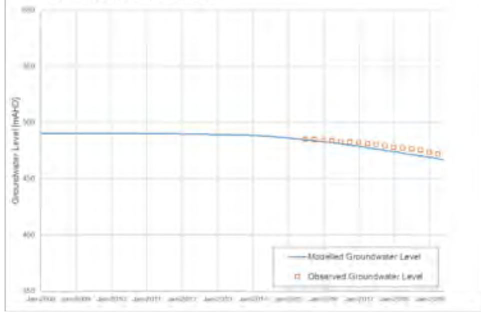

MB15BFH002 Tertiary BS4

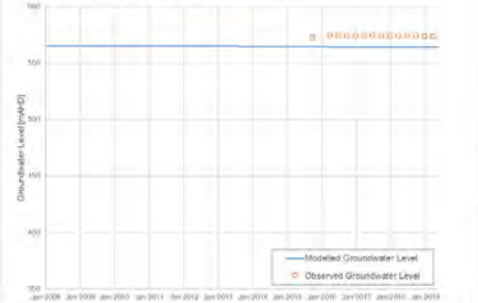

MB16BS4B0002 Mineralised Brockman BS4

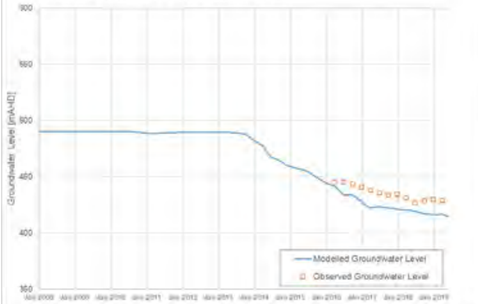

MB16BS4B0003 Brockman BS4

MB16BS4B0004 Mineralised Brockman BS4

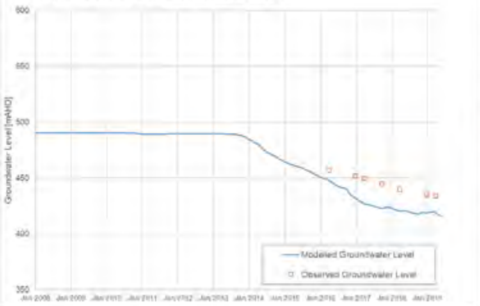

MB16BS4B0005 Mineralised Brockman BS4

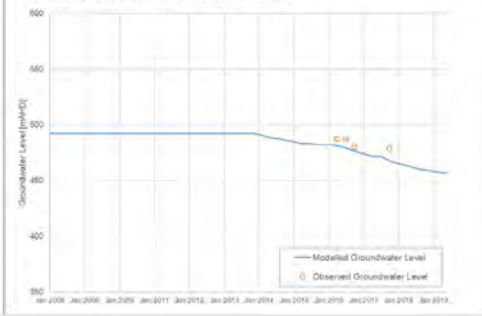

MB17BS4B0002 Mineralised Brockman BS4

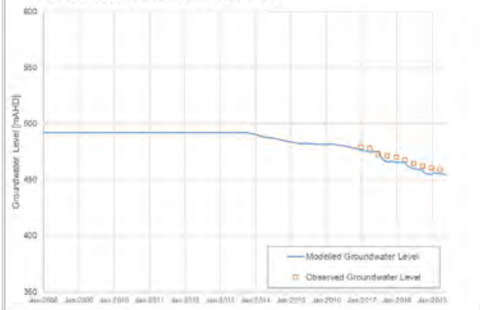

MB17BS4B0003 Mineralised Brockman BS4

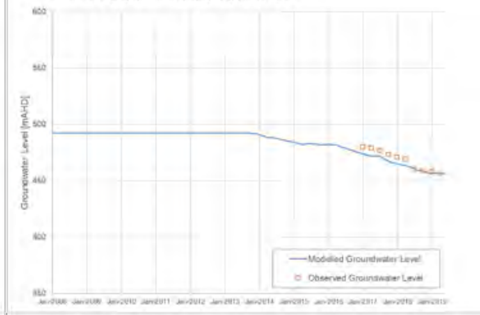

MB16BS4B0006 Mineralised Brockman BS4

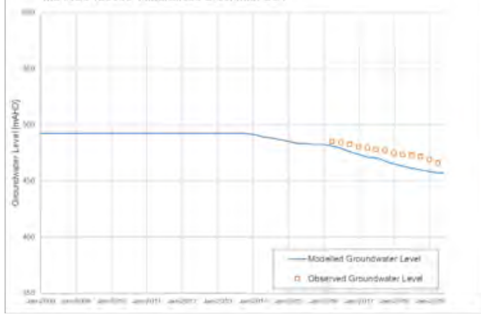

MB17BS4B0001 Brockman BS4

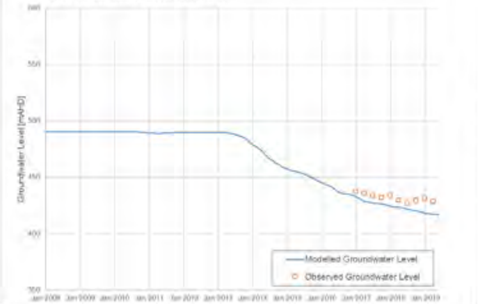

MB17BS4B0004 Brockman BS4

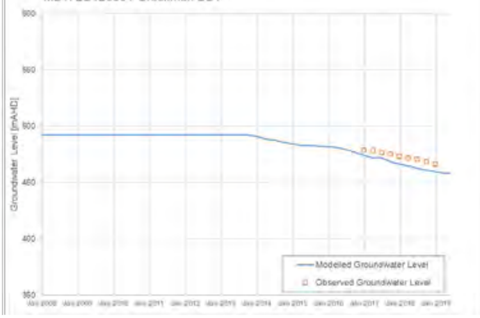

MB17BS4B0005 Brockman BS4

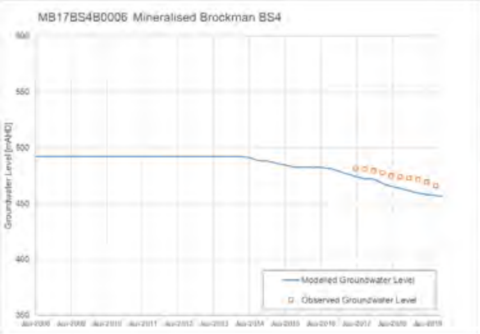
MB17BS4B0006 Mineralised Brockman BS4
Modelled Groundwater Level
Observed Groundwater Level

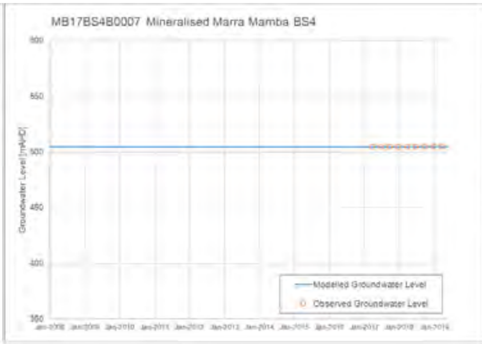
MB17BS4B0007 Mineralised Marra Mamba BS4
Modelled Groundwater Level
Observed Groundwater Level

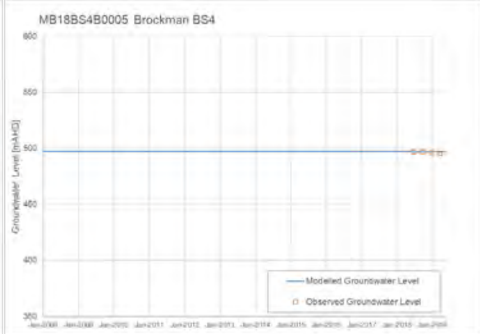
MB18BS4B0005 Brockman BS4
Modelled Groundwater Level
Observed Groundwater Level

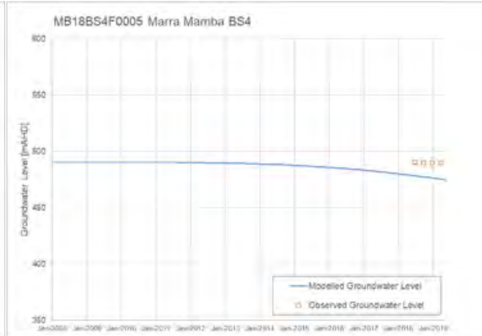
MB18BS4F0005 Marra Mamba BS4
Modelled Groundwater Level
Observed Groundwater Level

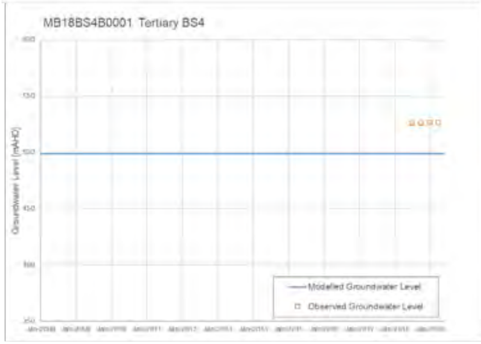
MB18BS4B0001 Tertiary BS4
Modelled Groundwater Level
Observed Groundwater Level

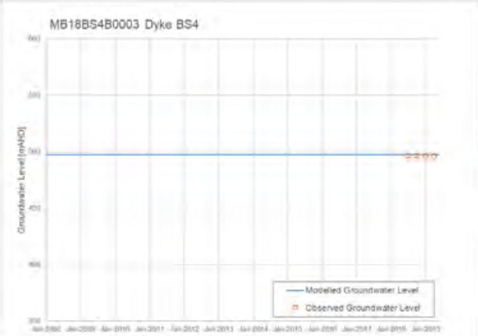
MB18BS4B0003 Dyke BS4
Modelled Groundwater Level
Observed Groundwater Level


MB18BS4M0004 Wittenoom BS4
Modelled Groundwater Level
Observed Groundwater Level

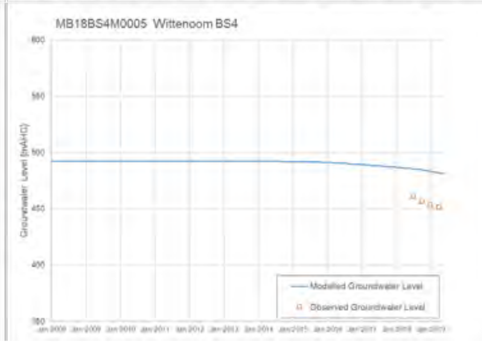
MB18BS4M0005 Wittenoom BS4
Modelled Groundwater Level
Observed Groundwater Level

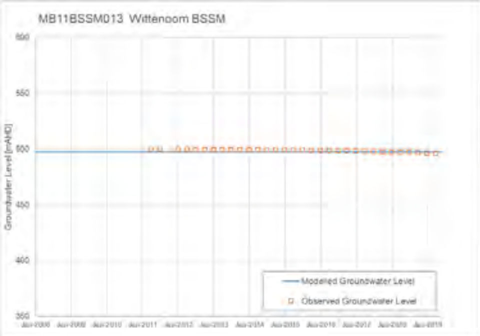
MB11BSSM013 Wittenoom BSSM
Modelled Groundwater Level
Observed Groundwater Level

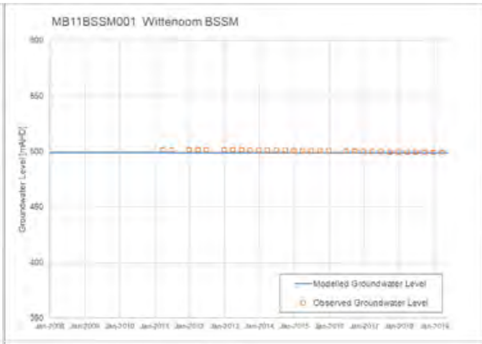
MB11BSSM001 Wittenoom BSSM
Modelled Groundwater Level
Observed Groundwater Level

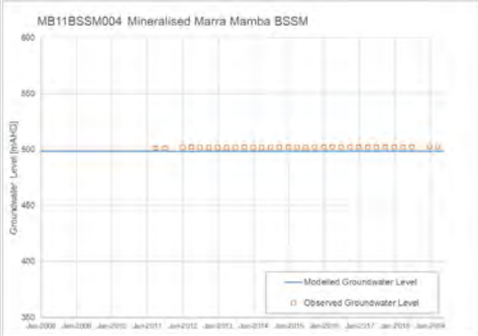
MB11BSSM004 Mineralised Marra Mamba BSSM
Modelled Groundwater Level
Observed Groundwater Level

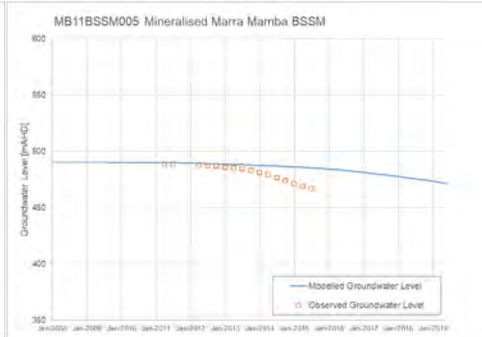
MB11BSSM005 Mineralised Marra Mamba BSSM
Modelled Groundwater Level
Observed Groundwater Level

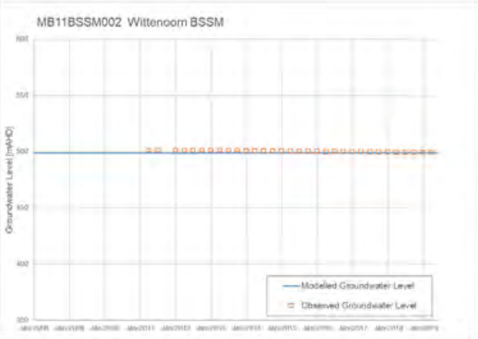
MB11BSSM002 Wittenoom BSSM
Modelled Groundwater Level
Observed Groundwater Level

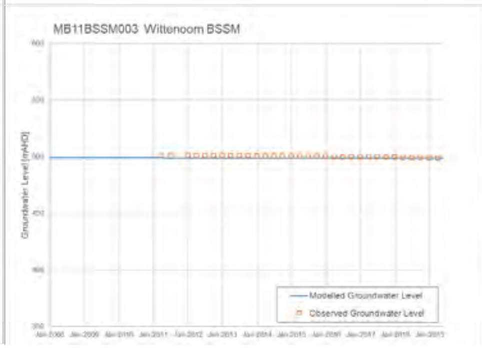
MB11BSSM003 Wittenoom BSSM
Modelled Groundwater Level
Observed Groundwater Level

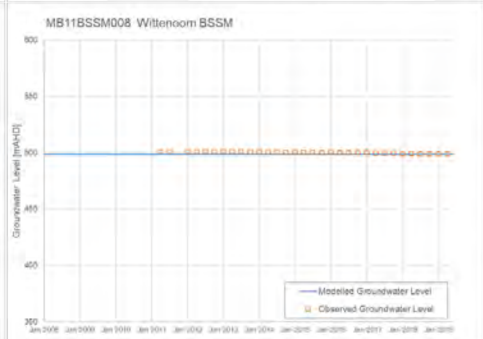
MB11BSSM008 Wittenoom BSSM
Modelled Groundwater Level
Observed Groundwater Level

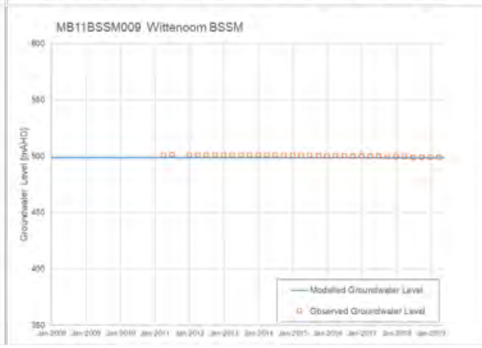
MB11BSSM009 Wittenoom BSSM
Modelled Groundwater Level
Observed Groundwater Level

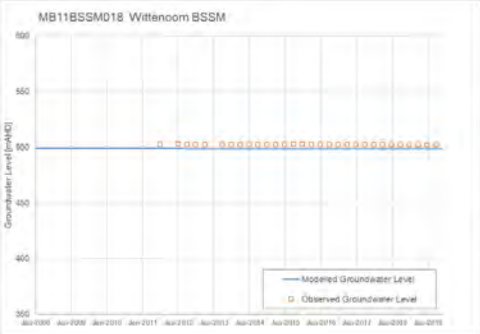
MB11BSSM018 Wittenoom BSSM
Modelled Groundwater Level
Observed Groundwater Level

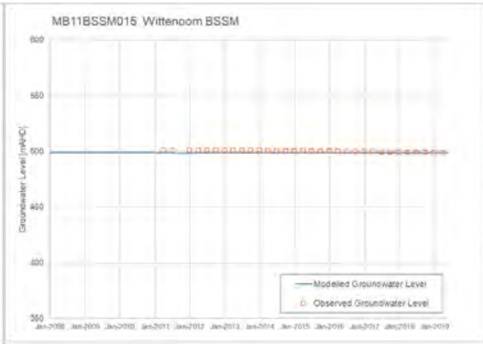
MB11BSSM015 Wittenoom BSSM
Modelled Groundwater Level
Observed Groundwater Level

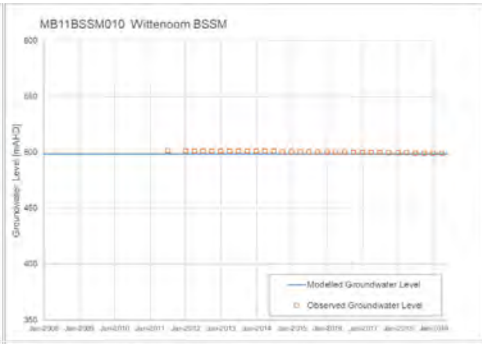
MB11BSSM010 Wittenoom BSSM
Modelled Groundwater Level
Observed Groundwater Level

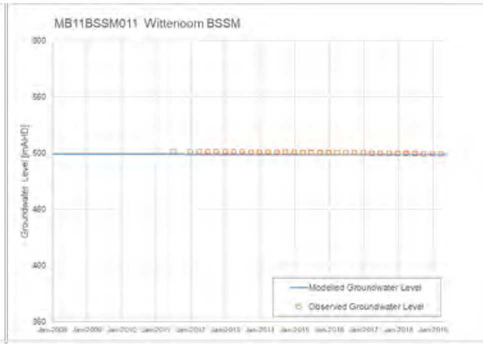
MB11BSSM011 Wittenoom BSSM
Modelled Groundwater Level
Observed Groundwater Level

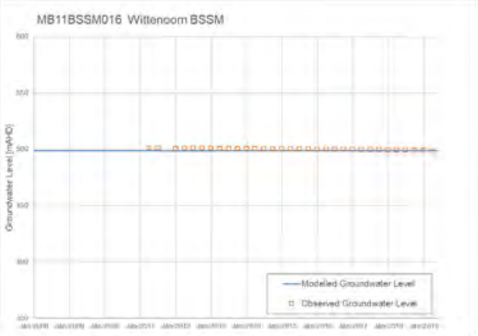
MB11BSSM016 Wittenoom BSSM
Modelled Groundwater Level
Observed Groundwater Level

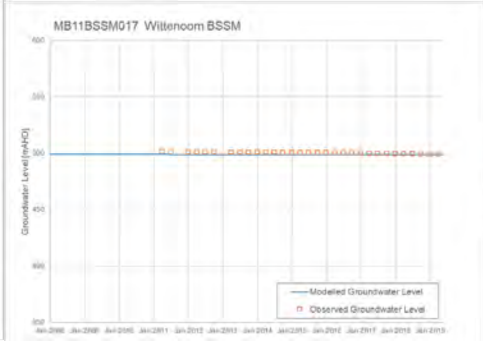
MB11BSSM017 Wittenoom BSSM
Modelled Groundwater Level
Observed Groundwater Level

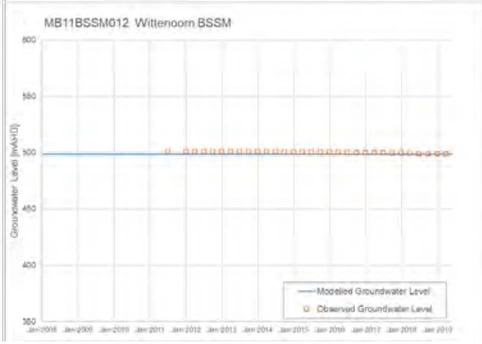
MB11BSSM012 Wittenoom BSSM
Modelled Groundwater Level
Observed Groundwater Level

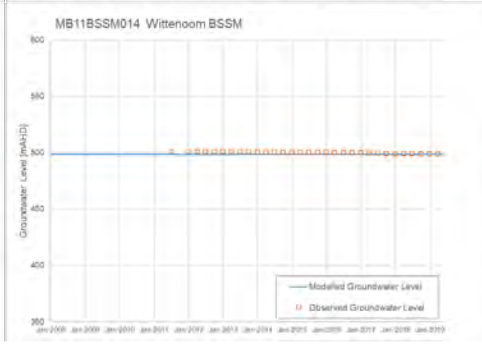
MB11BSSM014 Wittenoom BSSM
Modelled Groundwater Level
Observed Groundwater Level

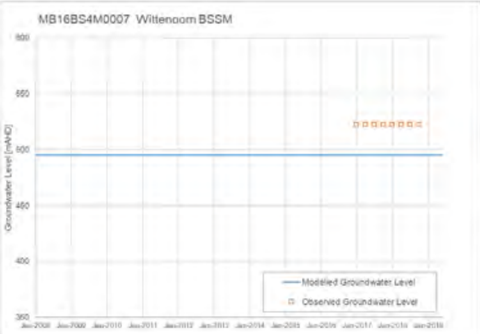
MB16BS4M0007 Wittenoom BSSM
Modelled Groundwater Level
Observed Groundwater Level

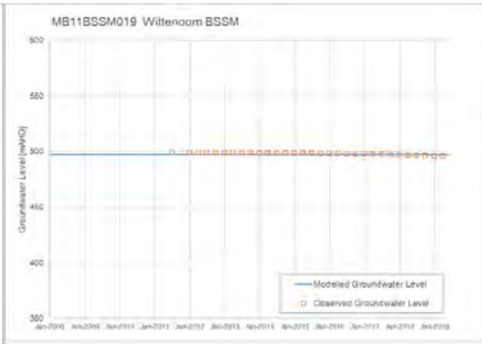
MB11BSSM019 Wittenoom BSSM
Modelled Groundwater Level
Observed Groundwater Level

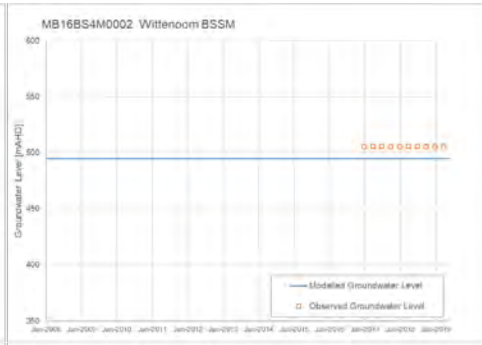
MB16BS4M0002 Wittenoom BSSM
Modelled Groundwater Level
Observed Groundwater Level

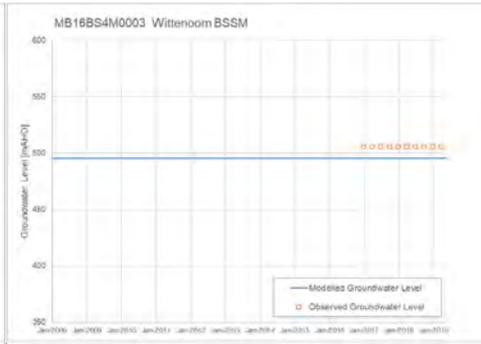
MB16BS4M0003 Wittenoom BSSM
Modelled Groundwater Level
Observed Groundwater Level

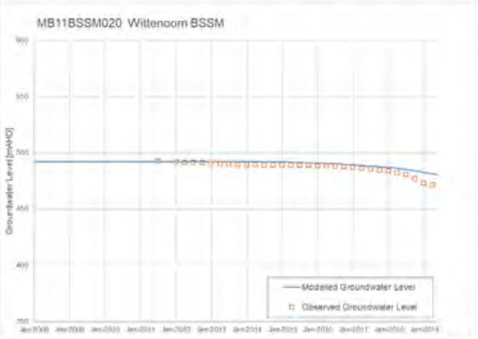
MB11BSSM020 Wittenoom BSSM
Modelled Groundwater Level
Observed Groundwater Level

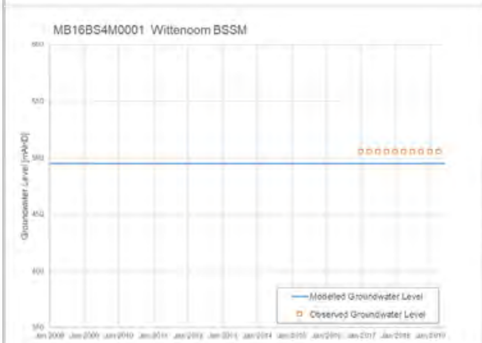
MB16BS4M0001 Wittenoom BSSM
Modelled Groundwater Level
Observed Groundwater Level

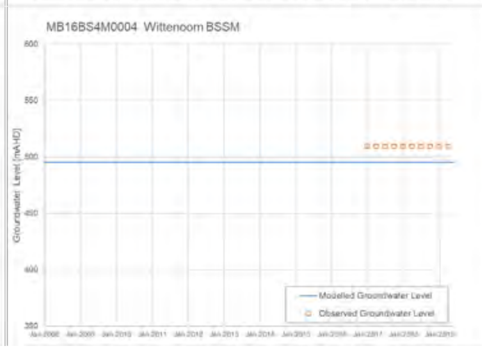
MB16BS4M0004 Wittenoom BSSM
Modelled Groundwater Level
Observed Groundwater Level

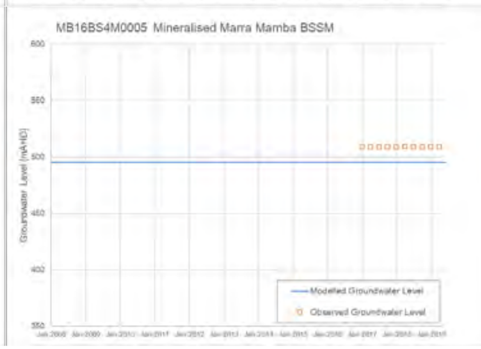
MB16BS4M0005 Mineralised Marra Mamba BSSM
Modelled Groundwater Level
Observed Groundwater Level

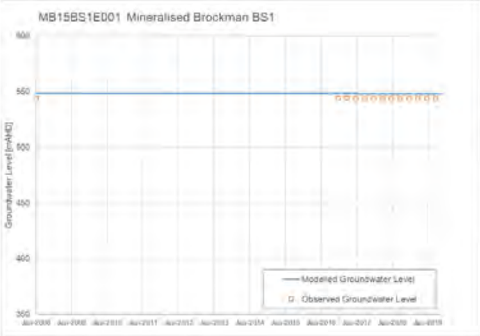
MB15BS1E001 Mineralised Brockman BS1
Groundwater Level (mAHD)
Modelled Groundwater Level
Observed Groundwater Level

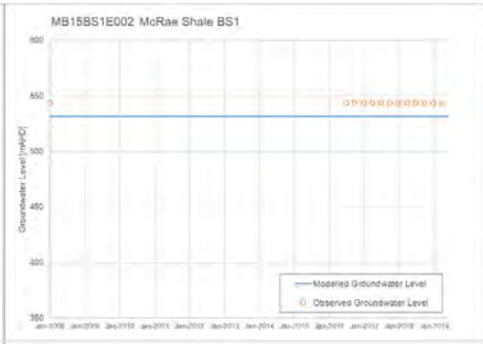
MB15BS1E002 McRae Shale BS1
Groundwater Level (mAHD)
Modelled Groundwater Level
Observed Groundwater Level

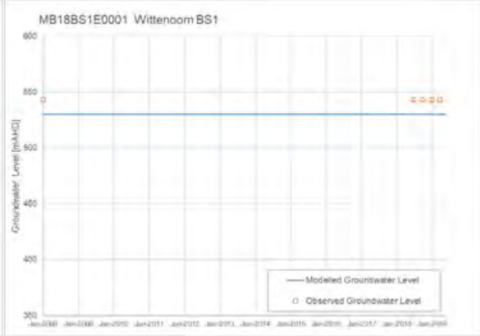
MB18BS1E0001 Wittenoom BS1
Groundwater Level (mAHD)
Modelled Groundwater Level
Observed Groundwater Level

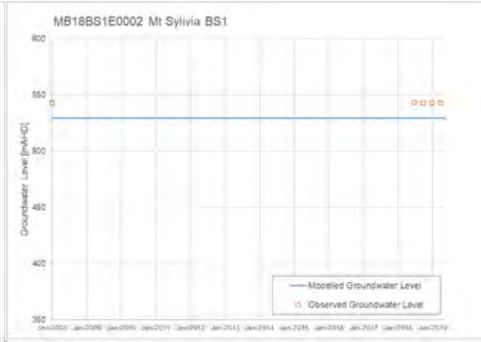
MB18BS1E0002 Mt Sylvia BS1
Groundwater Level (mAHD)
Modelled Groundwater Level
Observed Groundwater Level

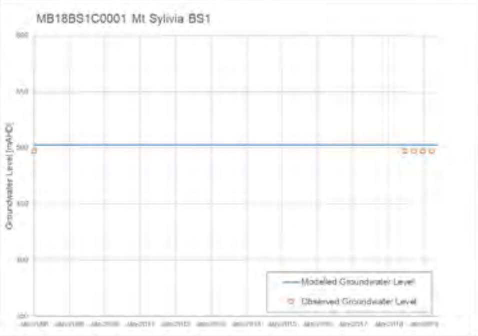
MB18BS1C0001 Mt Sylvia BS1
Groundwater Level (mAHD)
Modelled Groundwater Level
Observed Groundwater Level

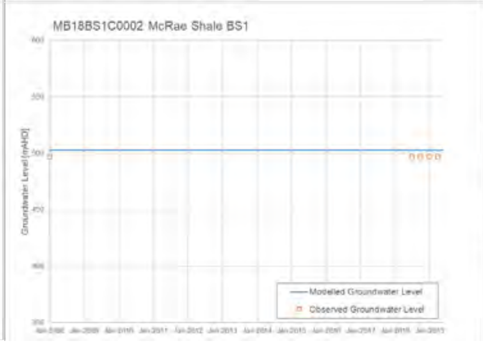
MB18BS1C0002 McRae Shale BS1
Groundwater Level (mAHD)
Modelled Groundwater Level
Observed Groundwater Level

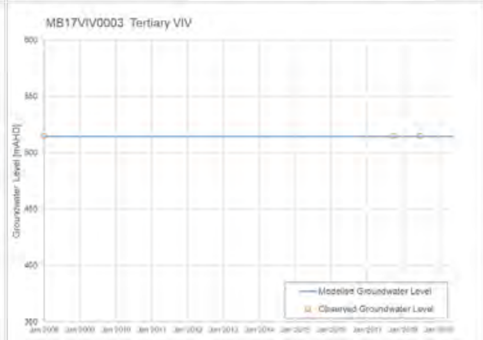
MB17VIV0003 Tertiary VIV
Groundwater Level (mAHD)
Modelled Groundwater Level
Observed Groundwater Level

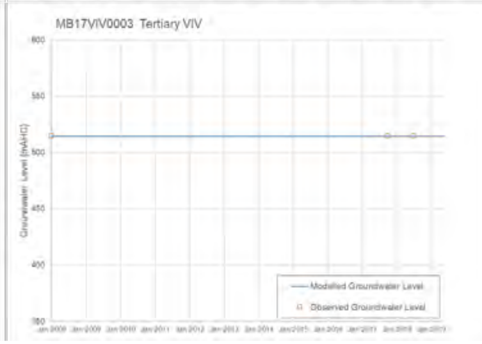
MB17VIV0003 Tertiary VIV
Groundwater Level (mAHD)
Modelled Groundwater Level
Observed Groundwater Level


MB17BS30001 Wittenoom BS3
Groundwater Level (mAHD)
Modelled Groundwater Level
Observed Groundwater Level

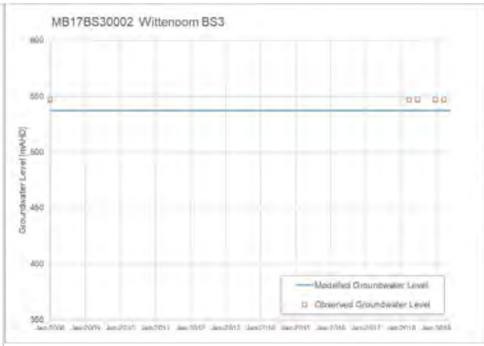
MB17BS30002 Wittenoom BS3
Groundwater Level (mAHD)
Modelled Groundwater Level
Observed Groundwater Level

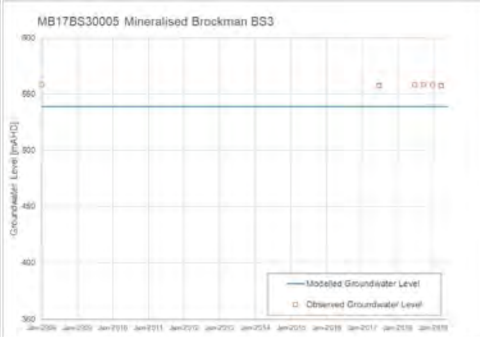
MB17BS30005 Mineralised Brockman BS3
Groundwater Level (mAHD)
Modelled Groundwater Level
Observed Groundwater Level

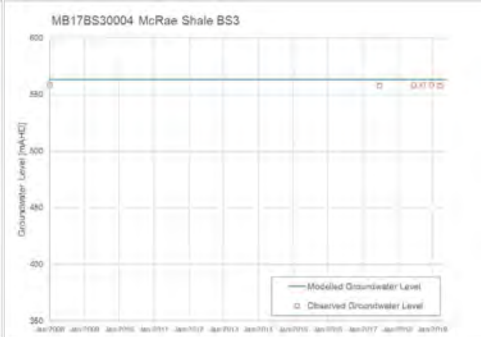
MB17BS30004 McRae Shale BS3
Groundwater Level (mAHD)
Modelled Groundwater Level
Observed Groundwater Level

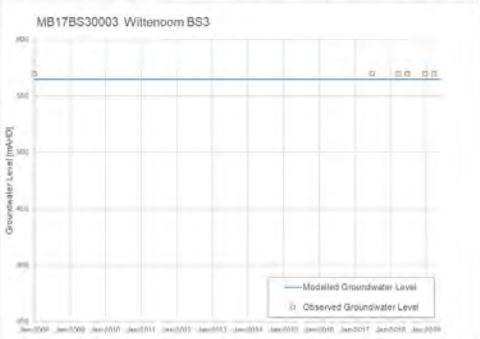
MB17BS30003 Wittenoom BS3
Groundwater Level (mAHD)
Modelled Groundwater Level
Observed Groundwater Level

APPENDIX C - LIFE OF MINE HYDROGRAPHS

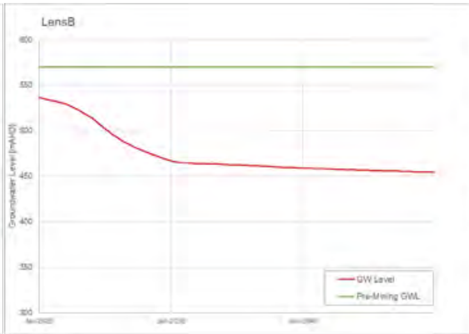

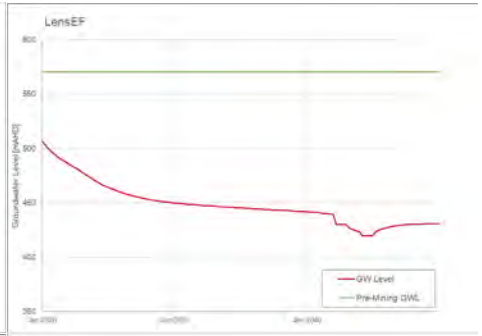

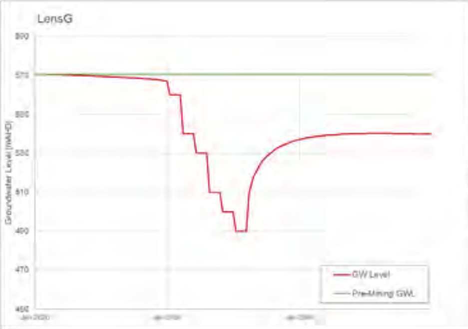

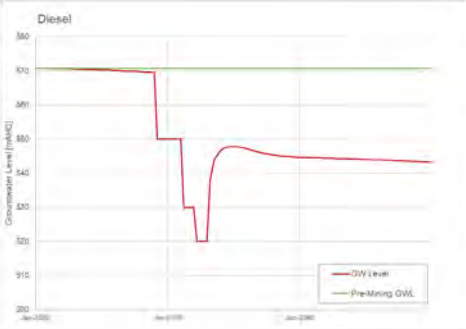

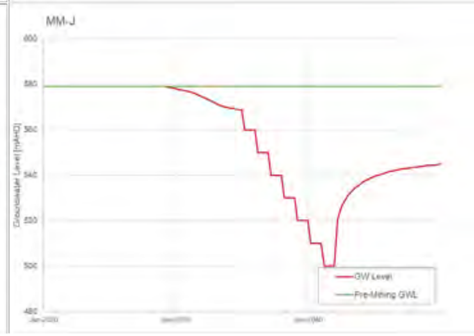

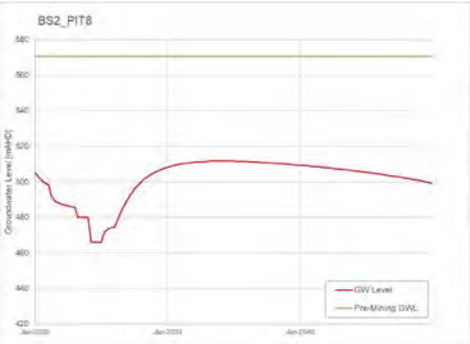

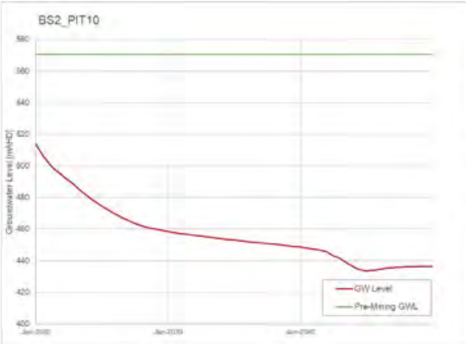

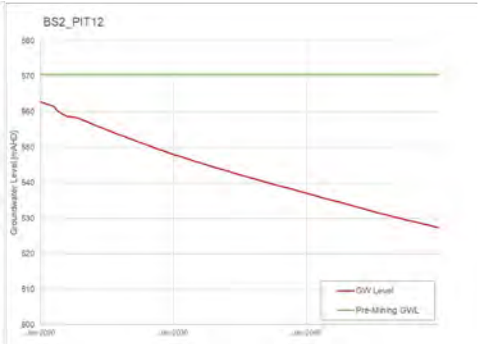

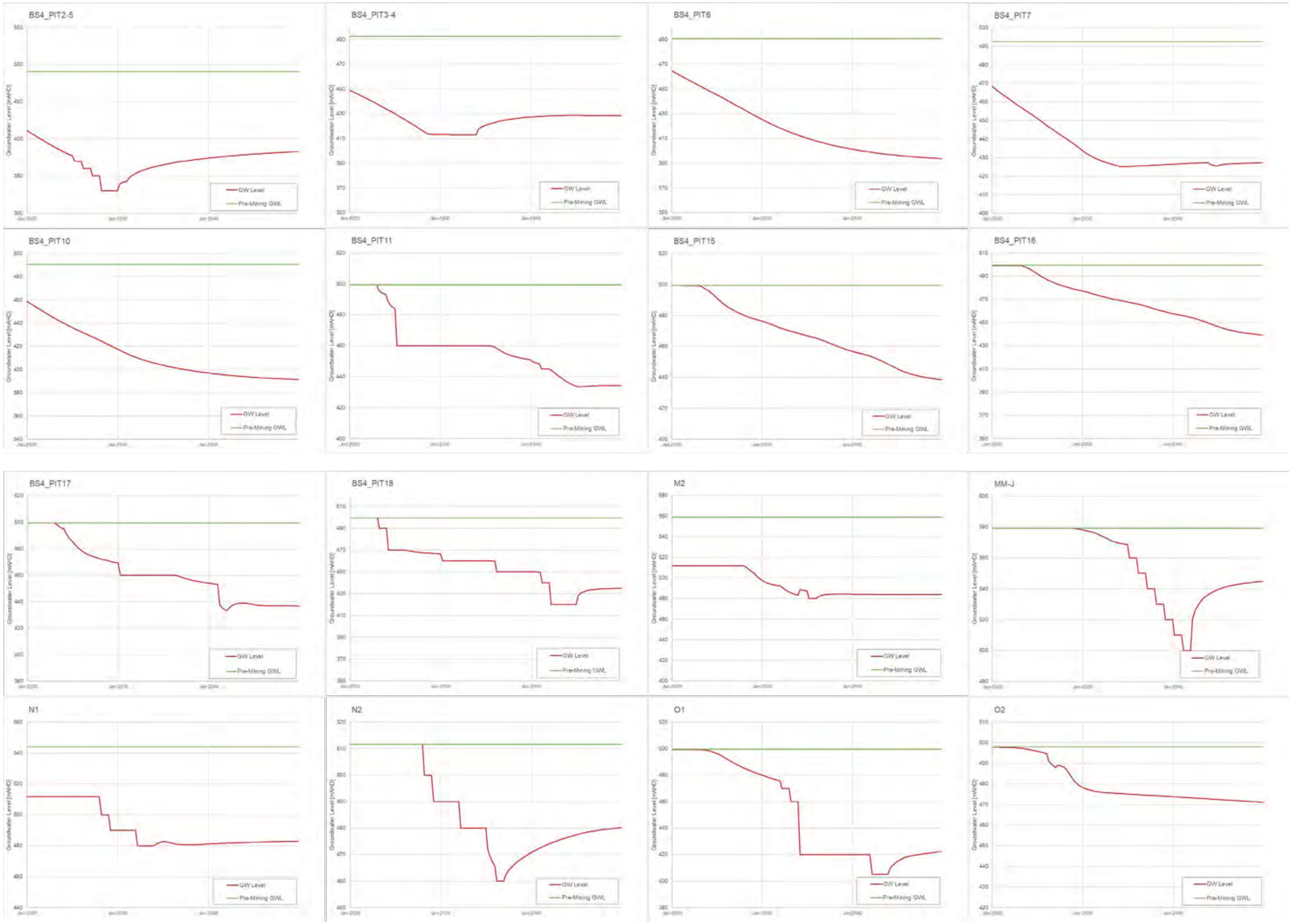
BS4_PIT2-5
BS4_PIT3-4
BS4_PIT6
BS4_PIT7
BS4_PIT10
BS4_PIT11
BS4_PIT15
BS4_PIT16
BS4_PIT17
BS4_PIT18
M2
MM-J
N1
N2
O1
O2
GW Level
Pre-Mining GWL

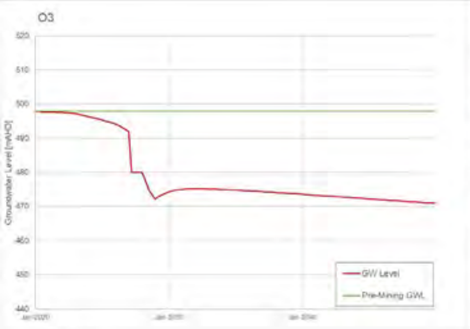
O3
Groundwater Level [mAHD]
GW Level
Pre-Mining GWL

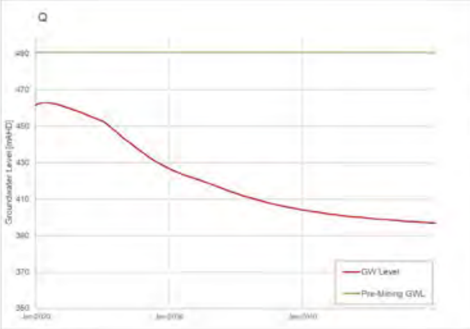
Q
Groundwater Level [mAHD]
GW Level
Pre-Mining GWL

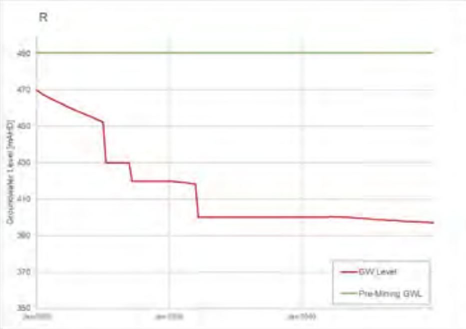
R
Groundwater Level [mAHD]
GW Level
Pre-Mining GWL

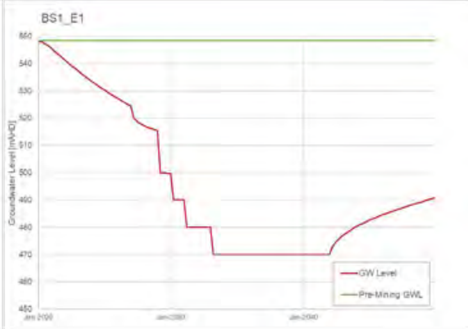
BS1_E1
Groundwater Level [mAHD]
GW Level
Pre-Mining GWL


BS1_E2
Groundwater Level [mAHD]
GW Level
Pre-Mining GWL

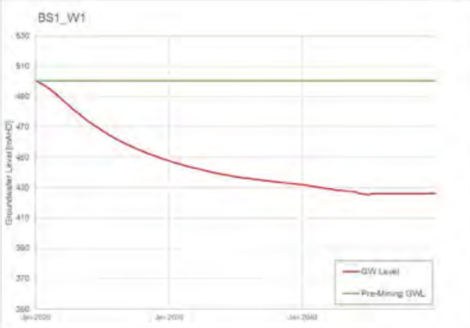
BS1_W1
Groundwater Level [mAHD]
GW Level
Pre-Mining GWL


BS1_W2
Groundwater Level [mAHD]
GW Level
Pre-Mining GWL

APPENDIX D - RECOVERY HYDROGRAPHS FOR OPEN VOIDS

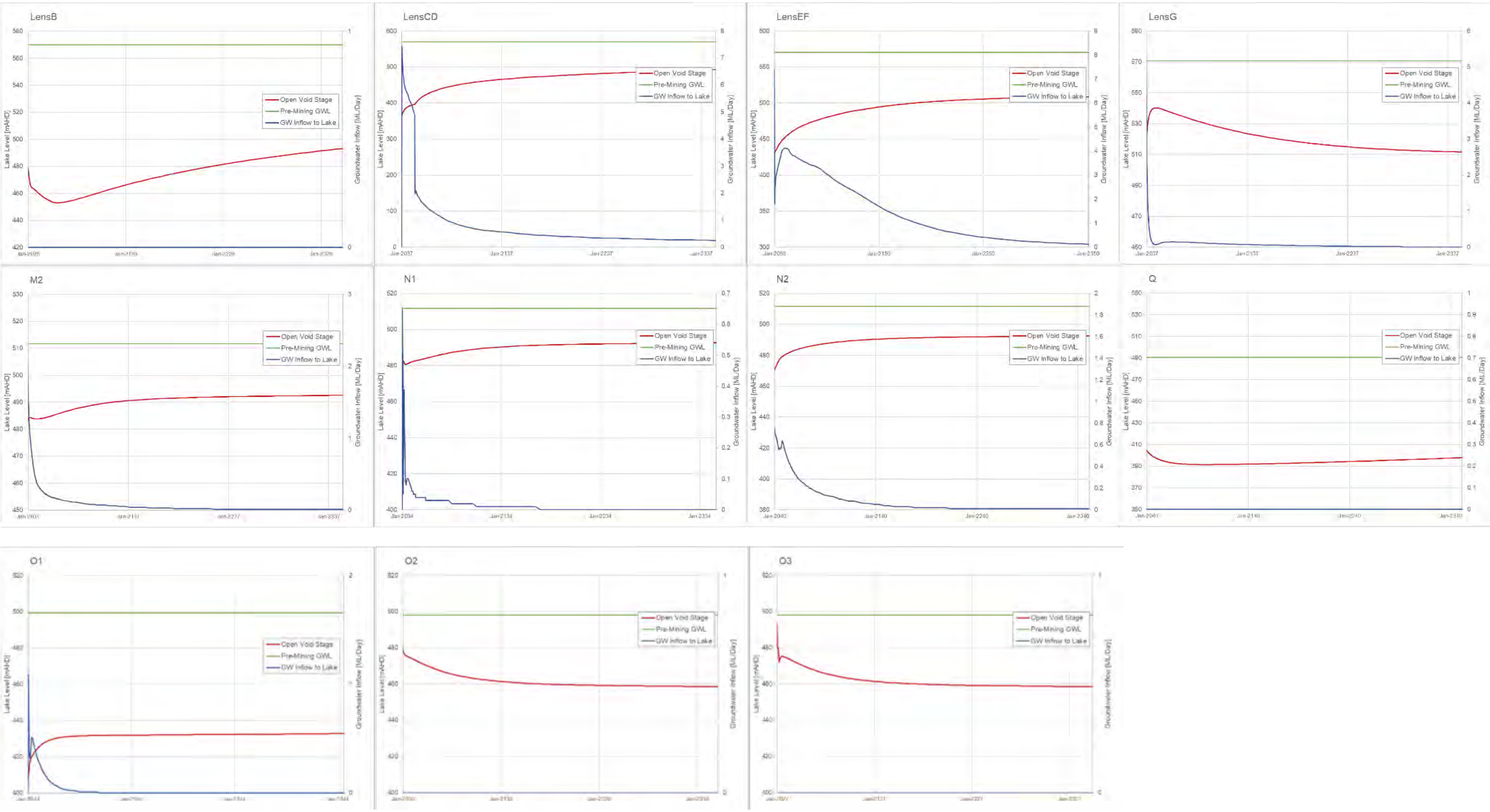

APPENDIX E - RECOVERY HYDROGRAPHS FOR BACKFILLED PITS

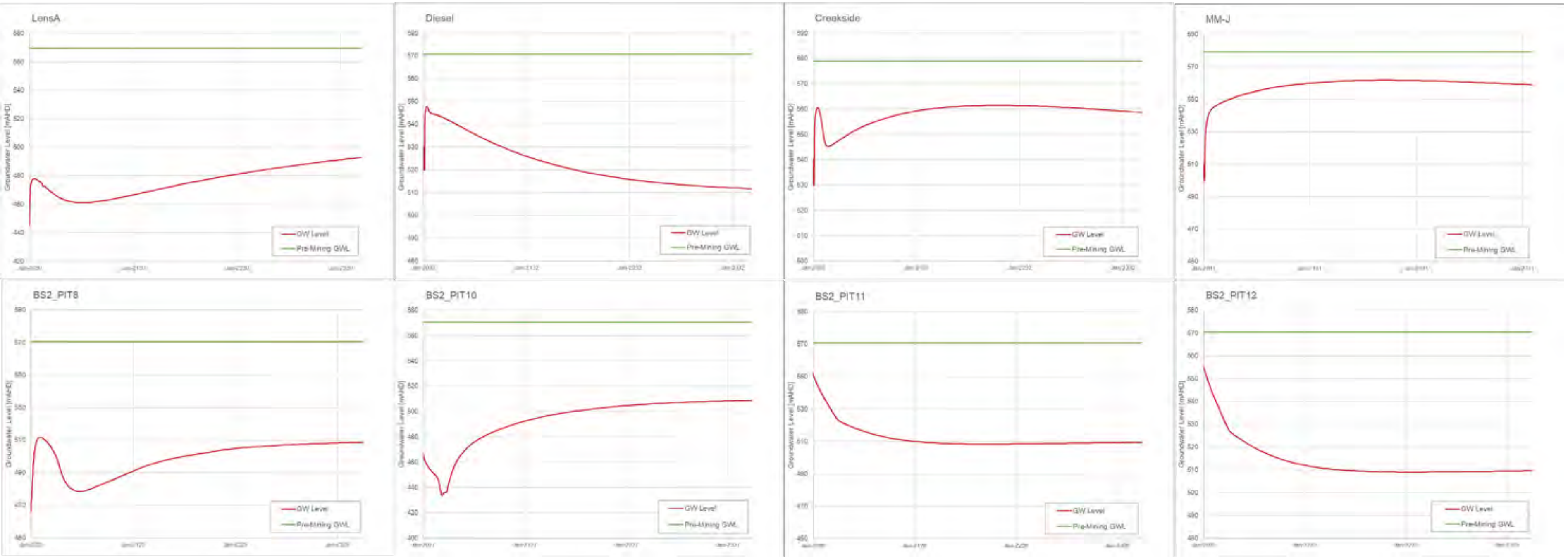

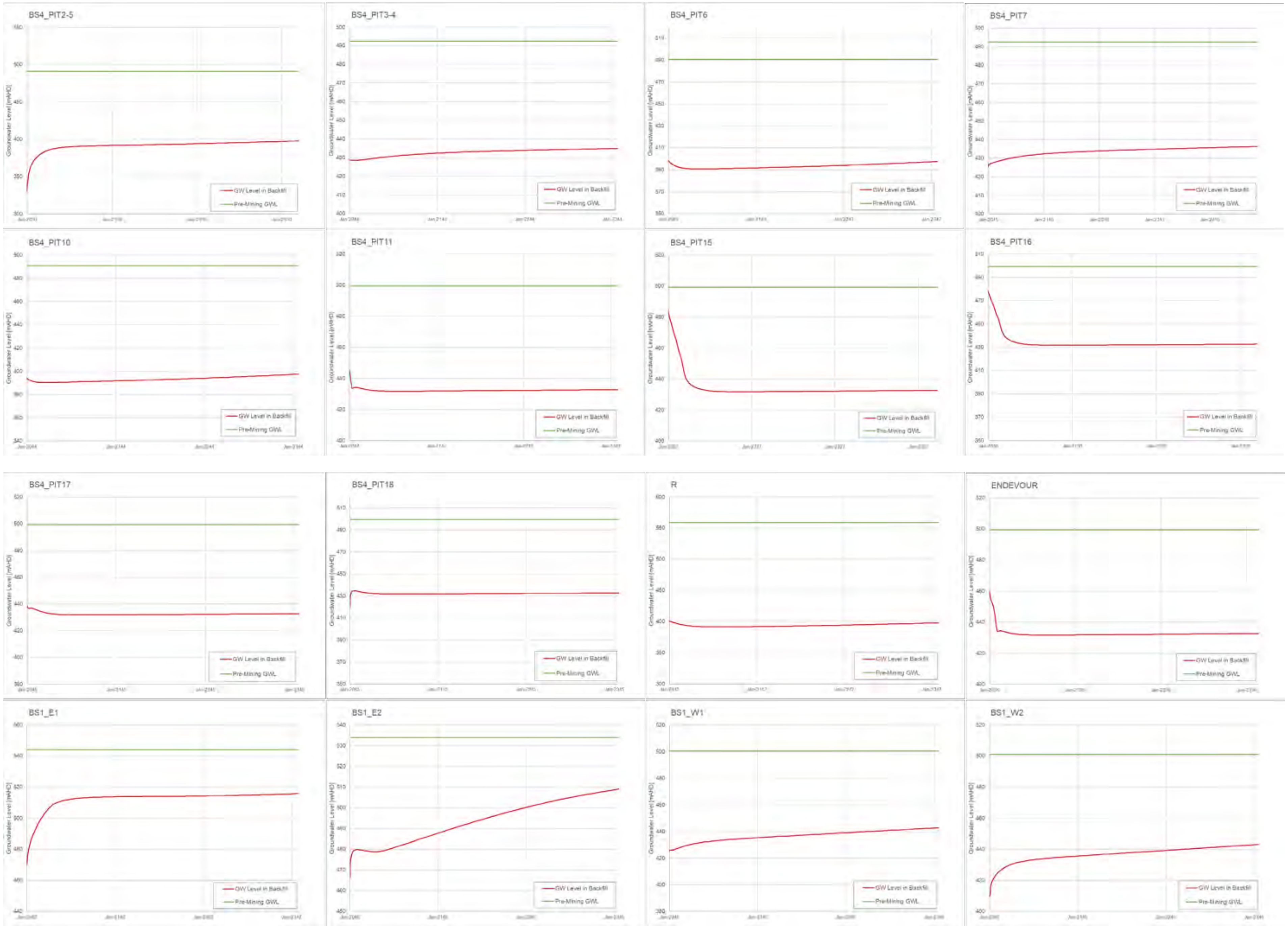
BS4_PIT2-5
BS4_PIT3-4
BS4_PIT6
BS4_PIT7
BS4_PIT10
BS4_PIT11
BS4_PIT15
BS4_PIT16
BS4_PIT17
BS4_PIT18
R
ENDEVOUR
BS1_E1
BS1_E2
BS1_W1
BS1_W2
Groundwater Level (mAHD)
GW Level in Backfill
Pre-Mining GWL